Copyright Warning & Restrictions

The copyright law of the United States (Title 17, United States Code) governs the making of photocopies or other reproductions of copyrighted material.

Under certain conditions specified in the law, libraries and archives are authorized to furnish a photocopy or other reproduction. One of these specified conditions is that the photocopy or reproduction is not to be "used for any purpose other than private study, scholarship, or research." If a, user makes a request for, or later uses, a photocopy or reproduction for purposes in excess of "fair use" that user may be liable for copyright infringement,

This institution reserves the right to refuse to accept a copying order if, in its judgment, fulfillment of the order would involve violation of copyright law.

Please Note: The author retains the copyright while the New Jersey Institute of Technology reserves the right to distribute this thesis or dissertation

Printing note: If you do not wish to print this page, then select "Pages from: first page # to: last page #" on the print dialog screen

ABSTRACT

CORROSION STUDIES OF STAINLESS STEEL BLADES

by
Dhruv Shrenikkumar Kothari

Corrosion is a subject of interest to interdisciplinary research communities that includes fields of materials science, chemistry, physics, metallurgy and chemical engineering. In order to understand the mechanisms of corrosion and the function of corrosion inhibitors, the reactions at the interfaces between the corrosive electrolyte and a steel surface, particularly at the initial stages of the corrosion process, need to be described. Naturally, these reactions are strongly affected by the nature and properties of the steel surfaces. It is however seen that the majority of recent corrosion and corrosion-inhibition investigations are limited to electrochemical testing, with ex situ analysis of the treated steels (post-exposure analysis). The characterization of materials and their surface properties, such as texture and morphology, are not being considered in most of the studies.

Similarly, in situ investigations of the initial stages of the corrosion reactions, using advanced surface characterization techniques, are scarce. In this thesis, attention is brought to the importance of surface features of carbon steels, such as texture and surface energy, along with defects and dislocation related to mechanical processing of carbon steels. This work is extended to a critical review of surface analytical techniques that are used for characterization of carbon steels in corrosive media with particular focus on examining steel surfaces treated with corrosion inhibitors. Further, emerging surface analysis techniques and their applicability to analyses of carbon steels in corrosive media are discussed.

Due to their good corrosion resistance, favorable mechanical properties, and

reasonable price regarding their excellent properties, martensitic stainless steels have, over recent decades, become one of the alloys that are increasingly used in blade manufacturing industry. Architects often design stainless steel exterior elements with higher polished surface, which are resistant to corrosion processes. The aim of this work is to investigate the influence of different types of surface finishes to stainless steel of quality AISI 440 on the corrosion properties of this steel. In order to achieve this goal, tests are performed on surface finishes in two different environments: in an NaCl aqueous solution, and in Acetic Acid. In addition to the methods used, surface roughness is also measured, and SEM-EDS surface analyses are performed. Based on the results of the performed analyses, it is found that, in the NaCl solution, the pitting potential depends strongly on the surface roughness and the surface finish. The evolution of the passive films on Martensitic 440 stainless steel in seawater and in pure 3.5 % NaCl and 3.5% acetic acid is studied using Scanning Electron Microscopy (SEM) and Energy Dispersive Spectroscopy (EDS). This thesis describes and evaluates the comparison of the effects of pure 3.5 % NaCl with acetic acid through surface and corrosion measurements.

CORROSION STUDIES OF STAINLESS STEEL BLADES

by
Dhruv S. Kothari

A Thesis
Submitted to the Faculty of
New Jersey Institute of Technology
in Partial Fulfillment of the Requirements for the Degree of
Master of Science in Materials Science and Engineering

Interdisciplinary Program in Materials Science and Engineering

May 2017

APPROVAL PAGE

CORROSION STUDIES OF STAINLESS STEEL BLADES

Dhruv S. Kothari

Dr. Nuggehalli M. Ravindra, Thesis Advisor — Date
Professor, Department of Physics, NJIT

Dr. Michael Jaffe, Committee Member — Date
Research Professor, Department of Biomedical Engineering, NJIT

Dr. Sagnik Basuray, Committee Member — Date
Assistant Professor, Department of Chemical, Biological and Pharmaceutical Engineering, NJIT

Dr. Alex Stein, Committee Member — Date
Chief Executive Officer, Harmon Sensors Inc.

BIOGRAPHICAL SKETCH

Author: Dhruv Shrenikkumar Kothari

Degree: Masters of Science

Date: May 2017

Undergraduate and Graduate Education:

- Master of Science in Materials Science and Engineering
  New Jersey Institute of Technology, Newark, NJ, 2017

- Bachelor of Engineering in Metallurgy Engineering,
  Indus Institute of Technology and Engineering, GTU, Ahmedabad, Gujarat, India, 2015

Major: Materials Science and Engineering

This Thesis is dedicated to my Mother Shilpa S. Kothari, Father Shrenikkumar Kothari and Sister Sweta S. Kothari. It is their love and support that gave me the ability to complete this work.

ACKNOWLEDGEMENT

I want to express my deepest gratitude to my supervisor, Dr. N.M. Ravindra, a respectable scholar, whose encouragement, guidance, and support from the beginning to the end enabled me to develop an understanding of the subject and also for giving me the privilege of working under his supervision. The knowledge and skills that I have learned from him especially those wonderful conversations about research, coursework and overall life, will be motivating me continuously in my future endeavors. I would also like to appreciate my committee members, Dr. Michael Jaffe, Dr. Sagnik Basuray and Dr. Alex Stein, for their precious support and time.

Special thanks to Dr Somenath Mitra from Chemistry Department and Ms. Samar Azizighannad, PhD Candidate, Interdisciplinary Program in Materials Science & Engineering, for helping me to perform the SEM-EDS analysis. Also, I would like to extend special thanks to my lab mates, Ms. Sita Rajyalaxmi Marthi and Mr. Asahel Banobre. I enjoyed working with them.

I thank my parents, Mr. Shrenikkumar Kothari and Mrs. Shilpa Kothari, whose help and emotional support has been of immense value to me. I thank my sister, Mrs. Sweta Kothari who encouraged me throughout my study.

Last but not least, thanks to my friends, Urvil Khatri, Javishk Shah, Jatin Jalora, Nirjar Shah, Aakash Sanghavi, Saloni Suthar, Bhargav Mehta, Harsh Desai and Pooja Devaraju, whose patience and encouragement played the greatest role in sustaining me through the challenge of this work. I will always be thankful to them.

TABLE OF CONTENTS

TABLE OF CONTENTS
(continued)

TABLE OF CONTENTS
(continued)

Chapter **Page**

TABLE OF CONTENTS
(continued)

Chapter **Page**

TABLE OF CONTENTS
(continued)

LIST OF FIGURES

LIST OF FIGURES
(continued)

LIST OF FIGURES
(continued)

LIST OF FIGURES
(continued)

LIST OF FIGURES
(continued)

LIST OF FIGURES
(continued)

LIST OF TABLES

CHAPTER 1

INTRODUCTION

Corrosion engineering is the application of science and art to prevent or control corrosion damage economically and safely. In order to perform this function properly, the corrosion engineer must be well versed in the following: practices and principles of corrosion; the chemical, metallurgical. physical and mechanical properties of materials; corrosion testing; the nature of corrosive environments; the availability and fabrication of materials; and design. The expert must also have the usual attributes of the engineer-a sense of human relations, integrity, the ability to think and analyze an awareness of the importance of safety, common sense of organization and of prime importance, a solid feeling for economics. In solving corrosion problems, the corrosion engineer must select the method that will maximize profits [1]. The importance of corrosion studies is three folds [2].

The first area of significance is economics including the objective of reducing material losses resulting from the corrosion of piping, tanks, metal components of machines, ships, bridges, marine structures, and so on.

The second area is improved safety of operating equipment which, through corrosion, may fail with catastrophic consequences. Examples are pressure vessels, boilers, metallic containers for toxic materials, turbine blades and rotors, bridges, airplane components, and automotive steering mechanisms. Safety is a prime consideration in the design of equipment for nuclear-power plants and disposal of nuclear wastes.

The third is conservation, applied primarily to metal resources - the world's supply of these is limited, and the wastage includes corresponding losses of energy

and water reserves that are associated with the production and fabrication of metal structures.

In the chemical, petrochemical, food processing, construction and transportation industries where corrosion and high temperature oxidation are major concerns, stainless steels are ubiquitous due to their high toughness and resistance to general corrosion (Fig 1). Despite advancements in steel making technology, these materials require a greater initial investment due to the high costs and low tolerances of alloying elements. The presence of a strongly adhering, several nanometer thick chromium oxide (passive) layer on the surface limits reaction kinetics and gives this class of materials the resistance to general corrosion and oxidation. However, stainless steels are susceptible to various forms of localized attack in chloride-containing environments including: stress corrosion cracking (SCC), pitting corrosion, crevice corrosion and inter-granular corrosion (IGC). A fundamental understanding of the influence of microstructure on these mechanisms will allow modifications of alloy chemistry, plastic deformation, heat treatment, service environment and maintenance so that localized corrosion can be mitigated, making this class of material a more sustainable alternative.

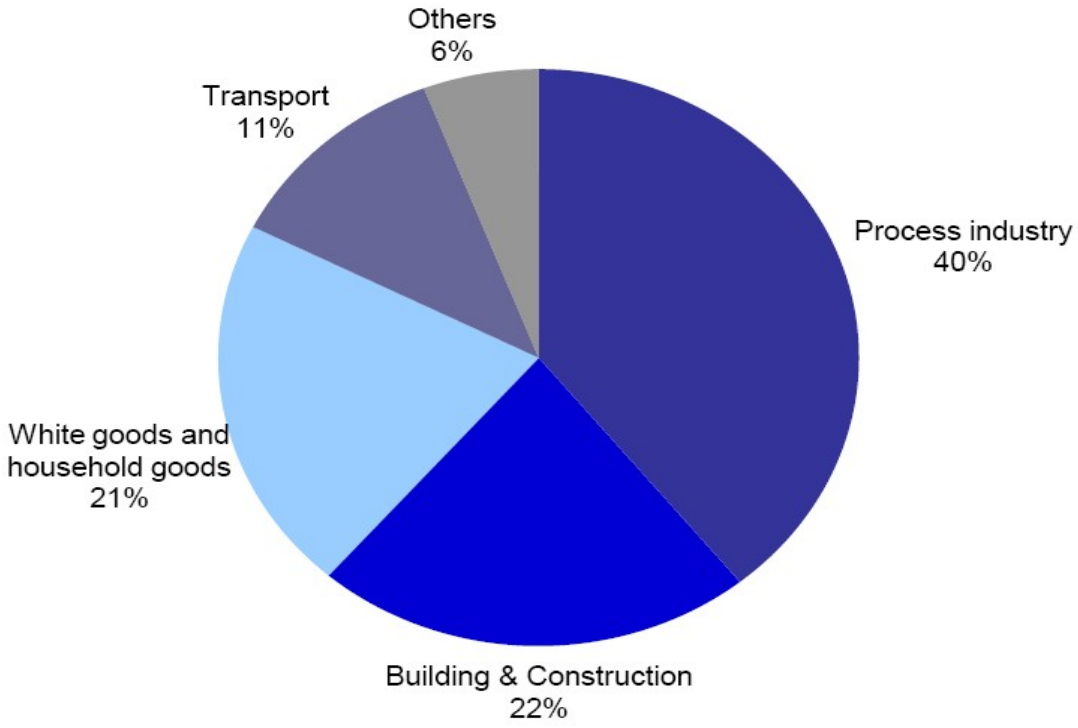

Figure 1.1 Percentage of stainless steel consumption by application in 2009; includes all grades [1].

1.1 Definition of Corrosion

Corrosion may be defined in several ways [1-3].

- Destruction or deterioration of a material because of reaction with its environment.
- Destruction of materials by means other than straight mechanical effect.
- Extractive metallurgy in reverse.
- Undesirable interaction of a material with its environment.

1.2 Corrosion of Metals and Alloys

The corrosion occurs because of the natural tendency for most metals to return to their natural state; e.g., iron in the presence of moist air will revert to its natural state, iron oxide. Metals can be corroded by the direct reaction of metal to a chemical and electrochemical reaction. The driving force that makes metals corrode is a natural sequence of their temporary existence in the metallic form.

Thermodynamically, corrosion is the ability of the metal to revert to compounds which are more stable, i.e., present in the nature initially [4].

Wagner and Traud, in 1938, utilized the mixed-potential theory, which consists of two simple hypotheses:

- Any electrochemical reaction can be divided into two or more partial oxidation and reduction reactions.
- There can be no net accumulation of electric charge during an electrochemical reaction.

From this, it follows that during the corrosion of an electrically isolated metal sample, the total rate of oxidation must equal the total rate of reduction [1].

Electrochemical corrosion, as shown in Fig. (1.2), is the most important classification of corrosion. Four conditions must exist before electrochemical corrosion can proceed:

- There must be something that corrodes (the metal anodes).
- There must be a cathode.
- There must be a continuous conductive liquid path (electrolyte, usually liquid, condensate, salts, other contaminations).
- There must be a conductor to carry the flow of electrons from anode to cathode.

This conductor is usually in the form of metal-to-metal contact as in bolted or riveted joints**.**

The rates of oxidation reaction may equal the rate of reduction reaction[1,5].

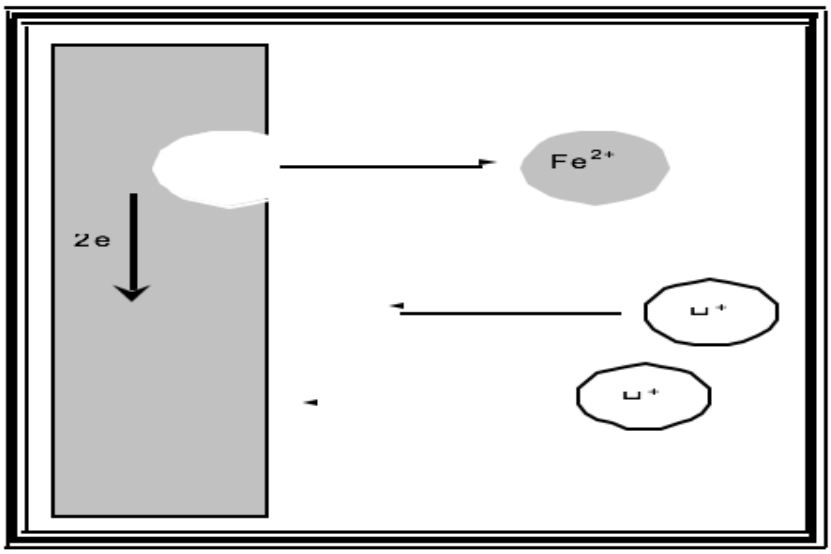

Figure 1.2 Simple model describing the electrochemical nature of corrosion processes. [1,5]

Figure 1.3 shows the basics of corrosion and the elimination of any one of the five conditions will stop corrosion. An unbroken (perfect) coating on the surface of the metal will prevent the electrolyte from connecting the cathode and anode so that the current cannot flow. Therefore, no corrosion will occur as long as the coating is unbroken.

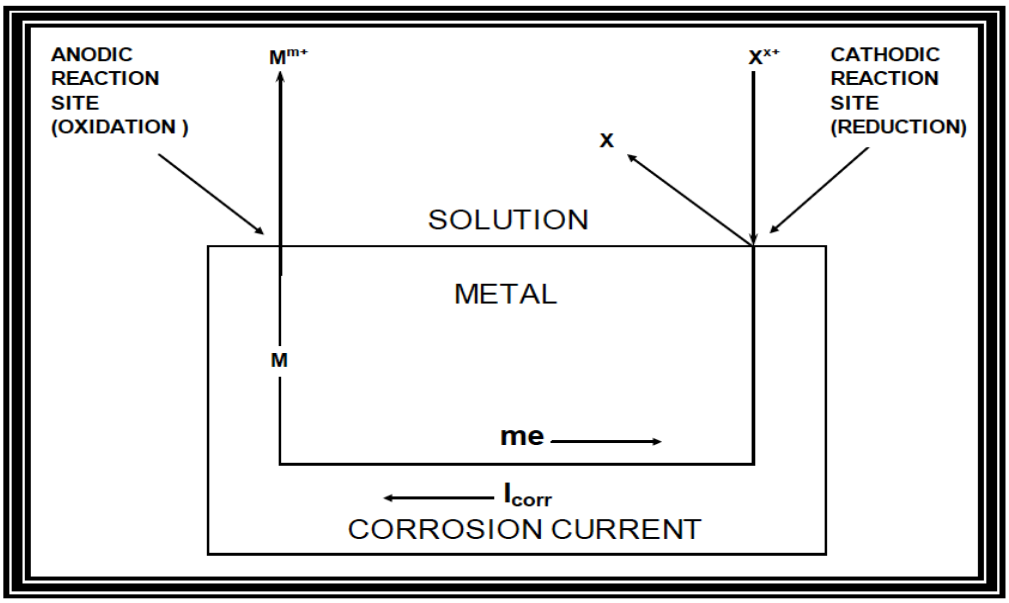

Figure 1.3 The basic corrosion process. [1]

1.3 Classification of Corrosion

Corrosion has been classified in many different ways. One method divides corrosion into low-temperature and high temperature corrosion. Another separates corrosion into direct chemical and electrochemical corrosion. The preferred classification here is:

- Wet corrosion.
- Dry corrosion.

Wet corrosion occurs when a liquid is present. This usually involves aqueous solutions or electrolytes and accounts for the greatest amount of corrosion by far. A common example is corrosion of steel in water or acid.

Dry corrosion occurs in the absence of a liquid phase or above the dew point of the environment. Vapors and gases are usually the corroding agents. Dry corrosion is most often associated with high temperatures. An example is attack on steel by furnace gases. The presence of even small amounts of moisture could change the corrosion completely. For example, dry chlorine is practically non corrosive to

ordinary steel but moist chlorine, or chlorine dissolved in water, is extremely corrosive and attacks most of the common metals and alloys. The reverse is true for titanium - dry chlorine gas is more corrosive than wet chlorine [1,4].

1.4 Types of Corrosion

It is convenient to classify corrosion by the forms in which it manifests itself, the basic for classification being the appearance of corroded metal. Each form can be identified by mere visual observation. In most cases, the naked eye is sufficient but sometimes magnification is helpful or required. Valuable information for the solution of a corrosion problem can often be obtained through careful observation of the corroded test specimens or failed equipment. Examination before cleaning is particularly desirable [1,4].

Some of the eight forms of corrosion are unique, but all of them are more or less interrelated. The eight forms are:

- Uniform (or General) attack
- Galvanic (or Two-metal) corrosion
- Crevice corrosion
- Pitting
- Intergranular corrosion
- Selective leaching, or parting
- Erosion corrosion
- Stress corrosion.

1.5 Principle of Electrochemical Corrosion

Corrosion in aqueous environments occurs by an electrochemical mechanism. The phenomenon involves electrons and ions and can be separated into two partial reactions, anodic (oxidation) and cathodic (reduction) [6]. At anodic sites, an oxidation reaction occurs which is the loss of electrons. For this reaction to take place, a simultaneous reduction process – a net gain of electrons – will occur at cathodic sites [7, 8]. The anodic reaction of the metal is of the form

$$M \rightarrow M^{n+} + n^{e} \qquad (1.1)$$

Depending on the corroded metals, **examples of some anodic reaction are:**

$Zn \rightarrow$	$Zn^{2+} + 2^{e-}$	Zinc corrosion	(1.2)
$Fe \rightarrow$	$Fe^{2+} + 2^{e-}$	Iron corrosion	(1.3)
$Al \rightarrow$	$Al^{3+} + 3^{e-}$	Aluminum corrosion	(1.4)
$Fe^{2+} \rightarrow$	$Fe^{3+} + e^{-}$	Ferrous ionoxidation	(1.5)
$H_2 \rightarrow$	$2H^{+} + 2^{e-}$	Hydrogen oxidation	(1.6)
$2H_2O \rightarrow$	$O^2 + 4H^{+} + 4e^{-}$	Oxygen evolution	(1.7)

Cathodic reaction of the metal is of the form:

$$X^{x+} + x^{e-} \rightarrow X \qquad (1.8)$$

The reduction of dissolved oxygen and release of hydrogen gas by the reduction of

hydrogen ions are the most common reactions during aqueous corrosion of metals [7]. However, there are other cathodic reactions encountered during the corrosion process**.**

Examples of these are:

$$O_2 + 2H_2O + 4e \rightarrow 4OH \quad \text{Oxygen reduction (neutral solution)} \qquad (1.9)$$

$$2H^+ + 2e \rightarrow H_2 \quad \text{Hydrogen evolution (in acid solution)} \qquad (1.10)$$

$$Cu^{2+} + 2e \rightarrow Cu \quad \text{Copper plating (metal deposition)} \qquad (1.11)$$

$$Fe^{3+} + e \rightarrow Fe^{2+} \quad \text{Ferric ion reduction} \qquad (1.12)$$

The two reactions, anodic and cathodic, are complementary events and must proceed at the same rate. Anodic and cathodic sites can form on the surface of the metal for many reasons: composition or grain size differences, discontinuities on the surface, impurities or inclusions in the metal, local differences in the environment (e.g., temperature, oxygen, or salt concentration), localized stresses. The basic corrosion process is shown in Figure 1.16. For electrochemical corrosion to take place, there are four fundamental requirements [9]: An anode, a cathode, a conducting environment for ionic movement (electrolyte), and an electrical connection between the anode and cathode for the flow of (electron) current. If any of these elements is missing or disabled, electrochemical corrosion cannot occur.

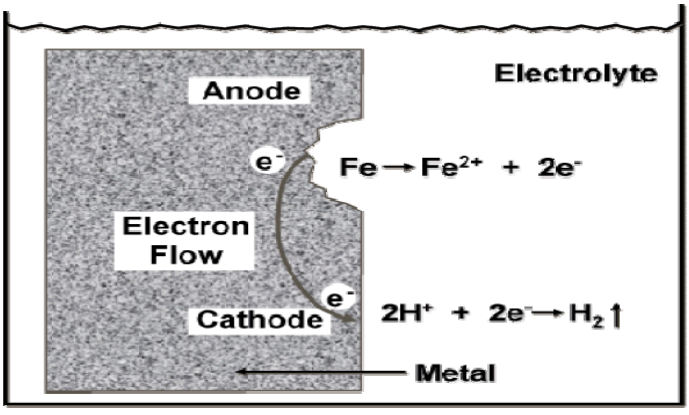

Figure 1.4 Example of basic corrosion process.[1]

1.6 Corrosion Thermodynamics and Kinetics

When considering a metal in a specific environment, a number of questions need to be addressed, including: will the metal corrode in this environment, and if yes, how fast will it corrode? These questions can be answered by studying the thermodynamics and kinetics of corrosion.

1.6.1 Thermodynamics of Electrochemical Corrosion

Thermodynamics gives an understanding of the energy changes involved in the electrochemical reactions of corrosion. These energy changes provide the driving force and control the direction for a chemical reaction. Therefore, thermodynamics shows how conditions may be adjusted to make the corrosion impossible; when corrosion is possible, thermodynamics cannot predict the rate; corrosion may range from fast to very slow process [3].

A metal will exhibit a potential with respect to its environment. This potential is dependent on the ionic strength and composition of the electrolyte, the temperature, the metal or the alloy itself, and other subsidiary factors. The potential of a galvanic cell is the sum of the potentials of the anodic and cathodic half cells in the environment surrounding it. From thermodynamic considerations, the potential of an electrochemical reaction can be related to the change in Gibbs free energy , ΔG = G (products) – G (reactants), as shown in the equation below [5]:

$$\Delta G = nFE \qquad (1.1)$$

where, n is the number of electrons participating in the reaction, F is Faraday's constant (96,500 Coulomb/mole), and E is the electrode potential. The potential of the Galvanic cell will depend on the concentrations of the reactants and products of the

respective partial reactions, and on the pH of the aqueous solutions in contact with the metal. Corrosion will not occur unless the spontaneous direction of the reaction (that is, $\Delta G < 0$) indicates metal oxidation. A negative free energy change (ΔG) indicates that the stability of the products is greater than that of the reactants. The change in electrode potential as a function of concentration is given by the Nernst equation [3, 5]:

$$E = E^{o} + 2.3(RT / n F) \quad \log (ox)^{x} / (red) \qquad (1.2)$$

where E^{o} is the standard electrode potential, (ox) is the activity of an oxidized species, (red) is the activity of the reduced species, and x and r are stoichiometric coefficients involved in the respective half cell reactions. The application of thermodynamics to corrosion phenomena has been generalized by the use of potential-pH plots (Pourbaix diagrams). Such diagrams are constructed from calculations based on the Nernst equation, above, and the solubility data for various metal compounds. From these diagrams, it is possible to differentiate regions of potential as a function of pH in which metal is either immune (no corrosion) or will be passivated by a thin film [10, 11]. Example of such diagrams is shown in Figure 1.5 which represents iron in an aqueous solution. The diagram gives regions of existence: iron is inert and stable (region A), actively dissolve (region B) or the oxide layer can form (region C).

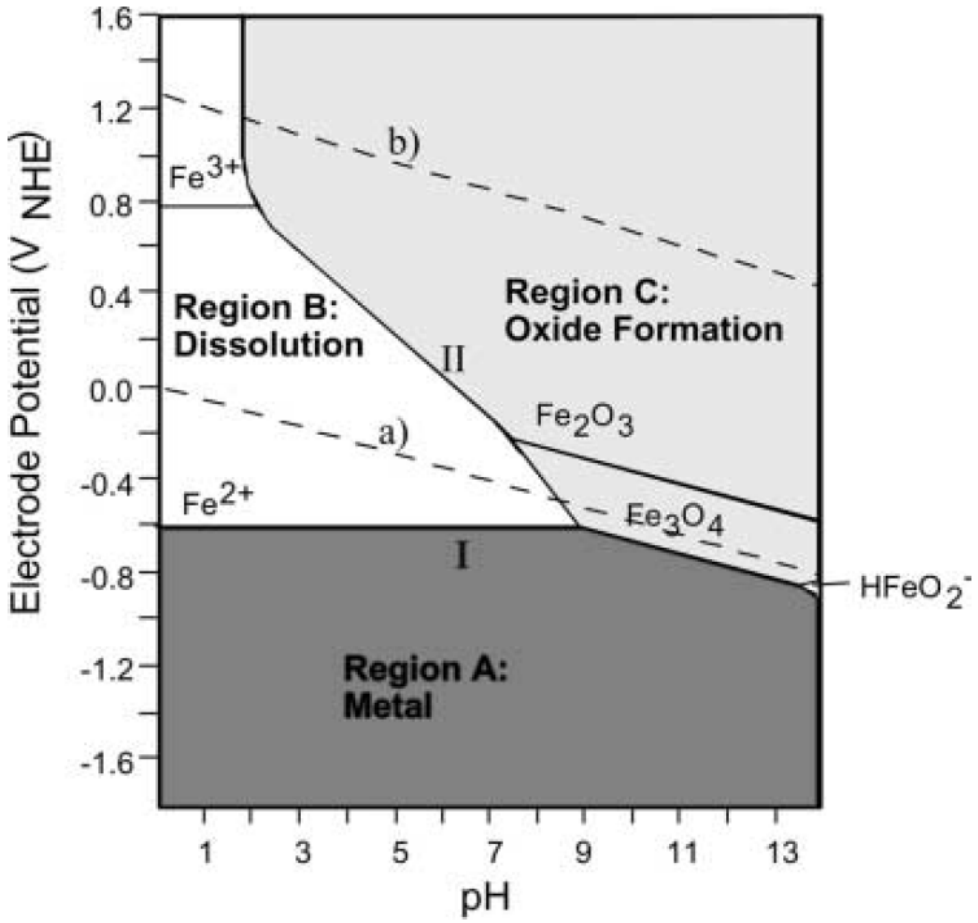

Figure 1.5 Simplified E/pH diagram (Pourbaix diagram) for iron-water system at 25°C. The potentials are given vs. normal hydrogen electrode (NHE) [2].

1.6.2 Kinetics of Electrochemical Corrosion

Corroding systems are not in equilibrium; the oxidation and reduction reactions in the corroding metal each occur at a potential displaced from its equilibrium value [12]. Thus, kinetic studies of the processes are necessary. A system is out of equilibrium when the potential is displaced from the equilibrium potential by the application of an external voltage or by the spontaneous production of a voltage away from equilibrium. This deviation in potential is defined as polarization (η) [5].

$$\eta = | E - E_{eq}| \qquad (1.3)$$

where, E_{eq} is the equilibrium potential.

There are mainly three types of polarization in any electrochemical cell: (1) Activation polarization, (2) Concentration polarization, and/or (3) Resistance polarization [13, 14].

1.6.2.1 Activation Polarization. A system is referred to be as activation controlled when the rate of the electrochemical process is controlled by the charge transfer across the metal solution interface. For anodic and cathodic polarization on activation controlled system, the activation polarization for the anodic reaction (ηa (A)) can be expressed as:

$$\eta_a (A) = \beta_A \log i_A / i_o \qquad (1.4)$$

where,

i_A = Anodic current density (A/cm2)

i_o = Exchange current density (A/cm2)

β_A = Tafel slope for the anodic reaction

An identical expression can be written for the cathodic reaction.

1.6.2.2 Concentration Polarization. When the transport of ions or molecules to or away from the metal surface determines the rate of the electrochemical process, the system is said to be under concentration polarization (η_c), or transport control. For example, when the cathodic process in corroded system depends on the reduction of dissolved oxygen, the diffusion of oxygen to the metal surface will often limit the rate of corrosion.

The concentration polarization can be expressed as:

$$\eta_c = 2.3RT/nF * \log (1\ i/i_{lim}) \quad (1.5)$$

where, i_{lim} = Limiting current density

1.6.2.3 Resistance Polarization. Resistance polarization (η_r) is a consequence of the Ohmic resistance in the system. It is the sum of the resistance in the electrolyte ($R_{sol.}$) and the resistance of any apparent scale on the surface (R_{scale}):

$$\eta_r = i \Sigma R \quad (1.6)$$

where, $\Sigma R = R_{sol.} + R_{scale}$

High-resistivity solutions and insulating films deposited at either the cathode or anode restrict or completely block contact between the metal and the solution and will promote a high-resistance polarization. The total polarization (η_{total}) across an electrochemical cell is the sum of the above individual polarizations:

$$\eta_{total} = \eta_a + \eta_c + \eta_r \quad (1.7)$$

1.6.2.4 Rate of Corrosion and Faraday's law. The rate of electron flow to or from a reacting interface is a measurement of the reaction rate [3]. The electron flow is conveniently measured as the magnitude of a current; therefore, the current can be used to determine the reaction rate of the process through Faraday's law. If we consider the anodic metal oxidation reaction in equation 1.1 ($M \rightarrow M^{n+} + n^{e-}$)

$$Q = nFm/M \quad (1.8)$$

where,

Q = the electrical charge (coulomb)

F= Faraday's constant (96500 coulombs/mole)

n= Number of electrons transferred

m = Mass of metal oxidized (g)

M= Atomic weight of metal (g/mole)

Also, this can be expressed in terms of the rate of the reaction:

$$I = nFK/M \quad (1.9)$$

where,

I = Corrosion current (A)

K = Rate of corrosion (g/s)

1.6.2.5 Mixed Potential Theory. Kinetic information of corroded surface is usually presented in graphical forms called Evans or polarization diagrams that represent the relation between the electrode potential and current density [15]. These diagrams are developed based on the principles of mixed potential theory. The theory of mixed potential was developed by Wagner and Traud in 1938 [16]. The theory proposes that the electron released during oxidation process (anodic) is consumed by a corresponding reduction process (cathodic). Therefore, the total rate of the oxidation reaction will equal the total rate of the reduction [17]. The cause of the entire process

is based on two factors. The oxidation and reduction reactions each have a unique half-cell electrode potential and exchange current density (I_o). The second factor is that, the half-cell potentials cannot coexist separately in the same conductive environment. There must be a polarization in potential to a common intermediate value referred to as the mixed potential.

Figure 1.6 illustrates the two half-cell reactions occurring when zinc is placed in an acid solution. The two half-cell potentials are plotted with respect to the corresponding current density of the half-cell reactions (I_o). The corrosion potential (E_{corr}) and the corrosion current density (i_{corr}) values are located where hydrogen reduction line and zinc oxidation line converge.

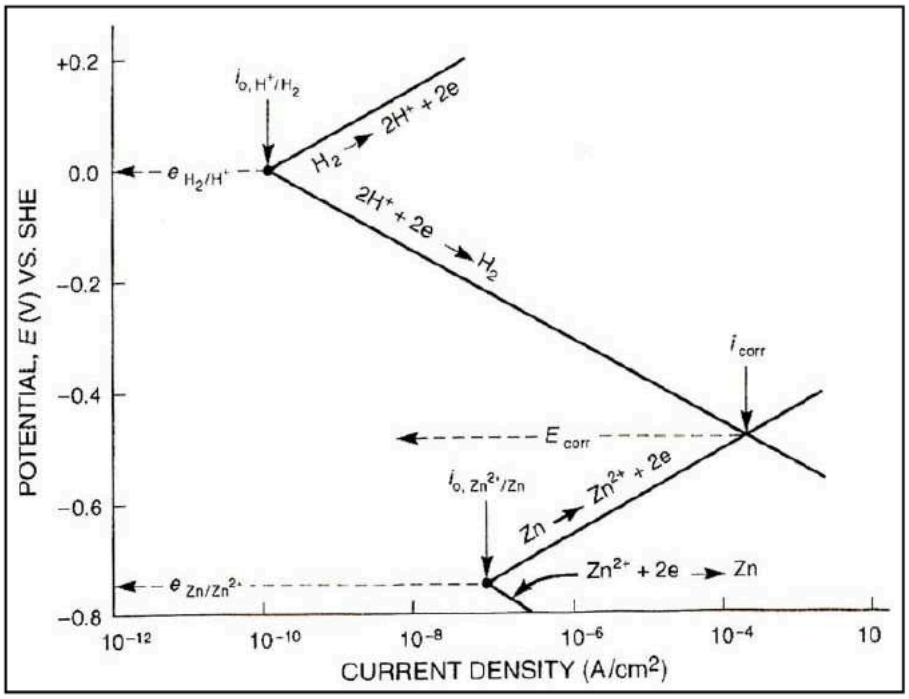

Figure 1.6 Schematic Evans diagram for zinc in acid solution shows the corrosion potential (E_{corr}) and corrosion current density (i_{corr}).[3]

1.7 Passivity to Corrosion

1.7.1 Introduction

All metals and alloys (commonly, gold is exception) have a thin protective corrosion product film present on their surface due to the reaction with the environment [18]. Some of these films are passive and on some metals and alloys have certain characteristics that enable them to provide more corrosion resistant metal surfaces. These protective surface films are responsible for the phenomenon of passivity [4, 19] which is the reason a metal does not corrode when it would be expected to corrode.

1.7.2 Definition of passivity

Two generally accepted definitions of the passivity have been reported [18, 20]

- A metal is passive if, on increasing its potential to more positive values, the rate of dissolution decreases (low corrosion rate, noble potentials)

- A metal is passive if it substantially resists corrosion in an environment where there is a large thermodynamic tendency to react (low corrosion rate, active potential).

Also, an additional definition has been provided by NACE/ASTM [21]; passive is the state of a metal surface characterized by low corrosion rates in potential region that is strongly oxidizing for the metal.

1.7.3 Active-passive Behavior

During anodic polarization, metals and alloys with a passivated surface will typically display a polarization curve of the shape shown in Figure 1.7. At a relatively low potential within the active region, when the potential value is plotted against log current density, the behavior is linear for normal metals. With the beginning of the formation of a passive layer, the measured current begins to decrease. The turning point on the curve, marking the beginning of this decrease, is known as the active-passive transition and the corresponding value of the applied potential is the primary passivation potential (E_{pp}). Also, in Figure 1.7, the current density decreases rapidly to a very low value called the passive current density (i_p) due to the formation of quite a passive layer.

With the presence of a stable uniform non-conducting layer (passive oxide) on the surface of the metal, the system enters a region where further increase in potential causes no noticeable increase in current density; this is the passive region. This current density remains relatively independent of the potential because it is controlled by the rate of dissolution of the passive film. In environments without aggressive species such as Cl-, with further increase in potential to more positive value, most of the metal passive oxides can be further oxidized to a more soluble state. Therefore, the effectiveness of the passivation layer is reduced and/or removed; so corrosion can re-occur. This region where the current density begins to increase again is called the transpassive region [22, 23]. For example, in the case of the protective layer of stainless steel containing chromium as Cr (III), when the potential is raised to the transpassive region, Cr (III) is oxidized to Cr (VI). However, for metals such as aluminum and tantalum, that can form electronically insulating passive oxide films, the passive region extends to very positive potentials and neither transpassive metal

dissolution nor oxygen evolution will occur [24]. Hoar [25] stated that four conditions, are usually, but not always, required for the passivity breakdown that initiates localized attack:

1) Critical potential: a certain critical potential must be exceeded.

2) Damaging species: such as chloride or higher atomic weight halides, are needed in the environment to initiate breakdown and propagate localized corrosion processes like pitting.

3) Induction time: an induction time exists, which starts with the initiation of the breakdown process (introduction of breakdown conditions) and ends when the localized corrosion density begins to rise.

4) Local sites: the presence of highly localized sites such as inclusions and second-phase precipitates.

Irrespective of the causes of the breakdown of the passive film, the result will be a fresh metal surface exposed to the environment leading to localized attack such as pitting, crevice, inter-granular corrosion or stress corrosion cracking [19, 26]. Further details will be discussed in the later section on pitting corrosion.

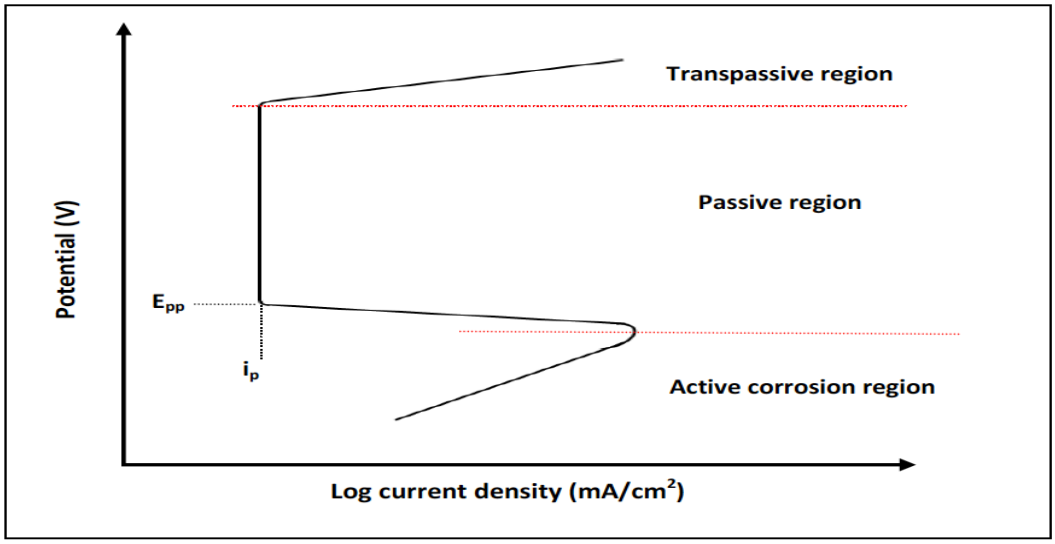

Figure 1.7 Schematic diagram showing current density vs. potential curve (anodic polarization curve) for metal with active, passive and transpassive potential range.

CHAPTER 2

PITTING AND CREVICE CORROSION OF STAINLESS STEEL

2.1 Introduction

Crevice and pitting corrosion are forms of localized corrosion, which means that the corrosion occurs in a limited area on the blades. The corrosion rate is often high and is generally higher than that for uniform corrosion, due to a large cathode/anode ratio. A severe attack is therefore usually observed, and the pit or crevice may cut through the pipe wall thickness to form a hole.

2.2 Pitting Corrosion

Pitting corrosion is defined as "localized corrosion of a metal surface, confined to a point or small area, that takes the form of cavities"[17]. Pitting is a deleterious form of localized corrosion and it occurs mainly on metal surfaces which owe their corrosion resistance to passivity. The major consequence of pitting is the breakdown of passivity; i.e. pitting, in general, occurs when there is breakdown of surface films when exposed to pitting environment. Pitting corrosion is complicated in nature because "oxide films formed on different metals vary one from another in electronic conduction, porosity, thickness, and state of hydration"[18].

Many engineering alloys, such as stainless steels and aluminum alloys, are useful only because of passive films, which are thin (nanometer-scale) oxide layers that form naturally on the metal surface and greatly reduce the rate of corrosion of the alloys. Such passive films, however, are often susceptible to localized breakdown,

resulting in accelerated dissolution of the underlying metal. If the attack initiates on an open surface, it is called pitting corrosion; at an occluded site, it is called crevice corrosion. These closely related forms of localized corrosion can lead to accelerated failure of structural components by perforation or by acting as an initiation site for cracking. Fig. (2.1) shows an example of deep pits on a metal surface[19].

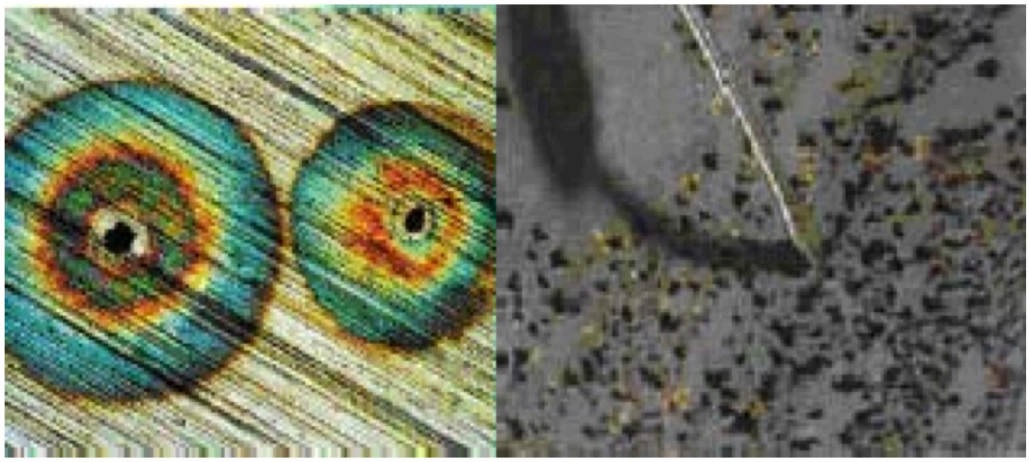

Figure 2.1 Deep pits in a metal. [19,20]

It should be noted that, whereas localized dissolution following breakdown of an otherwise protective passive film is the most common and technologically important type of pitting corrosion, pits can form under other conditions as well. For instance, pitting can occur during active dissolution if certain regions of the sample are more susceptible and dissolve faster than the rest of the surface.

Pitting corrosion is influenced by many different parameters, including the environment, metal composition, potential, temperature, and surface condition. Important environmental parameters include aggressive ion concentration, pH, and inhibitor concentration. Other phenomenological aspects of localized corrosion include the stochastic nature of the processes and the stages of localized attack,

including passive film breakdown, metastable attack, stable growth, and perhaps eventual arrest [21,22].

2.2.1 Principle of Pitting Corrosion

Pitting corrosion is an electrochemical oxidation-reduction process, which occurs within localized depths on the surface of metals coated with a passive film.

Anodic reactions inside the pit:

$$Fe = Fe^{2+} + 2^{e-} \text{ (dissolution of iron)} \quad (2.1)$$

The electrons given up by the anode flow to the cathode where they are discharged in the cathodic reaction:

$$1/2O_2 + H_2O + 2e^- = 2(OH) \quad (2.2)$$

As a result of these reactions, the electrolyte enclosed in the pit gains positive electrical charge in contrast to the electrolyte surrounding the pit, which becomes negatively charged.

The positively charged pit attracts negative ions of chlorine Cl^-, increasing acidity of the electrolyte according to the reaction:

$$FeCl_2 + 2H_2O = Fe(OH)_2 + 2HCl \quad (2.3)$$

pH of the electrolyte inside the pit decreases from 6 to 2-3, which causes further acceleration of the corrosion process. Large ratio between the anode and cathode areas

favors increase of the corrosion rate. Corrosion products ($Fe(OH)_3$) form around the pit resulting in further separation of its electrolyte.

Pitting corrosion is treated as a time-dependent stochastic damage process characterized by an exponential or logarithmic pit growth. Data from propulsion shaft of high-speed craft is used to simulate the sample functions of pit growth on metal surfaces. Perforation occurs when the deepest pit extends through the thickness of the propulsion shaft. Because the growth of the deepest pit is of stochastic nature, the time-to-perforation is modeled as a random variable that can be characterized by a suitable reliability model. It is assumed that corrosion will occur at multiple pits on both sides of the rivet depths and will cause multiple fatigue cracks. Therefore, system failure could occur due to the linkage between any two neighboring cracks.

2.2.2 Pit Initiation

An initial pit may form on the surface covered by a passive oxide film as a result of the following:

a. Mechanical damage of the passive film is caused by scratches. Anodic reaction starts on the metal surface exposed to the electrolyte. The passivity surrounding the surface acts as the cathode.

b. Particles of a second phase emerging on the metal surface. These particles precipitating along the grain boundaries may function as local anodes causing localized galvanic corrosion and formation of initial pits.

c. Localized stresses in the form of dislocations emerging on the surface may become anodes and initiate pits.

d. Non-homogeneous environment may dissolve the passive film at certain locations where initial pits form.

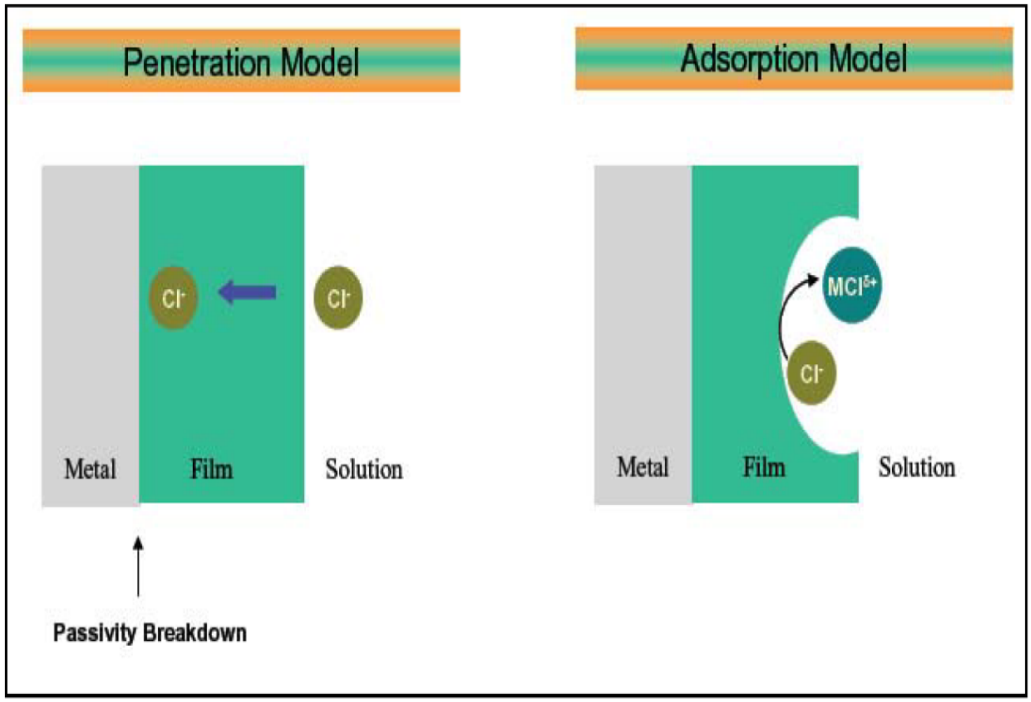

Figure 2.2 Models on passivity breakdown by Cl^-. [20]

2.2.3 Pitting Growth

In the presence of chlorine ions, pits are growing by autocatalytic mechanism. Pitting corrosion of stainless steel is illustrated in Figure 2.3. The actual pitting corrosion phenomenon is shown on propeller shaft of high speed craft, and the pit depth is measured with dial gauge as shown in Figure 2.4

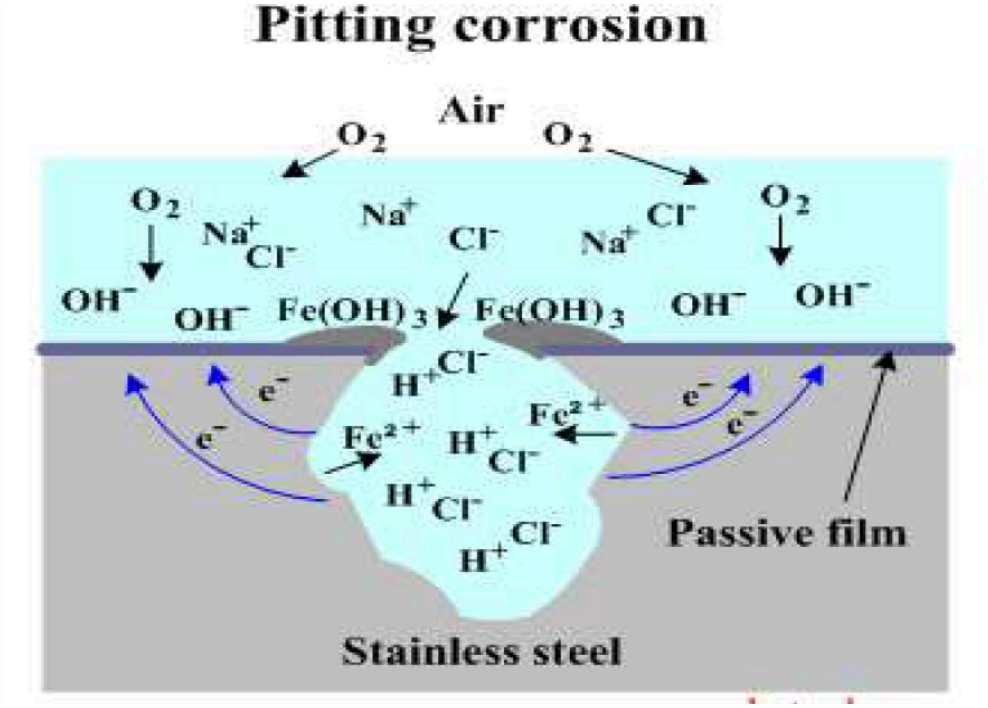

Figure 2.3 Pitting corrosion deep growth. [19,20]

Figure 2.4 Measuring depth of pitting. [19,20]

2.2.4 Metastable Pitting

Metastable pits are pits that initiate and grow for a limited period before repassivating (Figure 2.5). Large pits can stop growing for a variety of reasons, but metastable pits are typically considered to be those of micron size, at most, with a lifetime on the order of seconds or less. Metastable pits are important to understand because, under certain conditions, they continue to grow to form large pits. Metastable pits can form at potentials far below the pitting potential (which is associated with the initiation of stable pits) and during the induction time, before the onset of stable pitting at potentials above the pitting potential. These events are characterized by potential transients in the active direction at open circuit or under an applied anodic current, or anodic current transients under an applied anodic potential. Such transients have been reported in stainless steels [27,28-33] and aluminum [34,35] for many years. Individual metastable pit current transients can be analyzed for pit current density, and stochastic approaches can be applied to groups of metastable pits.

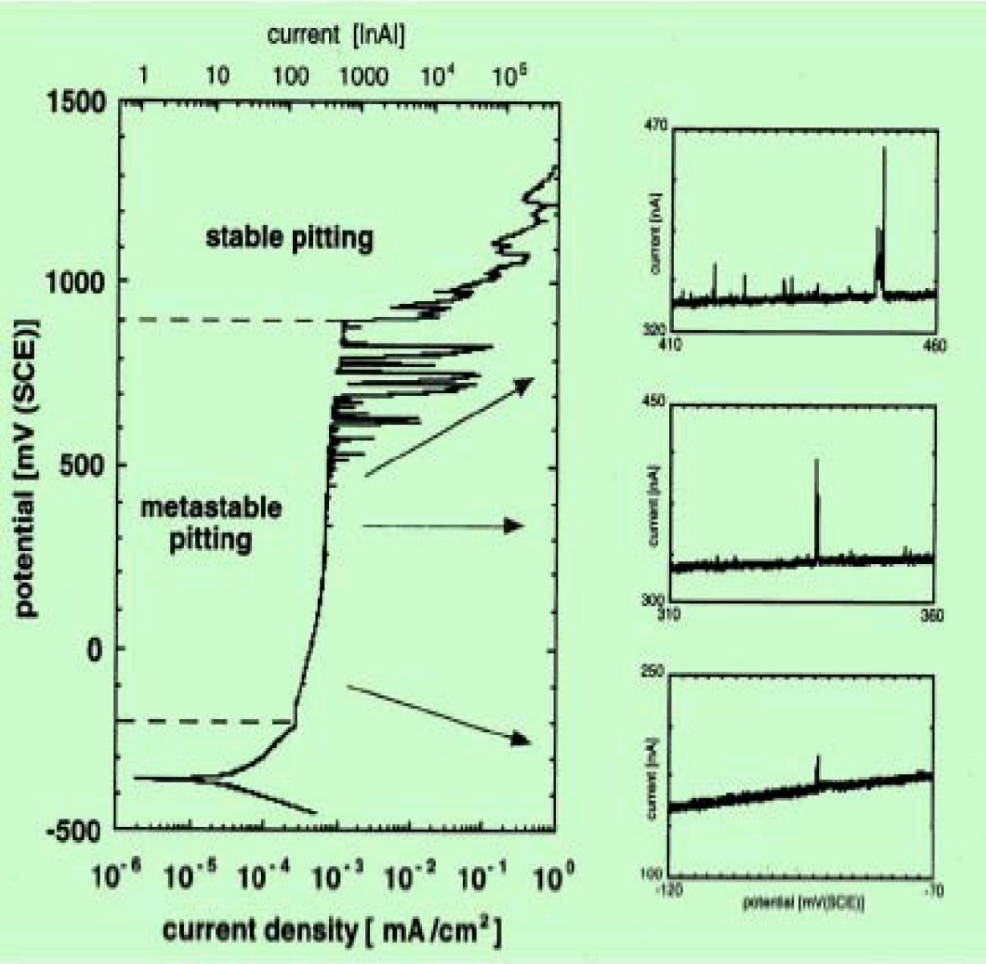

Figure 2.5 Typical potential current curve of stainless steel in Cl^- showing the different stages of localized corrosion. [20]

2.2.5 Transition from Pitting to Fatigue Crack Nucleation

The third stage is the transition from pit growth to fatigue crack nucleation, where mechanical effects such as the stress intensity factor come into play. The nucleation of the corrosion crack is essentially a competition between the processes of pit growth and crack growth. Two criteria are used to describe the transition process.

2.2.6 Short Crack Growth

The short crack growth stage involves chemical and microstructural factors and their interactions. Although much research has been done in this area, it has been difficult to derive an explicit formula for short crack growth, especially in corrosive environment. For computational simplicity, a probabilistic power law model is presented here to describe the relationship between the stress intensity factor and the growth rate. In this method, an empirically based probabilistic relationship is used to model the corrosion short crack growth.

2.2.7 Crack Coalescence

The linkage between any two neighboring cracks is considered to be the failure criterion at this stage.

2.3 Pitting Corrosion Behavior

Corrosion of metals and alloys by pitting constitutes one of the very major failure mechanisms. Pits cause failure through perforation and engender stress corrosion cracks. Pitting is a failure mode common to many metals. It is generally associated with particular anions in solution, notably the chlorine ion. The origin of pitting is small. Pits are nucleated at the microscopic scale and below. Detection of the earliest stages of pitting requires techniques that measure tiny events [24,25].

Stainless steels are used in countless diverse applications for their corrosion resistance. Although stainless steels have extremely good general resistance, stainless steels are nevertheless susceptible to pitting corrosion. This localized dissolution of an

oxide-covered metal in specific aggressive environments is one of the most common and catastrophic causes of failure of metallic structures. The pitting process has been described as random, sporadic and stochastic and the prediction of the time and location of events remains extremely difficult. Many contested models of pitting corrosion exist, but one undisputed aspect is that manganese sulphide inclusions play a critical role.

The chromium in steel combines with oxygen in the atmosphere to form a thin, invisible layer of chrome-containing oxide, called the passive film. The sizes of chromium atoms and their oxides are similar; so they pack neatly together on the surface of the metal, forming a stable layer only a few atoms thick. If the metal is cut or scratched and the passive film is disrupted, more oxide will quickly form and recover the exposed surface, protecting it from oxidative corrosion.

The passive film requires oxygen to self-repair; so stainless steels have poor corrosion resistance in low-oxygen and poor circulation environments. In seawater, chlorides from the salt will attack and destroy the passive film more quickly than it can be repaired in a low oxygen environment.

Some metals show preferential sites of pit nucleation with metallurgical microstructural and micro compositional features defining the susceptibility. However, this is not the phenomenological origin of pitting per se, since site specificity is characteristic only of some metals. A discussion of mechanisms of nucleation is presented; it is shown that the events are microscopically violent. The ability of a nucleated event to survive a series of stages that it must go through in order to achieve stability is discussed. Nucleated pits that do not propagate must repassivate. However, there are several states of propagation, each with a finite survival probability. Several variables contribute to this survival probability.

2.4 Electron Fractography of Fatigue Fracture with Pitting Corrosion

The evolution of corrosion pits on stainless steel immersed in chloride solution occurs in three distinct stages: nucleation, metastable growth and stable growth. A micro crack generated by pitting corrosion, forms the initial origin for fatigue fracture. But in fact, fatigue failure is not certainly caused at the deepest interior pitting depth. Due to the different shape of interior pitting depths as shown in Figure 2.6, some of them are hard to start or to continue the crack propagation and play a role of crack arrester, as shown in Figure 2.7. If the fracture is caused by the pitting depth as an inclusion, then continuous plastic deformation can be found around the pitting depth[26]. The dimples are generally equalized by overloaded tension, and elongated by shear or tearing, as shown in Figures 2.8 and 2.9.

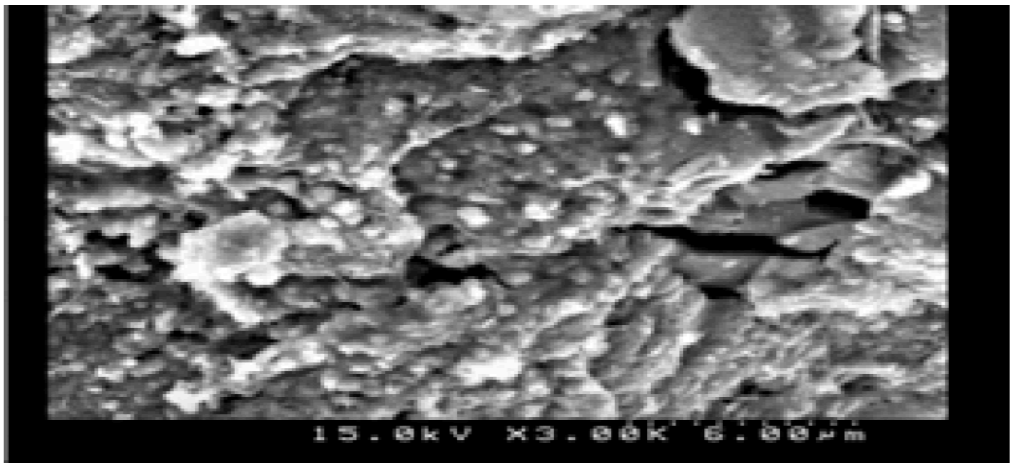

Figure 2.6 Interior pitting depth.

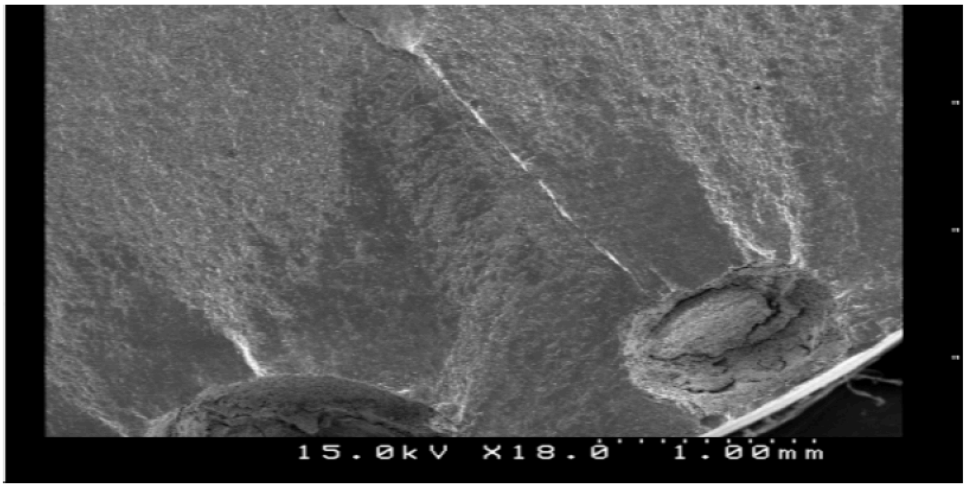

Figure 2.7 Fatigue failure arrester at interior pitting depth.

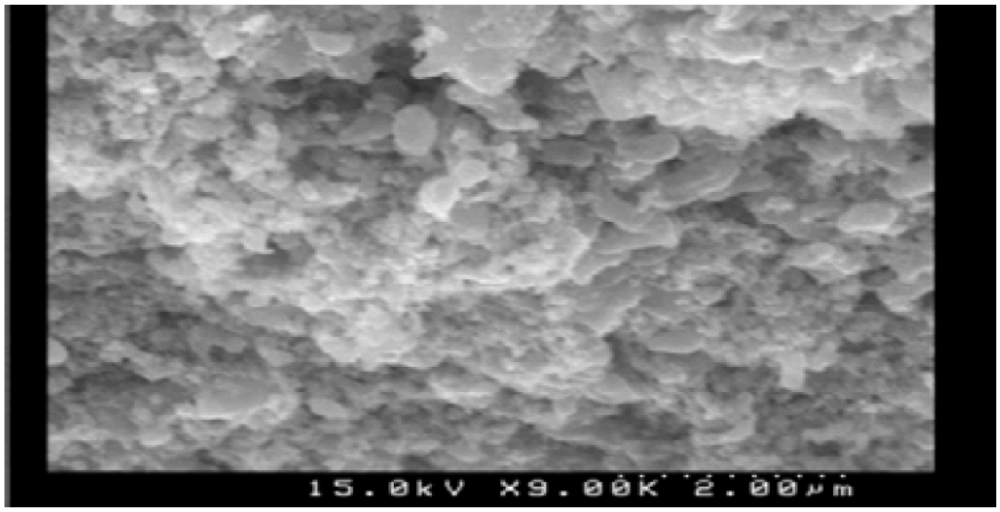

Figure 2.8 Equalized dimples around interior pitting depth.

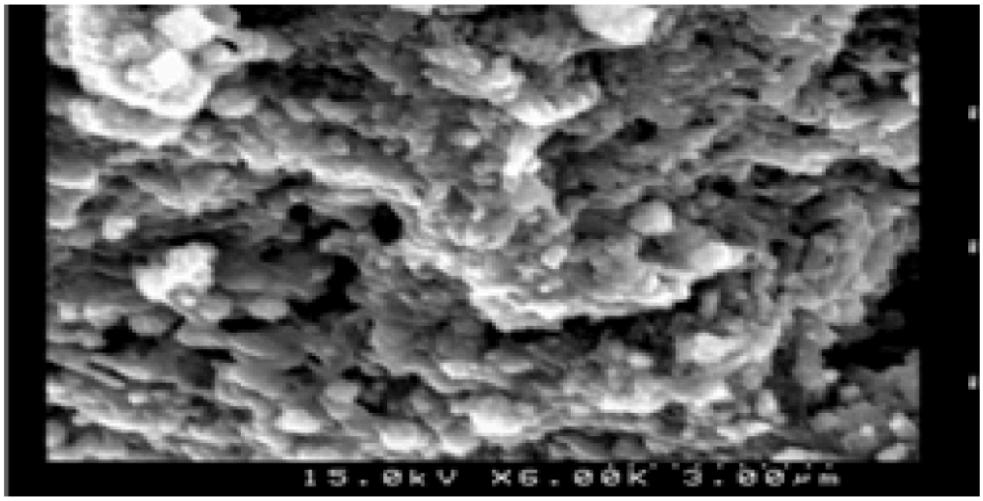

Figure 2.9 Elongated dimples around interior pitting depth.

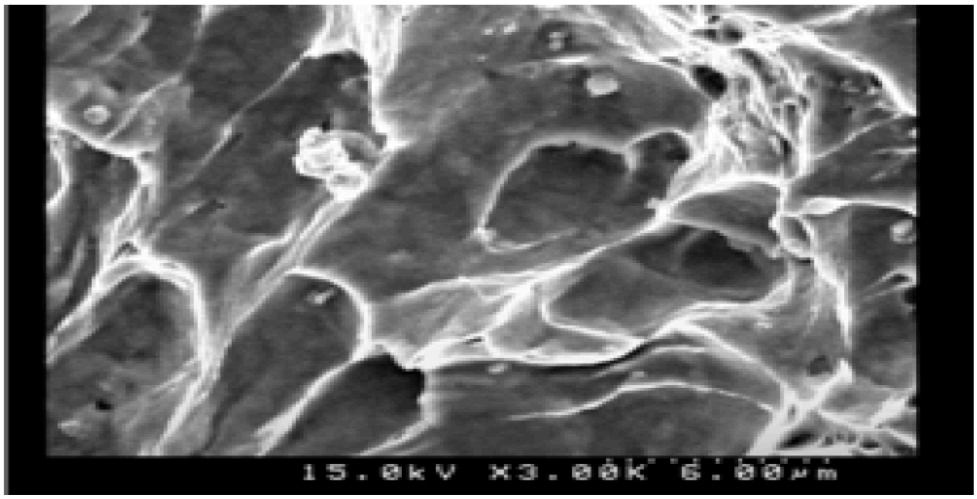

Figure 2.10 Typical cleavage fractures in fracture area (3000 times).

The features of cleavage failure can be seen by flat fractography as shown in Figure 2.10 and Figure 2.11 with 3000 and 1000 times magnification of Scanning Electron Microscopy (SEM) images respectively. Cleavage failure occurs by separation along crystallographic planes. This transgranular fracture is categorized to be the brittle fracture in the fracture area. There are several features that can be identified to be cleavage, namely, herringbone, tongues and river stream. Figure 2.12 and Figure 2.13 show the microscopic fractographics of river stream and tongue patterns, which have been seen in the study. At grain boundaries, the fracture plane or cleavage plane

changes because of the differences in crystallographic orientations. Cleavages are not only associated with transgranular fracture, but also with brittle particles as shown in Figure 2.14 and Figure 2.15 respectively.

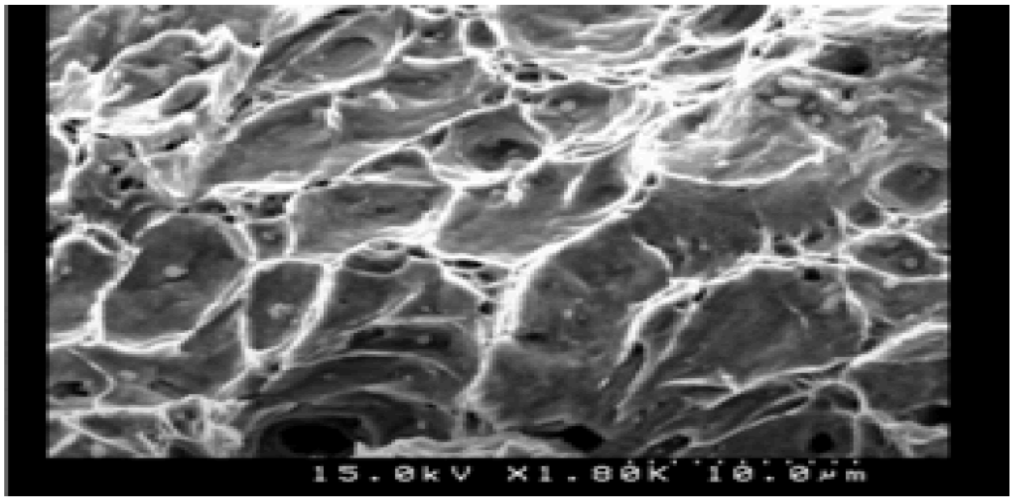

Figure 2.11 Typical cleavage fractures in fracture area (1000 times).

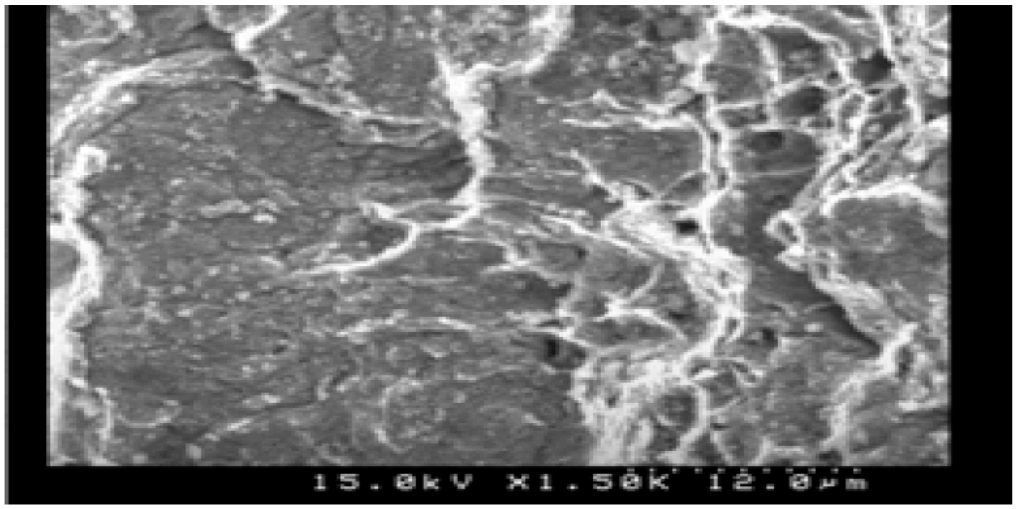

Figure 2.12 River pattern in fatigue propagation area (1500 times).

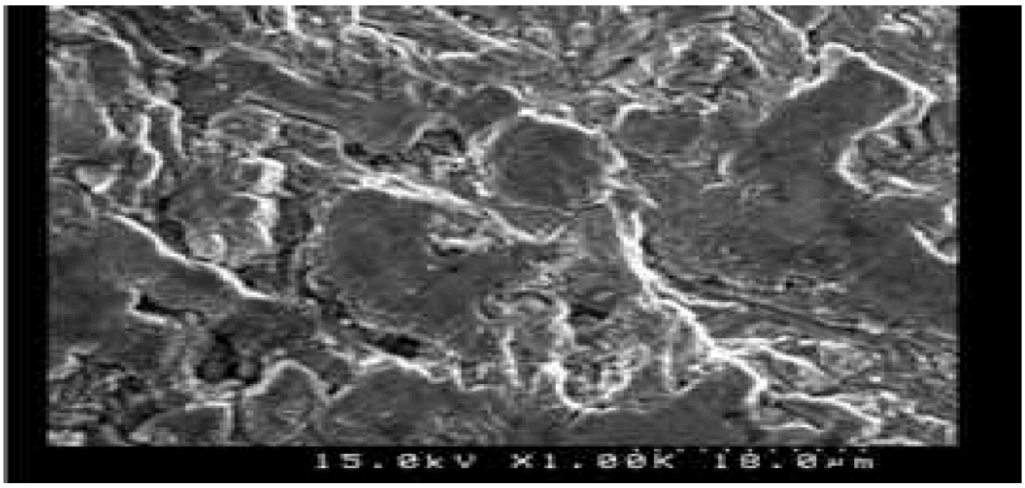

Figure 2.13 Tongue pattern in fatigue propagation area (1000 times).

Some metals can fail in brittle manner, but do not cleave. These fractures are identified as quasi-cleavage. They are similar to cleavage but their features are usually fairly flat and smaller, as shown in Figure 2.16 and Figure 2.17.

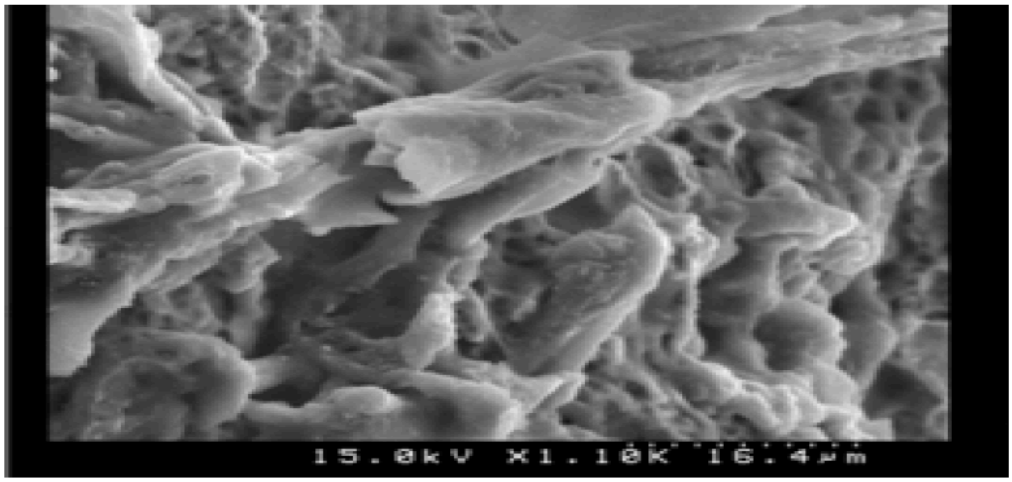

Figure 2.14 Cleavage with transgranular fracture in fatigue propagation area.

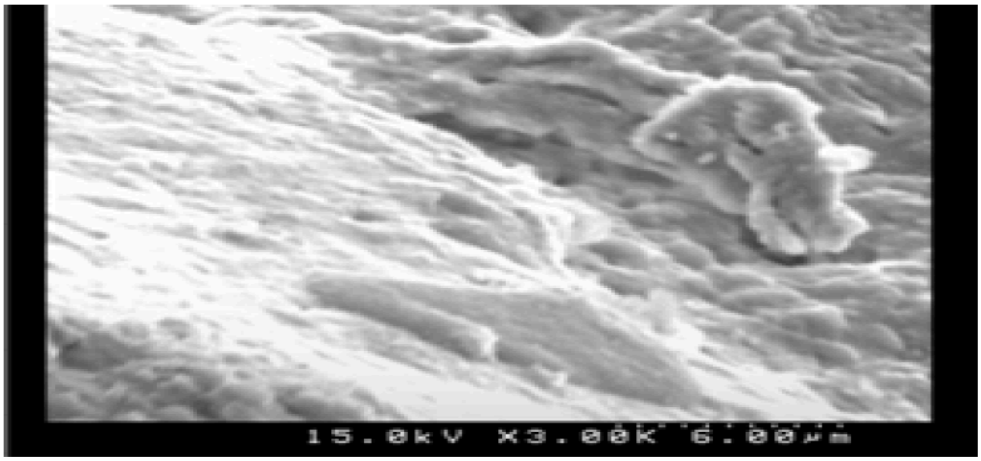

Figure 2.15 Cleavage with brittle particles in fracture area.

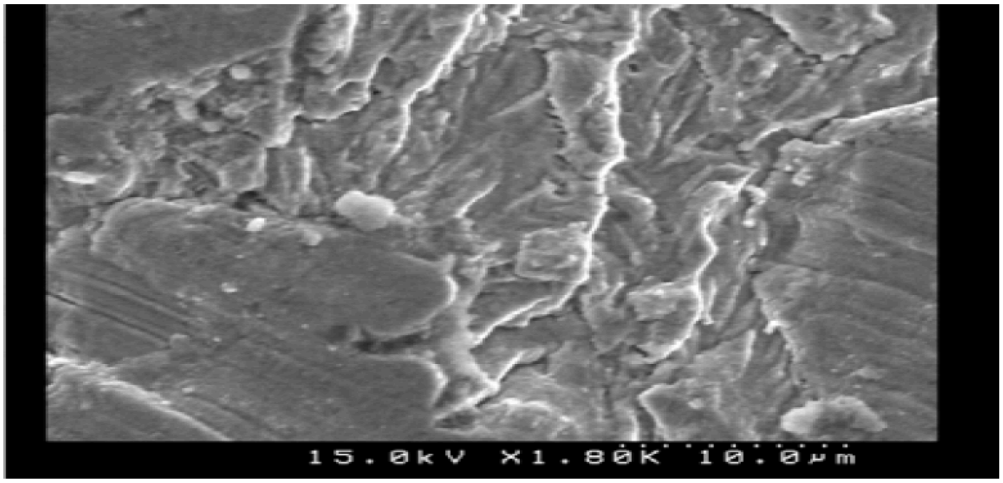

Figure 2.16 Quasi-cleavage in fracture area (I).

Also the intergranular fracture can occur by a number of causes; but it is generally possible to be identified fractographically by the features of grain contours, grain boundaries and triple points. Examples of this kind in intergranular fractures are tree pattern fracture and sub crack caused by the interior pitting depths, as shown in Figure 2.18 and Figure 2.19.

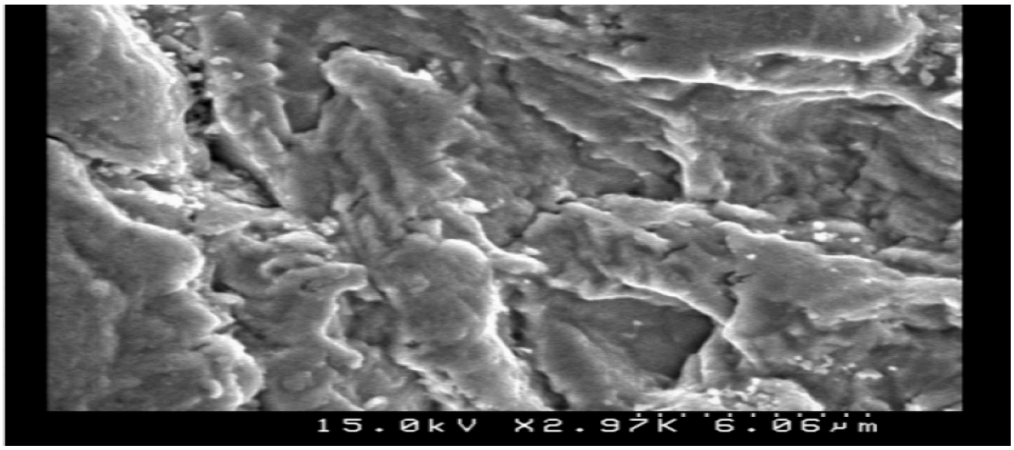

Figure 2.17 Quasi-cleavage in fracture area (II).

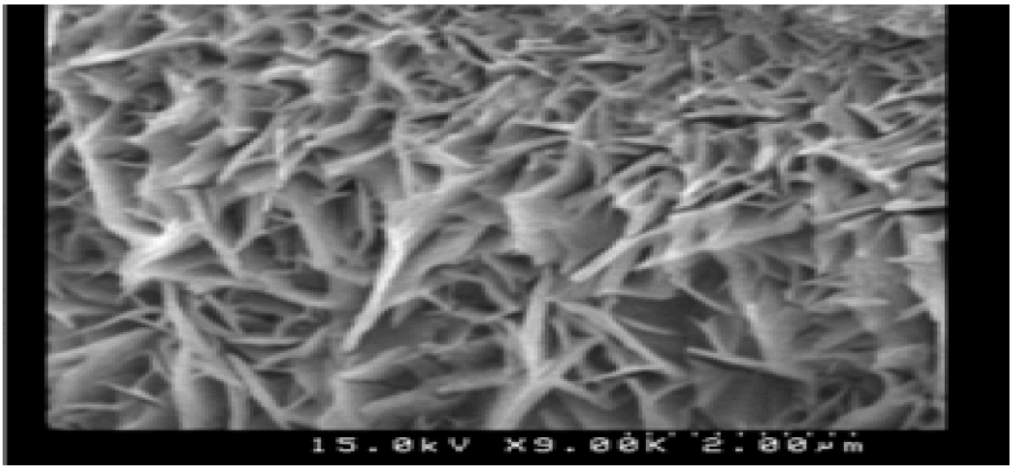

Figure 2.18 Tree pattern fracture caused by interior pitting depth.

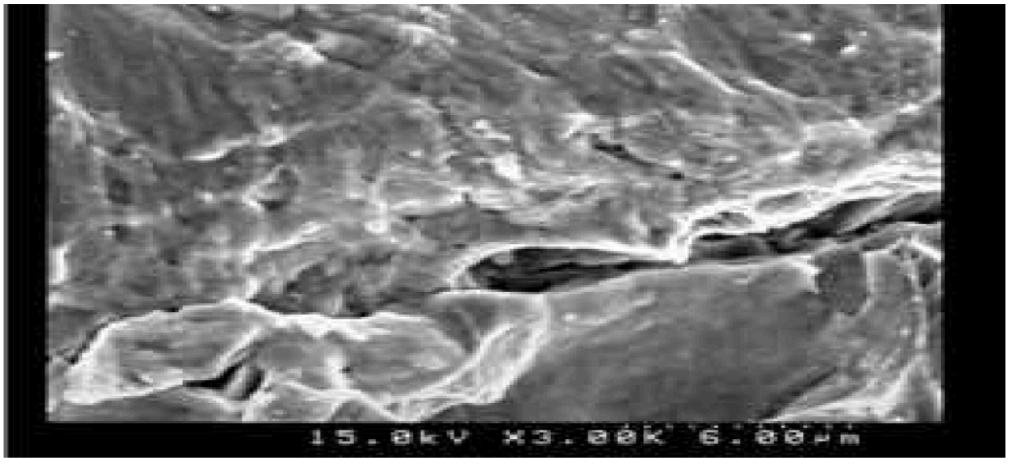

Figure 2.19 Sub-crack caused by interior pitting depth.

2.5 Initial Pitting Depth and Pitting Corrosion Behavior

Pitting corrosion is a localized form of corrosion by which cavities or depths are produced in the material. Pitting is considered to be more dangerous than uniform corrosion damage because it is more difficult to detect, predict and design against. Corrosion products often cover the pits. A small, narrow pit, with minimal overall metal loss, can lead to the failure of an entire engineering system.

2.5.1 Corrosion Pit Shapes

Pitting corrosion forms on passive metals and alloys like stainless steel when the ultra-thin passive film is chemically or mechanically damaged and does not immediately re-passivate. The resulting pits can become wide and shallow or narrow and deep which can rapidly perforate the wall thickness of a metal.

2.5.2 Pitting Shape by ASTM

Pitting corrosion can produce pits with their mouth open or covered with a semi-permeable membrane of corrosion products. Pits can be either hemispherical or cup-shaped. In some cases, they are flat-walled, revealing the crystal structure of the metal, or they may have a completely irregular shape. Pitting corrosion occurs when discrete areas of a material undergo rapid attack while most of the adjacent surface remains virtually unaffected.

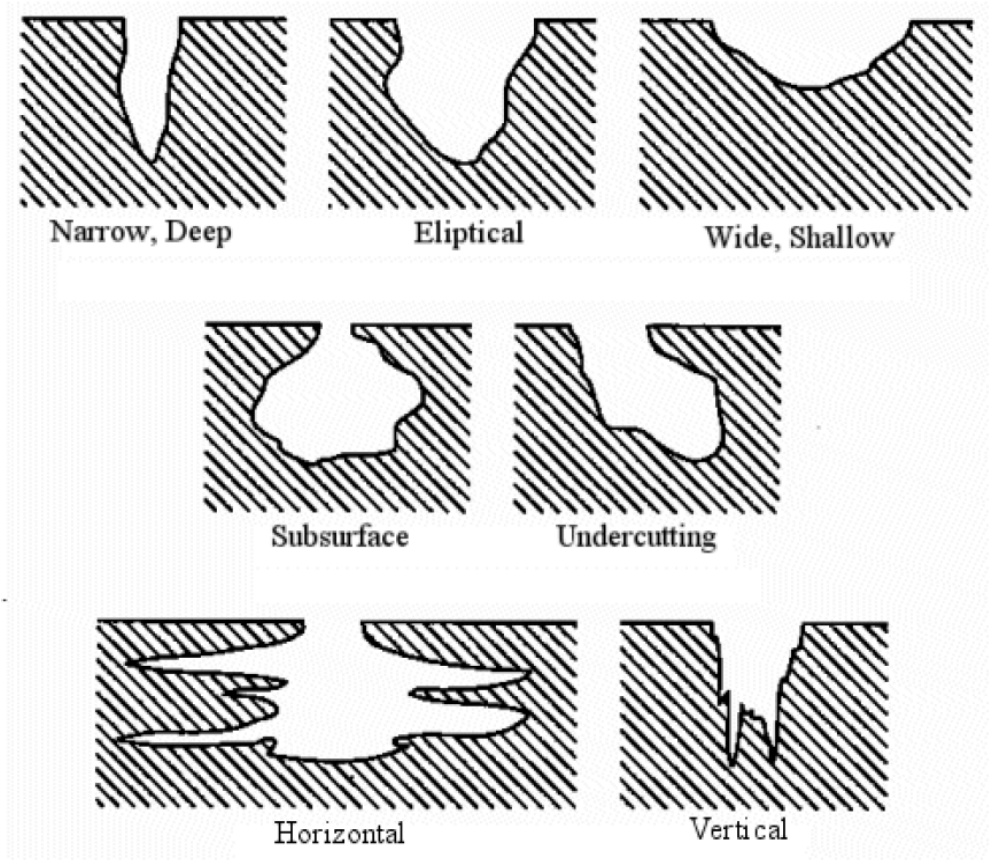

Figure 2.20 ASTM-G46 has a standard visual chart for rating of pitting corrosion.
Source: (http://www.corrosionclinic.com)

2.6 Experiment Pitting Shape

Localized chemical or mechanical damage to the protective oxide film and water chemistry factors which can cause breakdown of a passive film are acidity, low dissolved oxygen concentrations and high concentrations of chloride in seawater. The actual pitting shape was investigated by Scanning Electron Microscopy as shown in Figure 2.21 and Figure 2.22.

Figure 2.21 Pitting depth shape.

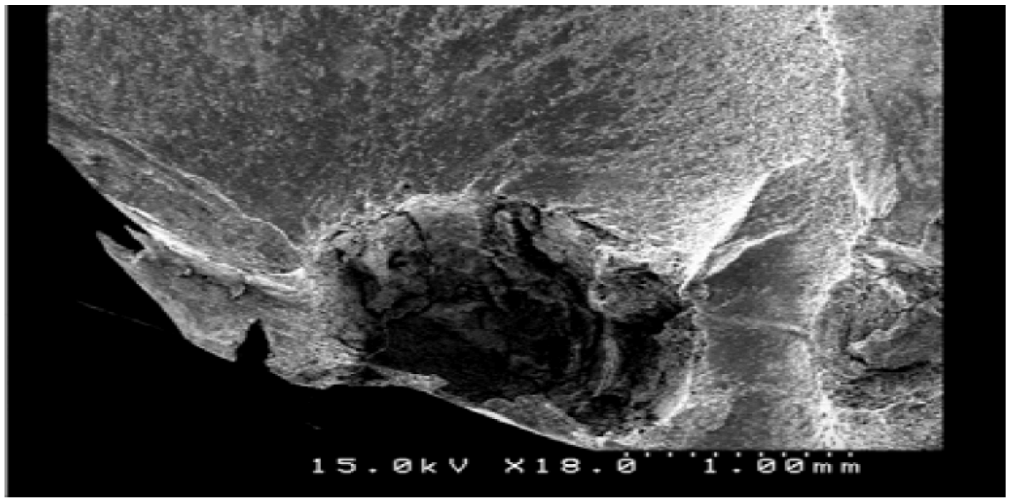

Figure 2.22 Pitting depth shape.

2.7 Pitting Corroding Rate

The grey systems are the systems that lack information, such as architecture, parameters, operation mechanism and system behavior, for example, for estimating the tendency of Typhoon landing in Taiwan [8]. There are a number of factors that affect the pitting corrosion rate of stainless alloys. The grey correlation analysis explains uncertain correlations between one main factor and all other factors in a given system. The grey correlation analysis method is based on the clustering approach in which the time factor is varied during the experiment period [23].

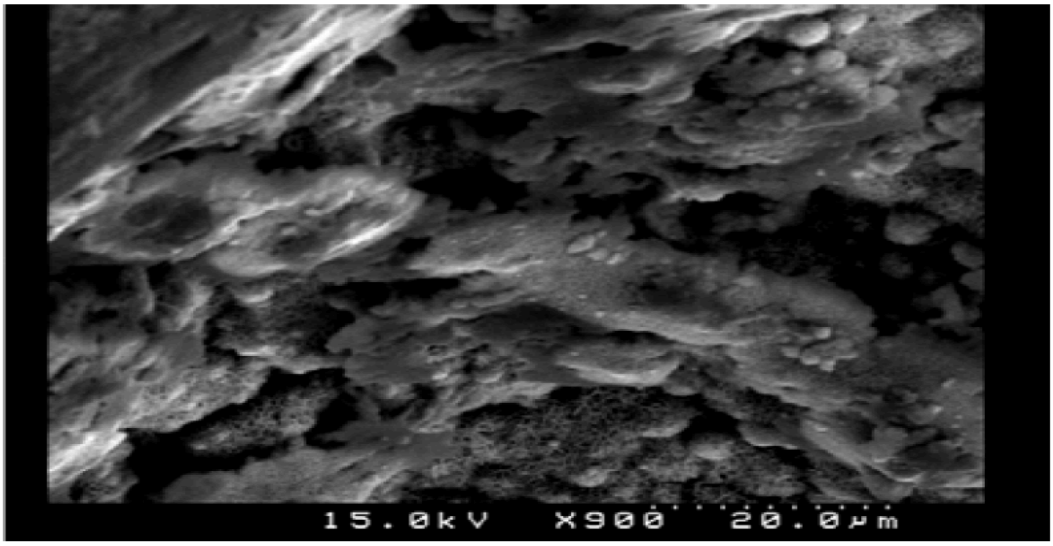

Figure 2.23 Transgranular fracture at interior pitting depth.

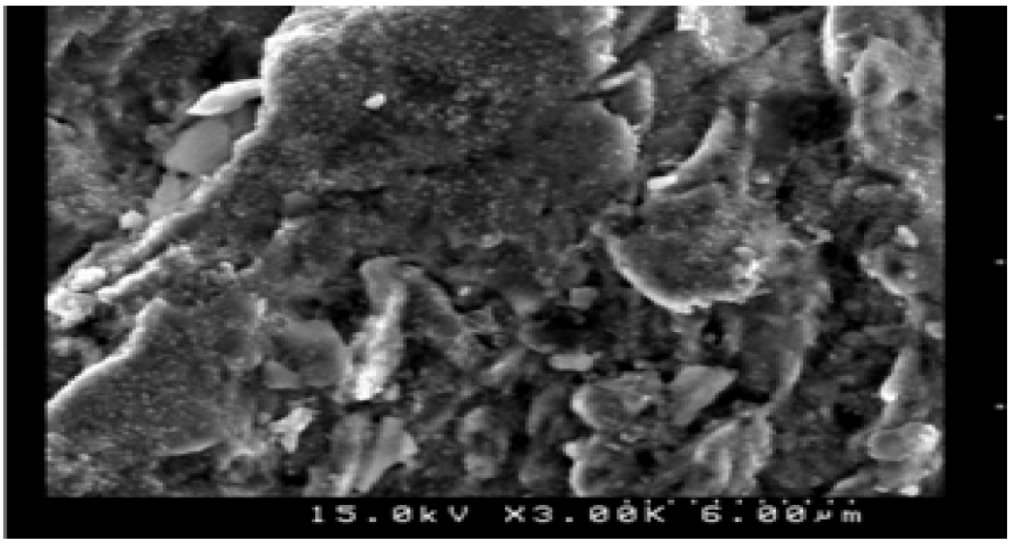

Figure 2.24 Intergranular fracture in the fracture area.

2.8 Effect of Temperature

Temperature is also a critical factor in pitting corrosion, because many materials will not pit at temperature below certain value, which is extremely sharp and reproducible [36-42]. This effect can be seen either by varying the temperature at a range of fixed applied potentials or by varying the potential for a range of constant temperature experiments. Fig. (2.25) is a plot of pitting and repassivation potentials for three different stainless steels in 1 M NaCl as a function of solution temperature [41-42]. At low temperatures, extremely high breakdown potentials are observed, corresponding to transpassive dissolution, and not localized corrosion. Just above the critical pitting temperature (CPT), pitting corrosion occurs at a potential that is far below the transpassive breakdown potential. This value of CPT is independent of the environmental parameters and applied potential over a wide range and is a measure of the resistance to stable pit propagation [57]. At higher temperatures, the pitting potential decreases with increasing temperature and chloride concentration. The CPT can be used, similar to pitting potential, as a means for ranking susceptibility to pitting

corrosion; the higher the CPT, the more resistant the alloy is to pitting [57]. If crevice corrosion is the primary concern, creviced samples can be used to determine a critical crevice temperature (CCT), which is typically lower than the corresponding CPT, Fig. (2.26). Aluminum alloys do not exhibit a CPT in aqueous chloride solutions at temperatures down to 0 °C (32 °F).

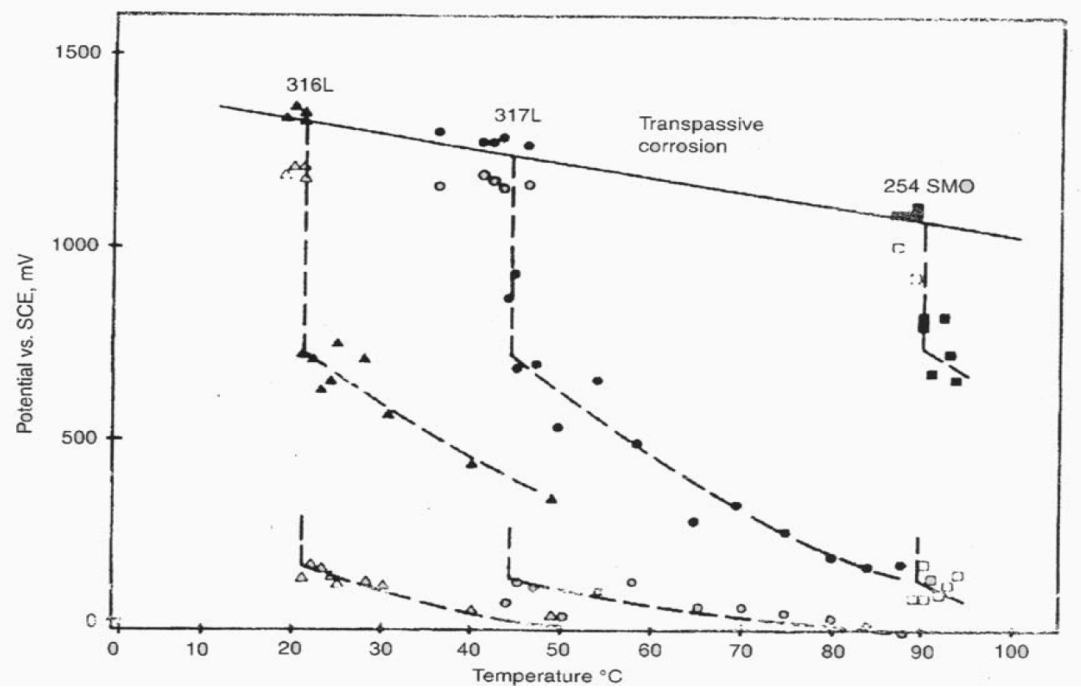

Figure 2.25 Pitting and repassivation potentials for three different stainless steels in 1 M NaCl as a function of solution temperature.[19]

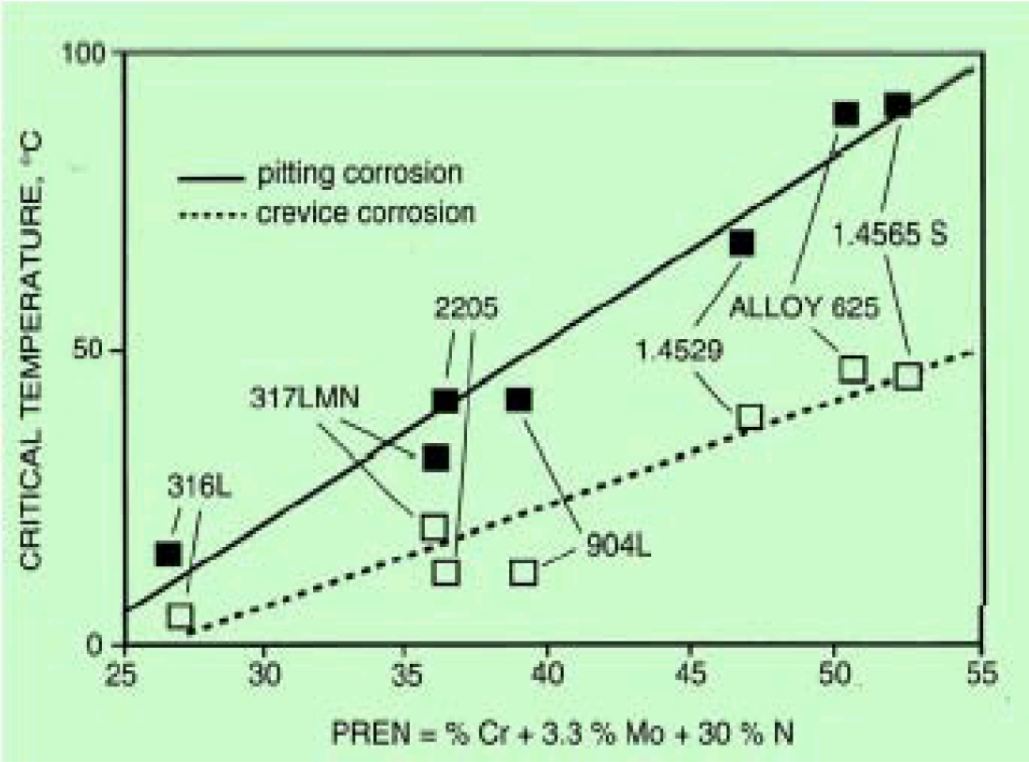

Figure 2.26 Variation in the critical pitting temperature and critical crevice corrosion temperature.[20]

2.9 Effect of pH

The effect of pH on the breakdown potential has not been much investigated. It is found with the exclusion of Pourbaix work[43] that the E_b value is almost constant within a large range of pH values [44-46].

Figure (2.27) shows that iron is thermodynamically immune in neutral and acid solutions (below line a) when $Fe^{+2} < 10^{-6}$ M. The metal goes passive on the right of line d. Iron does not dissolve at all at pH values between 9 and 13, owing to a passivating film of Fe_3O_4 or Fe_2O_3.

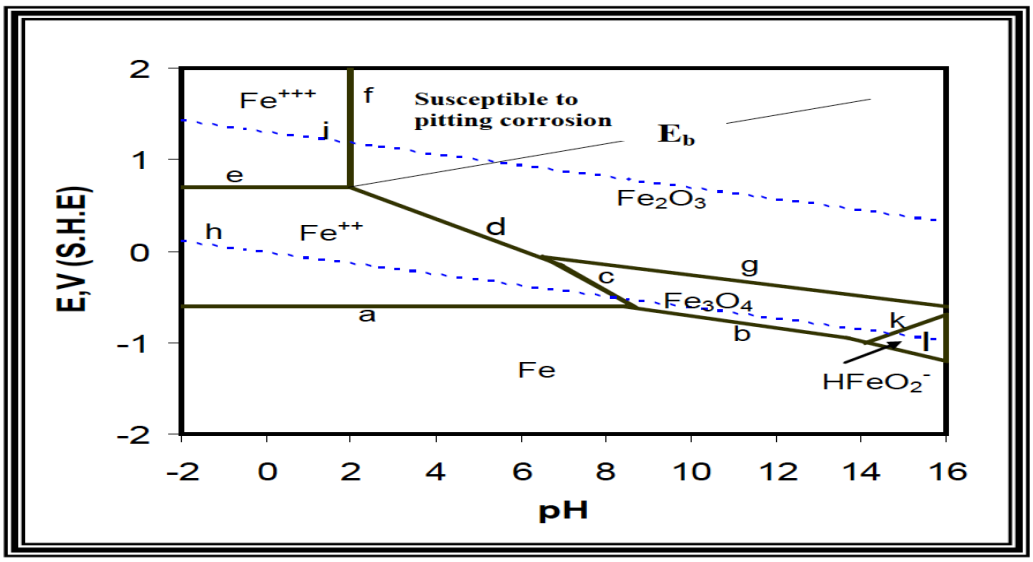

Figure 2.27 Pourbaix diagram for iron in water (298 K).[47]

2.10 Effect of Velocity

The attack on metal immersed in water may vary greatly, depending on the relative velocity between the water and the metal surface. For metals that show passive behavior or form other protective films in water, as most metals do, attack will occur where the changes in water velocity are most pronounced. Water corrosivity can be dramatically increased by dissolved gases, acids, salts, strong bases, entrained abrasives, high temperature, fluctuating pressure, cavitation, or impingement.

Relative difference in velocity between the metal and the aqueous corrosive medium influence any of the common varieties of iron or steel, including low-carbon or high-carbon steel, low-alloy steel, wrought iron, and cast iron. These corrode in slow-moving freshwater or seawater at almost the same rate, which is about 0.13 mm/year (0.005 in./year). At higher temperatures, with equal values of dissolved gas concentration, the rate tends to increase, but remains relatively low. Therefore, steel can be used for boilers in contact with deaerated water. Commercially pure aluminum typically corrodes less in aerated or deaerated fresh water than iron and carbon steels, making it a suitable material for handling distilled water [1,6,48].

2.10.1 Low Velocity Effects

Slow-moving and stagnant waters can prevent, damage, or remove passive films. The low velocity allows loosely adherent solid corrosion products to form on metal surfaces and allows debris to collect, which facilitates further corrosion damage. In closed systems, if a corrosion inhibitor is used, its effectiveness is often reduced where the water is stagnant or quiet.

In designing for corrosion control, stagnant zones should be eliminated by the following methods:

• Circulation of stagnant liquids or relative movement of metallic surfaces

• Allowing free drainage of water

• Filtering suspended solids

• Providing a N_2 blanket (carbon steels) or free access to O_2 (stainless steels). Weakly passivating metals such as carbon steels are attacked by high O_2, whereas strongly passivating metals such as stainless steels are protected by uniform O_2 distributions.

• Maintaining concentration of dissolved passivating chemicals such as O_2 by infusion or injection [6,48].

2.10.2 High-Velocity Effects

Swift-moving water may carry dissolved metal ions away from corroding areas before the dissolved ions can be precipitated as protective layers. Gritty suspended solids in water scour metal surfaces and continually expose fresh metal to corrosive attack.

In fresh water, as water velocity increases, it is expected that corrosion of steel first increases, then decreases, and then increases again. The latter occurs because erosive action serves to breakdown the passive state.

The corrosion of steel by seawater increases as the water velocity increases. The effect of water velocity at moderate levels is shown in Fig. (2.28), which illustrates

that the rate of corrosive attack is a direct function of the velocity until some critical velocity is reached, beyond which there is little further increase in corrosion. At much higher velocities, corrosion rates may be substantially higher. The effect of changes in water velocity on the corrosion resistance of stainless steels, copper alloys, and nickel alloys shows much variation from alloy to alloy at intermediate velocities. Type 440 Martensitic stainless steel may pit severely in typical seawater especially when stagnant and at velocities of less than 1 or 1.5 m/s (4 or 5 ft/s), but is usually very corrosion resistant at higher velocities. In seawater at high velocity, metals fall into two distinctly different groups: those that are velocity limited (carbon steels and copper alloys).and those that are not velocity limited (stainless steels and many nickel alloys).

Metals that are not velocity limited are subject to virtually no metal loss from velocity effects or turbulence short of cavitation conditions. The barrier films that form on these metals seem to perform best at high velocities with the full surface exposed and clean. Crevices and under deposit form from low-moving or stagnant seawater because of local breakdown of the film and pitting begins [48-51].

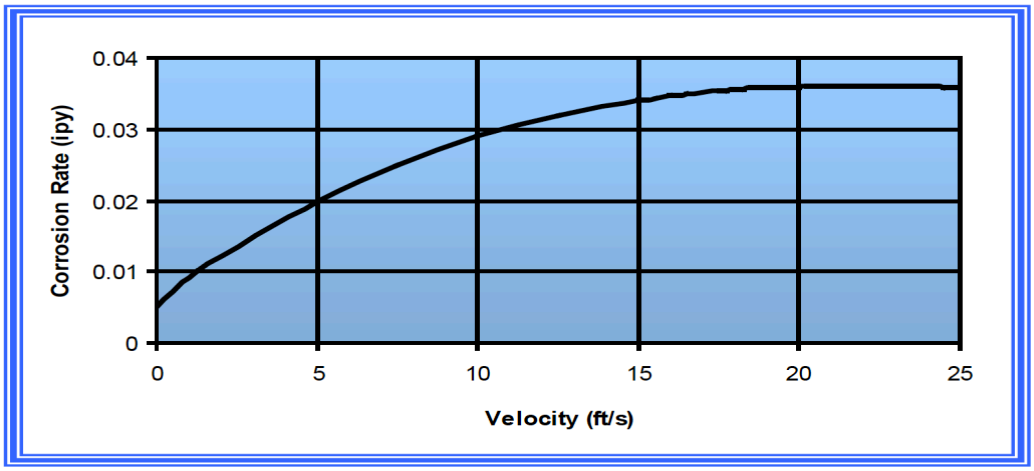

Figure 2.28 Effect of velocity of sea water at atmospheric temperature on the corrosion rate of steel. [48]

2.11 Effect of Surface Condition

The exact condition of a surface can have a large influence on the pitting behavior of a material. In general, samples prepared with a rough surface finish are more susceptible to pitting and exhibit a lower pitting potential. For example, the pitting potential of type 302 stainless steel with a 120-grit finish was shown to be approximately 150 mV lower than that for the same material with a 1200-grit finish over a range of chloride concentrations [75]. The effect of surface roughness on pitting is related to the stabilization criteria described subsequently. Rougher surfaces have more occluded sites, which can sustain the conditions that are required for active dissolution at lower current densities and thus lower potentials because of the longer diffusion path length and slower rate of diffusion.

For stainless steels, heat treatment, grinding, and abrasive blasting have been reported to be detrimental to pitting resistance, whereas pickling in HNO_3 + HF scales or passivation in HNO_3 is beneficial [57]. Heat treatments in air generate a chromium oxide scale and a chromium-depleted region under the scale. The seal is typically removed mechanically, and the chromium-depleted region is removed by pickling[57]. Other common surface defects include heat tint from welding, embedded iron particles from machining, and MnS inclusions. The detrimental effects of these defects are minimized and the overall-surface condition improved by passivation in nitric acid, which increases the chromium content of surface oxide film.

The effects of surface condition on localized corrosion are significant enough that care must be taken not to apply experimental data collected on samples with special preparation to a real application without taking the surface condition into account [56].

2.12 Evaluation of Pitting Damage

Pitting is a localized type of attack, in which the rate of corrosion is greater at some areas than at others. If appreciable attack is confined to a relatively small fixed area of the metal, acting as anode, the resultant pits are described as deep. If the area of attack is relatively larger and not so deep, the pits are called shallow [2].

Since pitting is a localized form of corrosion, conventional weight loss tests cannot be used for evaluation of pitting damage because metal loss is very small and the instrument does not measure it. The depth of pits are complicated by the fact that there is a statistical variation in the depths of pits. Note that, the average pit depth is a poor way to estimate pit damage, since it is the deepest pit that causes failure. Therefore, a measurement of maximum pit depth over time would be a reliable way of expressing pitting corrosion.

However, once pitting starts, penetration of the metal at an ever increasing rate will take place. In addition, pits tend to undermine or cut the surface as they grow [1].

Depth of pitting is sometimes expressed by the term (pitting factor). This is the ratio of deepest metal penetration to average metal penetration as determined by the weight loss of the specimen. A pitting factor of unity represents uniform attack as shown in Figure. (2.29). Iron buried in the soil corrodes with formation of shallow pits, whereas stainless steels immersed in seawater characteristically corrode with formation of deep pits [2].

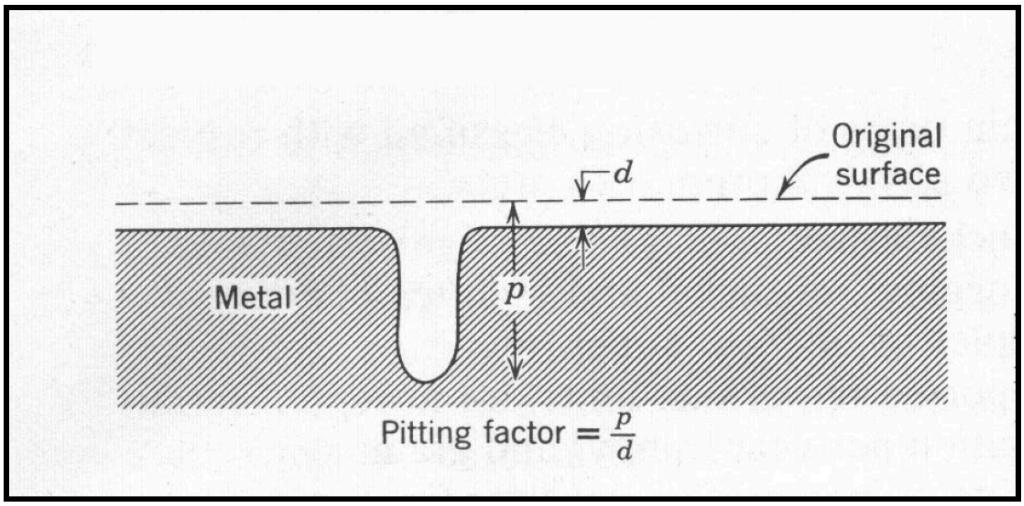

Figure 2.29 Sketch of deepest pit with relation to average metal penetration and the pitting factor. [24]

2.13 Pitting Resistance Equivalent Number (PREN)

In order to quantify the effect of alloying elements on the pitting resistance of the stainless steels alloys, Pitting Resistance Equivalent Number (PREN) can be used and this number can give a good indication of the pitting resistance of stainless steels based on their compositions. However, PREN cannot be used to predict whether a particular grade of materials will be suitable for a given application where pitting corrosion may be a hazard. The most commonly used formula to calculate the PREN value is [95-98].

$$\mathbf{PREN = \%Cr + 3.3\ x\ \%Mo + 16\ x\ \%N} \qquad (2.1)$$

Other formulas give greater weight to nitrogen, with factor of 27 or 30. But because nitrogen level is relatively modest in most of stainless steels alloys, this factor does not have a dramatic effect on ranking. From the formula, it is clear that grades with high chromium, molybdenum and nitrogen content are more resistant to pitting corrosion.

2.14 Crevice Corrosion

In an electrolyte high in chloride, a confined (occluded) zone linked, for example, to bad design, favors the accumulation of chloride ions. The progressive acidification of the medium in this zone facilitates the de-stabilization of the passive layer. When the pH in this zone reaches a critical value called « depassivation pH »,corrosion starts.

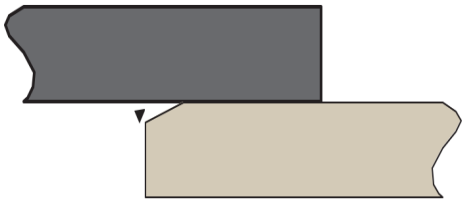

Figure 2.30 Confined zone acidification

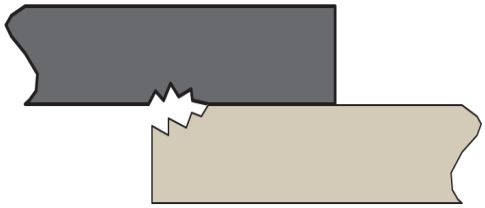

Figure 2.31 Break in passive layer attack.

Source:https://www.google.com/search?q=google+images+corrosion+steel&source=lnms&tbm=isch&sa=X&ved=0ahUKEwjL5XPjNnTAhUB4yYKHcscBawQ_AUICigB&biw=800&bih=547

Once corrosion is initiated, its propagation occurs by active dissolution of the material in the crevice. In the laboratory, we simulate this type of corrosion by recording the potentiodynamic scans in chloride mediums of increasing acidity.

If, on a recording, we detect a current peak (activity), crevice corrosion is starting; in the opposite case, repassivation takes place. Activity peak measurement for a pH lower than the depassivation pH can then be considered to quantitatively compare the speed of crevice corrosion propagation for different grades. This value is sensitive to the alloy elements which improve the passivation and limit active dissolution, principally molybdenum, nickel and chromium. The speed of propagation is also a function of local aggressiveness and temperature of the medium.

2.15 Mechanism of Crevice Corrosion

The crevice corrosion mechanism is dependent on several parameters and it may change accordingly with a change in the parameters. This attack happens in a restricted area, often a narrow fissure with a width of normally only a few micrometers. These fissures can occur where there are external agents such as paint remnants, tape or insulation, that forms a crevice against the pipe surface. The chemistry within the fissure develops differently from the rest of the bulk solution. Several mechanisms were proposed for crevice corrosion, since any single mechanism fails to explain all aspects of crevice corrosion. Here, only deoxygenation-acidification, also called the passive dissolution mechanism, of crevice corrosion proposed by Oldfield and Sutton is briefly explained to give an introduction to crevice corrosion. In fissures, the most common reduction reaction, which is a requirement in order to introduce crevice corrosion, is the oxygen reduction reaction. Other reduction reactions may also occur, for example, reduction by chloride ions. The only reduction reaction at the cathode is the proton (H^+) or water reduction reaction; in the case where no oxidizing agent is left in the pit, or depletion of oxygen is called deoxygenation. This is caused by very slow oxygen diffusion into the crevice and, therefore, a concentration gradient builds up between the crevice and the outer passive surface of the material. Hydroxide forms in the crevice in alkaline seawater, causing a rise in the pH. This is the first part of the initiation phase.

The second step is hydrolysis-acidification, which is directly induced by the deoxygenation. The depletion of oxygen causes the cathode reaction to move to the outer passive surface, where oxygen is more easily accessible, while the oxidation of

the components of the alloy continues in the crevice. The components in AISI 440 that dissolve are Cr, Fe, Mo and Ni, where the formation of chromium hydroxide seems to exert the most influence on the pH. The dissolution causes a predominance of cations; so anions, that is, chlorides, start migrating into the crevice to restore electro neutrality. These components of the alloy hydrolyze simultaneously producing protons which lower the pH in the crevice, thereby causing acidification. The last step in the initiation phase is activation, which is when the critical solution chemistry is aggressive enough to cause oxide film breakdown. The time until all the three steps have occurred is normally called the initiation time and is discussed in this section. There is no attack of the crevice in this phase; the attack occurs in the propagation phase. The initiation phase consists of the evolution of an aggressive crevice solution in which a steady state develops and this phase is assumed to occur much faster than the propagation phase that follows.

The propagation phase that comes after initiation is shown in Figure 2.32. It can be seen from the graph that the corrosion current rapidly increases. As the crevice continues to corrode, its growth is directed towards the mouth of the crevice. It is the IR (I = Current; R = Resistance) drop that limits its growth. The resistance decreases as the corrosion progresses towards the crevice mouth, causing an increase in the current. It can be seen from the graph that IR limits the growth. The resistance decreases as it grows towards the mouth, while the current increases. The anodic current limit is attained when the growth of the crevice reaches the mouth, and the IR drop no longer limits the corrosion reaction. The dissolution of metal or the cathodic reaction at the surface are the limiting factors of corrosion. After a while, the corrosion rate starts decreasing due to an increased resistance in the solution between the oxidation of the metal in the crevice and the cathode reaction on the bare surface.

The products of corrosion that build up at the crevice mouth are the reason for this behavior. Another reason that limits the corrosion rate is the cathodic reaction reducing proton to hydrogen, which increases the pH of the solution.

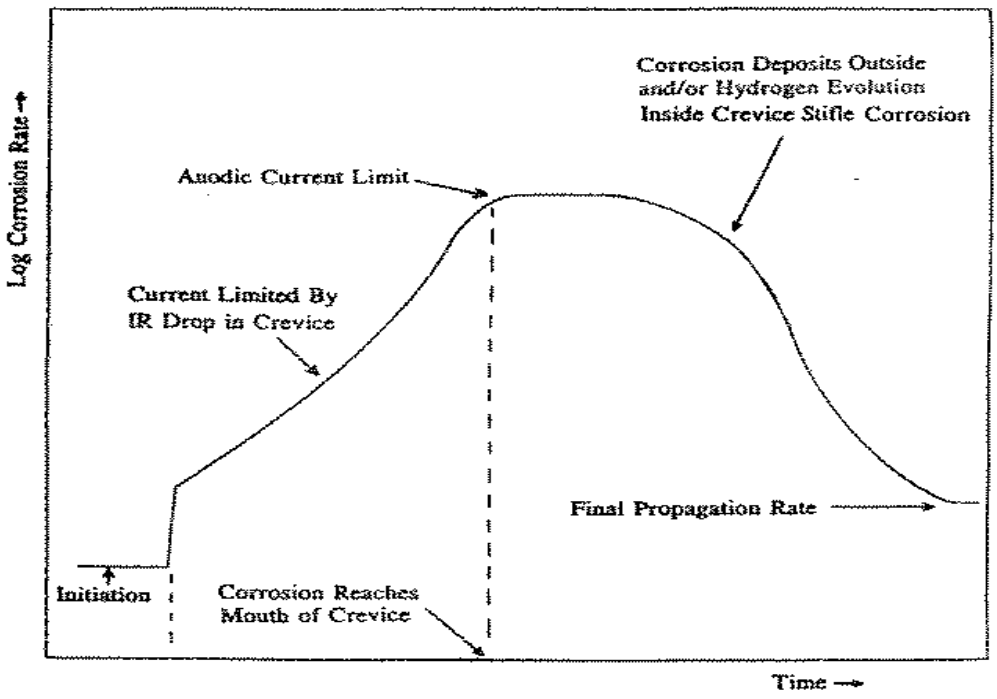

Figure 2.32 Diagram presenting the corrosion rate of crevice corrosion against time.
Source:https://www.google.com/search?q=google+images+corrosion+steel&source=lnms&tbm=isch&sa=X&ved=0ahUKEwjL5XPjNnTAhUB4yYKHcscBawQ_AUICigB&biw=800&bih=547

The Oldfield and Sutton model is criticized due to tests of changes in solution composition during the initiation stage of crevice corrosion. The three elements tested were Cr, Fe and Ni. It was shown that Cr does occur in very small amounts before breakdown of the passive film, compared to the actual amount of Cr in the alloy. After breakdown, the Cr content increased considerably and the possible reasons for this were tested. Adsorption and pH drop were evaluated during only one experiment and thereafter ruled out as possible reasons for the corrosion behavior.

Acidification (pH drop) did not occur in the crevice before breakdown, unlike in the Oldfield and Sutton model and is therefore a result and not a reason for the occurrence of breakdown. It was concluded from the results that the only possible reasons could be that the dissolved oxygen developed a surface oxide of chromium, or that chromium did not dissolve at all.

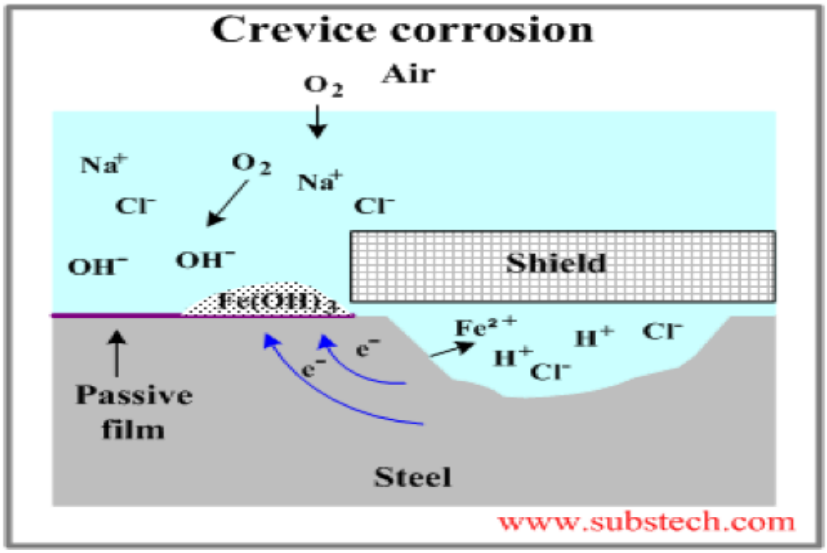

Figure 2.33 Crevice Corrosion Deep Growth.

Our first recommendation to avoid crevice corrosion is to optimize the design of the piece to avoid all artificial crevices. An artificial crevice can be created by a badly made joint, a rough or bad weld, deposits, gaps between two plates etc. If the confined zone is unavoidable, it is preferable to enlarge this zone and not to make it smaller. If the design of the pièce is not modifiable or if the fabrication process makes it difficult to avoid confined zones, the risk of crevice corrosion is very high. We recommend, in this case, choosing an appropriate grade, in particular a stainless steel austenitic or duplex phase when the product will be in contact with corrosive media or part of the process equipment.

2.16 Other Types of Corrosion

2.16.1 Intergranular Corrosion

At temperatures greater than 1035°C, the carbon is in solid solution in the matrix of the austenitic stainless steels. However, when these materials are cooled slowly from these temperatures or even heated between 425 and 815 °C, chromium carbide precipitates at the grain boundaries. These carbides have a higher chromium content in comparison to the matrix.

Consequently, the zone directly adjacent to the grain boundaries is greatly impoverished. The sensitization state takes place in several environments by privileged initiation and the rapid propagation of corrosion on the de-chromed sites.

For unstabilized ferritic stainless steels, the sensitization temperature is higher than 900°C.

In practice, this case of corrosion can be encountered in welded zones. The solution for the austenitic phase consists of using a low carbon grade called « L » (Low C%<0.03%) or a stabilized grade, and titanium or niobium stabilized ferritic grades. The volume of the piece permitting a thermal treatment of the quenching type (rapid cooling) at 1050/1100°C or a tempering of the welded piece can be performed.

2.16.2 Stress Corrosion

We mean by « stress corrosion » the formation of cracks which start after a period of long incubation and which, afterwards, can propagate very rapidly and provoke downtime of the equipment by cracking. This particularly dangerous phenomenon is the result of the combined effects of 3 parameters:

- temperature, since stress corrosion rarely develops under 50°C
- applied or residual stresses

- corrosiveness of the medium: presence of Cl-, H2S
- caustic media NaOH.

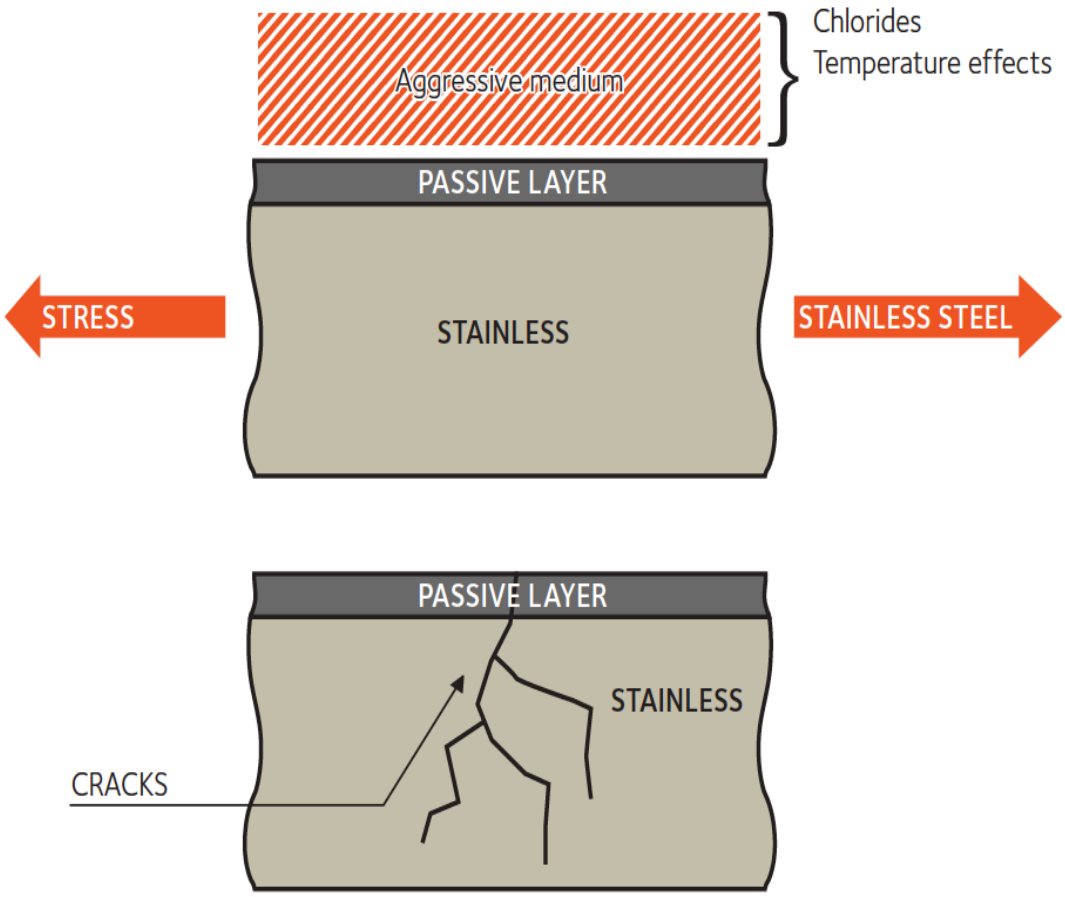

Figure 2.34 The metallurgical structure of stainless steels influences their behavior in this type of configuration. [58]

Although stress corrosion of ferritic can be provoked by particularly aggressive tests in the laboratory, their body cubic centered structure rarely renders them subject to this type of phenomena in practice. The face cubic centered structure of austenitic stainless steels can present a risk. In effect, it favors a mode of planar deformation which can generate very strong stress concentrations locally. As shown in the graph in Figure 2.36, this is particularly true for classic austenitic stainless steels with 8% nickel; an increase in nickel above 10% is beneficial. In austenitic stainless steels, the

austenitic stainless steels with manganese perform worse. The austeno-ferritic structure of the duplex gives them an intermediate behavior, very close to the ferritic in the chloride medium and even better in the H_2S medium.

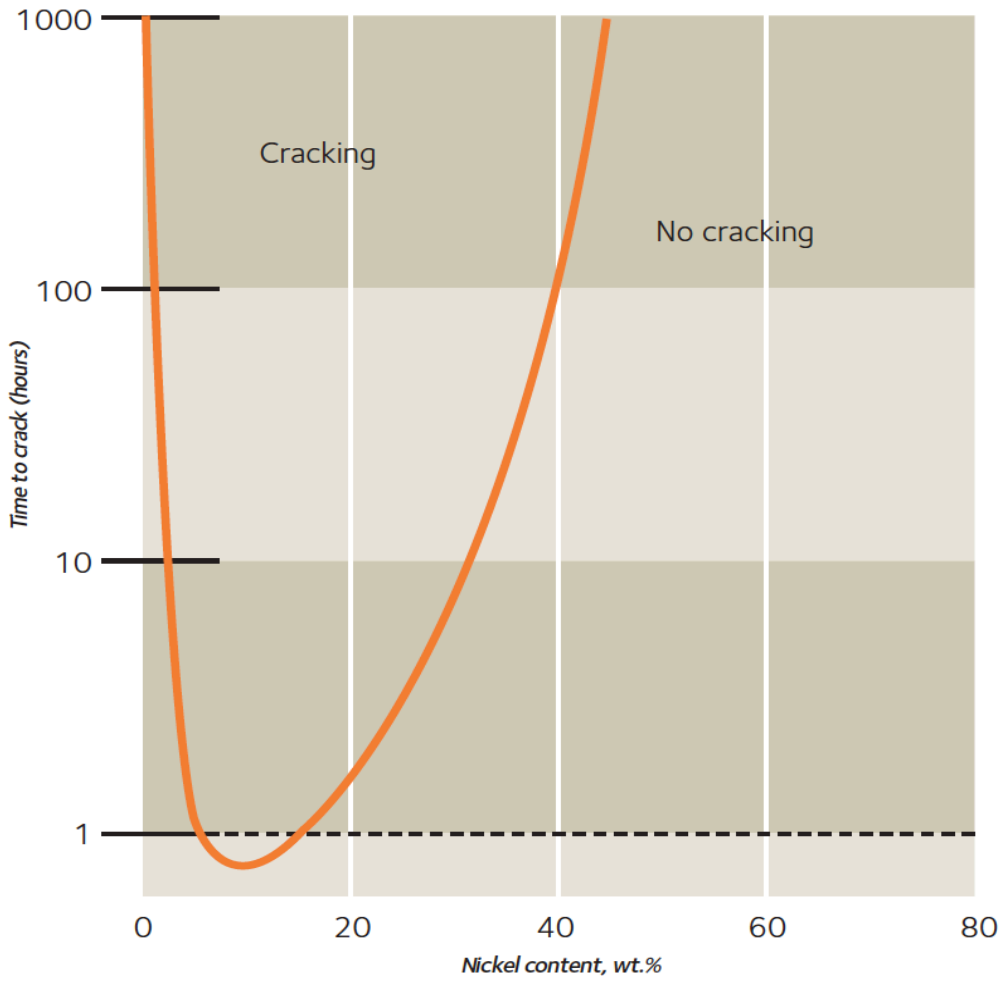

Figure 2.35 Effect of nickel content on the resistance to stress corrosion of stainless steel containing 18-20% chromium in magnesium chloride at 154°C.
Source: From a study by Copson [ref]. Physical Metallurgy of Stress Corrosion Cracking, Interscience, New York, 247 (1959).

In order to avoid this type of corrosion, the following steps must be taken:

- suppress the stresses or have a better redistribution, by optimizing the design or by a stress relieving treatment after forming and welding of the pieces concerned
- lower the temperature if possible
- if not practicable, choose the grade most adapted, favoring as a solution a ferritic or duplex phase but bearing in mind the other corrosion problems encountered.

2.16.3 Uniform Corrosion

This is the dissolution of all the affected points on the surface of the material which are attacked by the corrosive medium. On the micrographic scale, this corresponds to a regular uniform loss of thickness or loss of weight (uniform or generalized corrosion as opposed to localized corrosion). We see this corrosion in acid media. Indeed, below a critical pH value, the passive layer protecting the stainless steel is no longer stable and the material suffers a generalized active dissolution. The more acidic the medium, the faster the corrosion and the loss of thickness of the stainless steel. In the laboratory, we measure this speed of corrosion in an acid medium by examining the polarization curve (see Figure 2.37). An increasing potential scan is imposed on the metal and the corresponding intensity is recorded [58].

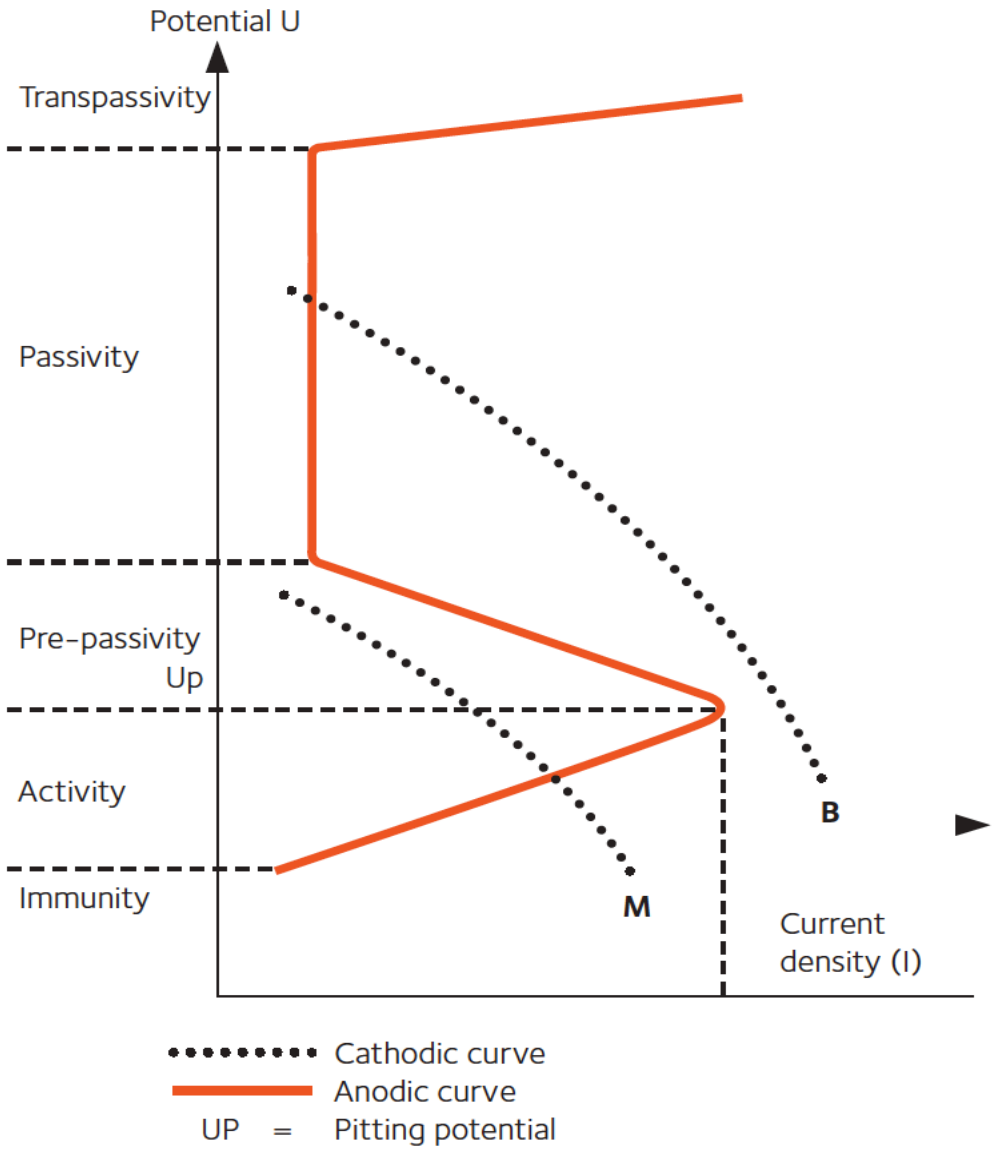

Figure 2.36 Polarization curve in an acidic medium.

- In a low oxidizing medium, the cathodic curve (M) cuts the anodic curve below the pitting potential; metal remains intact.
- In a strong oxidizing medium, the cathodic curve (B) cuts the anodic curve above the pitting potential; pits appear on the surface of the metal.

The maximum current reading of the activity peak allows us to classify the resistance of different grades to this type of corrosion. Generally, the higher the current, the faster and greater the dissolution, thus the less the grade the higher the resistance.

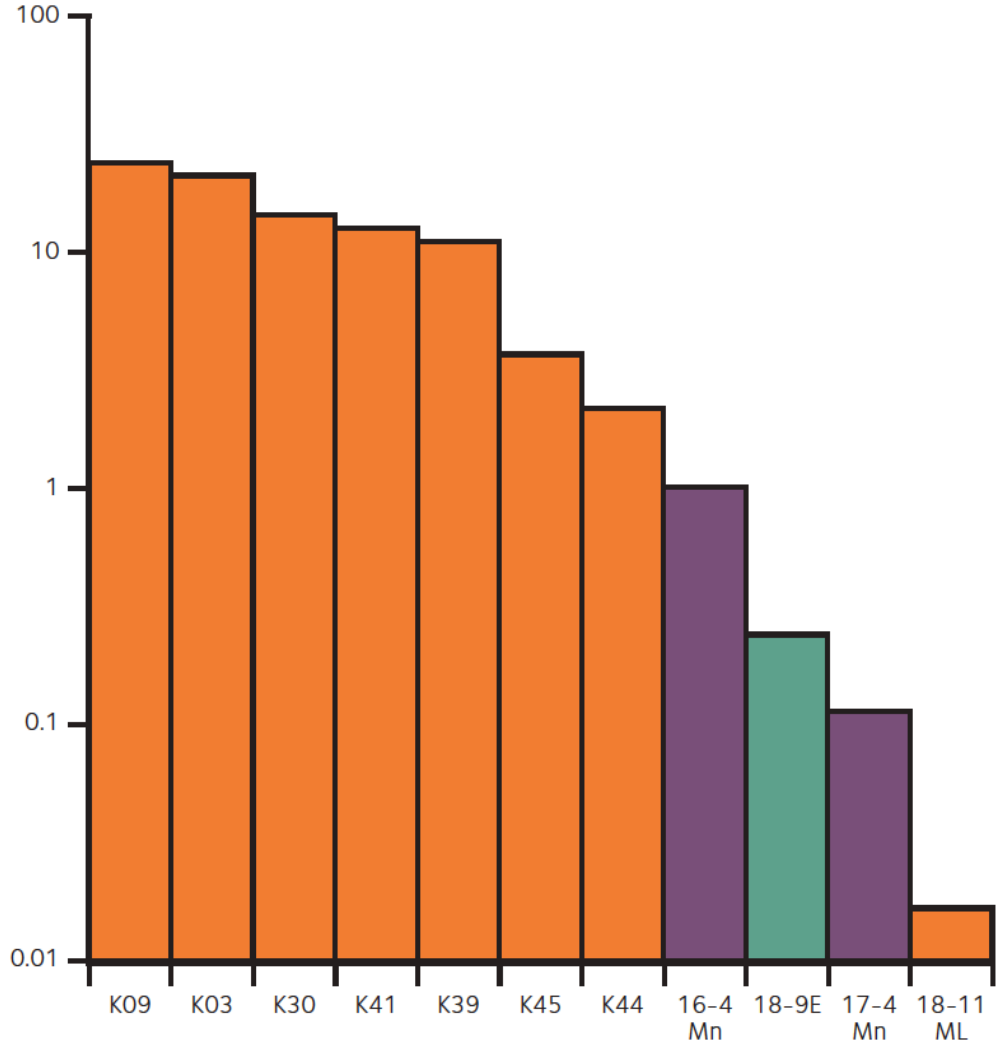

Figure 2.37 Critical current «icrit» at the peak maximum in H_2SO_4 2M de-aerated at 23°C.

In order to avoid this type of corrosion, appropriate grade is chosen in regard to the acid medium used. We note the favorable impact of chromium and molybdenum which reinforce the existing passive film but also the combined effect of the noble alloys (nickel, molybdenum and copper) which slow down the dissolution of the material when the stability is passive.

CHAPTER 3

STAINLESS STEELS

3.1 Introduction

For years, the food, beverage and pharmaceutical industries have used stainless steels in their process piping systems. Most of the time, stainless steel components provide satisfactory results. Occasionally, a catastrophic failure will occur [59].

Stainless steel is not a single alloy, but a large family of alloys with different properties that are characteristic of the alloys. There are hundreds of grades and subgrades in the stainless steel family, each designed for a special application. Chromium is the magic element that transforms iron into stainless steel. Stainless steel must contain at least 10.5% chromium to provide adequate resistance to rusting, and the more chromium the alloy contains, the better the corrosion resistance becomes. There is, however an upper limit to the amount of chromium the iron can hold. Therefore, additional alloying elements are necessary to develop corrosion resistance to specific media [1,22,59,60].

Stainless steels are iron based alloys containing a minimum of 12wt % chromium and up to 25wt % nickel with minor additions of carbon, nitrogen, molybdenum, tungsten, titanium, niobium, copper and selenium. Stainless steels are a class of versatile materials, which can be tailored to exhibit a wide range of engineering properties by alloy design and controlled mechanical treatments to meet the demanding conditions. This versatility has resulted in an enhanced demand for stainless steels in a broad variety of applications ranging from small pins to the construction of automobiles, petrochemical, space, aeronautics, ship building industries and nuclear power stations. Certain grades of stainless steel, because of

their biocompatibility, are used for the manufacture of biomedical implants.

Stainless steel is an alloy of iron. According to its definition, stainless steel must contain a minimum of 50% iron. If it contains less iron, the alloy system is named for the next major element. For example, if the iron is replaced with nickel-so that the iron is less than 50%-then it is called a nickel alloy. Chromium imparts a special property to the iron that makes it corrosion resistant. When the chromium is in excess of 10.5%, the corrosion barrier changes from an active film to a passive film. While the active film continues to grow over time in the corroding solution until the base metal is consumed, the passive film will form and stop growing. This passive layer is extremely thin, in the order of 10 to 100 atoms thick, and is composed mainly of chromium oxide which prevents further diffusion of oxygen into the base metal. But, chromium is also stainless steel's Achilles heel, and the chloride ion is stainless steel's nemesis. The chloride ion combines with chromium in the passive layer, forming soluble chromium chloride. As the chromium dissolves, free iron is exposed on the surface and reacts with the environment forming rust. Alloying elements like molybdenum will minimize this reaction. [61-63]

Other elements, as illustrated in Table (3.1), may be added for special purposes. These purposes include: high temperature oxidation resistance, sulfuric acid resistance, greater ductility, high temperature creep resistance, abrasion resistance, or high strength. Of all these elements, only chromium is required in order for stainless steel to be stainless. [62-63]

Table 3.1 Stainless steel alloying element and their purpose [64]

Chromium	Oxidation Resistance
Nickel	Austenite former - increases resistance to mineral acids and produces tightly adhering high temperature oxides
Molybdenum	Increases resistance to chlorides
Copper	Provides resistance to sulfuric acid precipitation hardener together with titanium and aluminum
Manganese	Austenite former - combines with sulfur, increases the solubility of nitrogen
Sulphur	Austenite former - improves resistance to chlorides, improves weldability of certain austenitic stainless steels, and improves the machinability of certain austenitic stainless steels
Titanium	Stabilizes carbides to prevent formation of chromium carbide precipitation hardener
Niobium	Carbide stabilizer - precipitation hardener
Aluminum	Deoxidizer - precipitation hardener
Carbon	Carbide former and strengthener

3.2 Classification of Stainless Steels

There are five classes of stainless steel: austenitic, ferritic, martensitic, duplex, and precipitation hardening. They are named in accordance with their microstructure resemblance to a similar microstructure in steel. The properties of these classes differ but are essentially the same within the same class. Table (3.2) lists the metallurgical characteristics of each class of stainless steel [64].

Table 3.2 Metallurgical Characteristics [64]

Austenite	Non-magnetic Non-hardenable by heat treatment Single phase from 0 (K) to melting point crystallographic form – face centered cubic Very easy to weld
Ferrite	Magnetic Non-hardenable by heat treatment crystallographic form - body centered cubic Low carbon grades easy to weld
Duplex	Magnetic Non-hardenable by heat treatment Contains both austenite and ferrite Easy to weld
Martensitic	Magnetic Heat treatable to high hardness levels crystallographic form – distorted tetragonal Hard to impossible to weld
Precipitation Hardening	Magnetic Crystallographic form - martensitic with microprecipitates Heat treatable to high strength levels Weldable

Stainless steels can be classified into five main groups in accordance with their metallurgical structure [19, 33, 34]:

- Austenitic
- Ferritic
- Martensitic
- Duplex (austenite/ferrite) and
- Precipitation-hardening alloy

Schaeffler diagram, as shown in Figure 3-3, is a useful way to determine the likely structure of a stainless steel. This diagram is based on the presence of ferrite or austenite in the stainless steel in terms of nickel and chromium equivalents [35].

The chromium equivalent (Cr eq.) has been determined using the most common ferrite forming elements [35]:

$$\text{Cr eq.} = (\text{Cr}) + 2(\text{Si}) + 1.5(\text{Mo}) + 5(\text{V}) + 5.5(\text{Al}) + 1.75(\text{Nb}) + 1.5(\text{Ti}) + 0.75(\text{W}) \quad (3.1)$$

The nickel equivalent ($Ni_{eq.}$) has likewise been determined with the familiar austenite forming elements:

$$\text{Ni eq.} = (\text{Ni}) + (\text{Co}) + 0.5(\text{Mn}) + 0.3(\text{Cu}) + 25(\text{N}) + 30(\text{C}) \quad (3.2)$$

In this thesis, the stainless steel alloys, 440, which are considered as martensitic type, were used. Thus, this group of martensitic stainless steels will be further described.

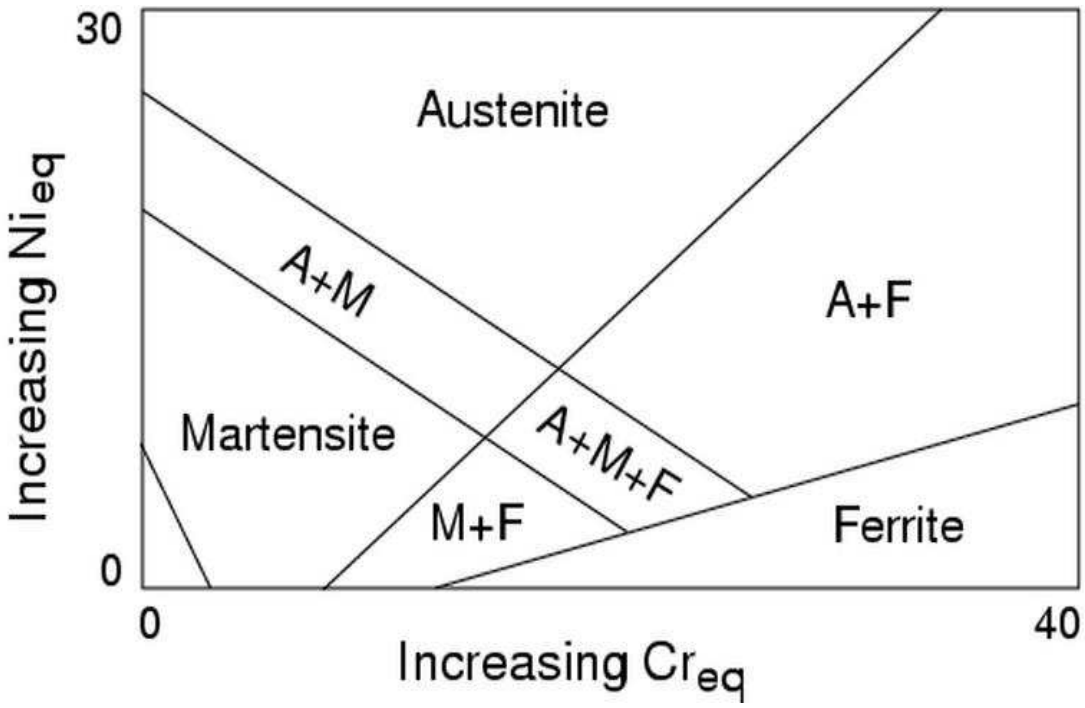

Figure 3.1 Schaeffler diagram, effect of alloying elements on the basic structure of Cr- Ni stainless steels. [35]

3.2.1 Ferritic Stainless Steels

Ferritic stainless steels (FSS) normally contain high chromium content (11 to 30 wt %), with carbon content in the range of 0.04 to 0.12 wt %. Apart from the basic elements, other alloying elements are added to ferritic stainless steels to improve the corrosion resistance or other special properties.

Ferrite stainless steels, because of their low carbon content and high chromium content, do not undergo the austenite to ferrite transformation, and therefore, they are not considered for hardening treatment.

3.2.2 Precipitation-Hardening Stainless Steels

Precipitation hardening stainless steels usually contain chromium 10 to 30wt % and nickel 4 - 7 wt % along with small amounts of molybdenum (1-3wt %). Precipitates in these alloys are formed by additions of small amount of Cu, Al, Ti and Nb. These alloys generally have high mechanical strength without significant loss of corrosion resistance due to the presence of precipitates. These steels are used in various applications, where high strength along with corrosion resistance are needed.

Precipitation hardening stainless steels can be grouped into three types namely martensitic, semi-austenitic and austenitic based on their martensitic start and finish temperatures and the resultant behavior upon cooling from a suitable solution treatment temperature.

3.2.3 Duplex Stainless Steels

Duplex stainless steels are a mixture of ferrite and austenite crystal structures. The percentage of each phase is dependent on the chemical composition and heat treatment. Most duplex stainless steels are intended to contain ~ equal amounts of ferrite and austenite phases in annealed conditions. The primary alloying elements are Cr, Ni, Mo and N. Duplex stainless steels have similar corrosion resistance to austenitic stainless steels except that they typically have better stress corrosion cracking resistance. Duplex stainless steels generally have greater tensile and yield strengths, but poorer toughness than austenitic stainless steels (Martins et al 2009). The higher amount of ferrite content in the duplex stainless steels enhances the resistance to stress corrosion cracking (Fargas et al 2009).

3.2.4 Austenitic Stainless Steels

Austenitic stainless steels are essentially ternary Fe-Cr-Ni alloys containing a minimum of 16wt % Cr and 7 to 20wt % Ni. They also contain small amounts of Mo (2-4wt %) and N (0.1-0.2wt %). These alloys are called as “austenite stainless steel”. since their structure remain austenitic (FCC, -iron type) at all normal heat treated condition. The most widely used austenitic stainless steels are the 300 series wrought material (304, 316, 317 etc.) and their cast counterparts (CF8, CF8M, CG8M etc.). They are widely used in various applications such as nuclear, power plants, petro-chemical industries and paper-pulp industries. Because of their versatile properties such as (i) outstanding strength and toughness, (ii) superior corrosion resistance, (iii) ease of fabrication and iv) good weldability, they are mainly considered for many engineering applications (Marshal, 1984). However, there are applications in which they do not have sufficient corrosion resistance in environments containing hot

concentrated chlorides and strength at the elevated temperatures, that is, above 400C. To overcome these problems, alloys with high nickel and high molybdenum contents have been developed for such high critical applications. Alloy 20 containing high Ni content is commonly used for these applications (Davison et al 1983).

Over the years, there has been continuous development and improvement of the austenitic stainless steel grades frequently resulting in higher alloyed variants. The first step in the sequence of new grades was quite logical to enhance high strength and resistance to pitting corrosion by increasing the amounts of: (i) molybdenum from 2wt % to 4wt%, (ii) chromium from 18 to 25wt % and (iii) nickel to 20wt %. For example, 904L grade was one of the first corrosion resistant grades of austenitic stainless steels developed for petro-chemical industries, which contains normally 4-5wt % Mo and 0.2wt % N. Subsequently, alloys with higher amounts of Mo content (6.5wt %) were developed to improve the resistance to crevice and pitting corrosion in chloride (3000 ppm) environments (Mats Liljas 1995). Increasing Mo content to ASS is represented somewhat of a technical challenge on the high alloyed austenitic stainless steel, because higher amount of Mo content promotes intermetallic phases at various temperatures (Maurer et al 1982). In the late 1970s, Avesta developed a high alloyed steel of 254 SMO with high amount of Mo (6.5wt %) and N (0.25wt %). This high nitrogen content permits high Mo content (about 6wt %) for the production of austenitic stainless steel over a wider range of section thicknesses and with excellent response to most types of welding (Wallen et al 2001). The direction of further developments in stainless steels is clearly the usage of nitrogen for its own merits and for its stability to permit higher chromium and molybdenum additions (Speidel 1991).

Recently, a major advancement that has taken place in austenitic stainless steel is the Avesta 654 SMO grade with increased Mo (7wt %) and nitrogen (0.3wt %)

contents. In this steel, the addition of higher amount of nitrogen (0.5wt % N) to SASS provides a significant increase in: (i) strength, (ii) toughness, (iii) pitting resistance and (iv) resistance to crevice corrosion. These enhanced properties of high alloyed SASS are achieved by the addition of appropriate combination of Cr, Mo and N (Speidel 1991). These steels offer a chloride resistant stainless steel that approaches the resistance of some nickel-based alloys (Wallen et al 2001).

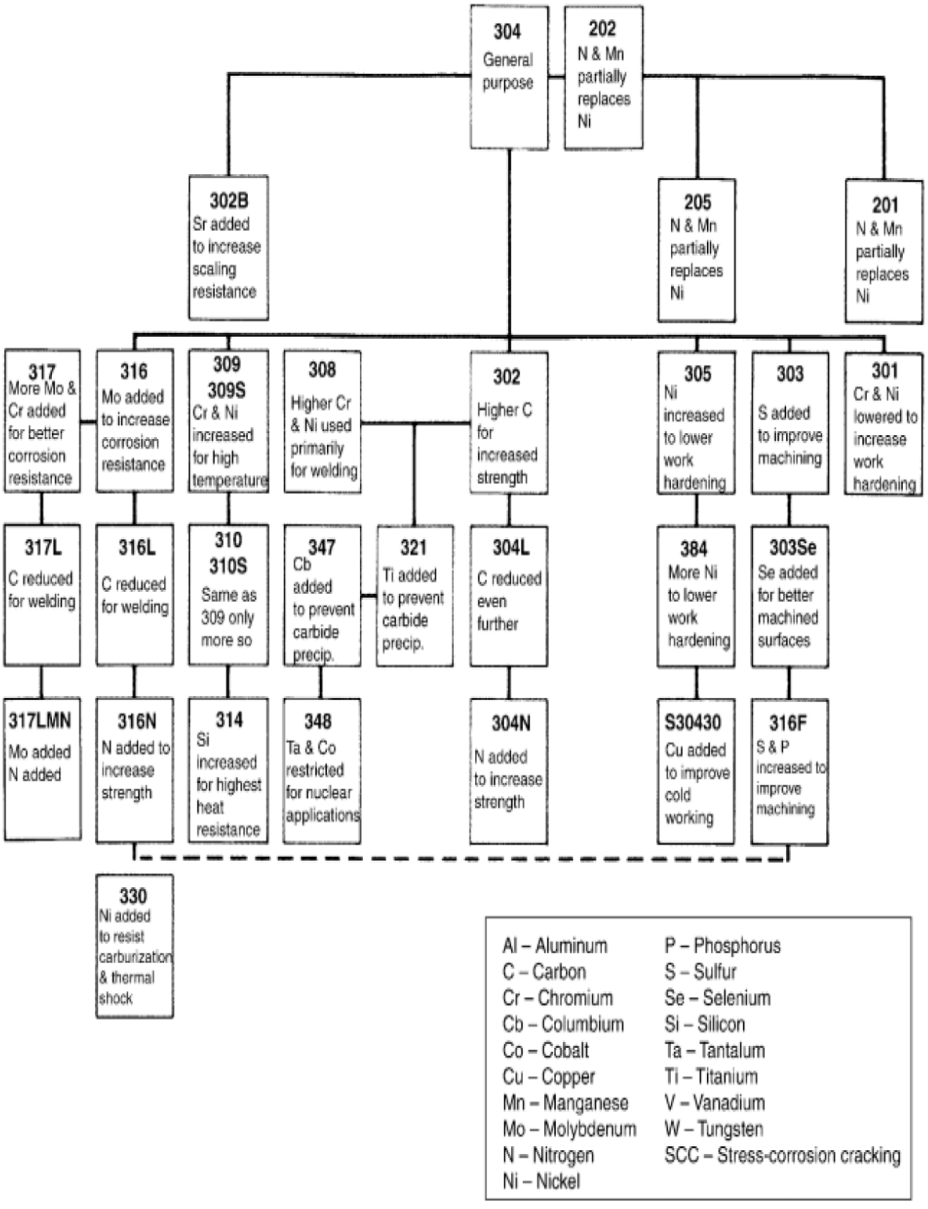

Fig 3.2 Austenitic Stainless steel family.
Source: www.asminternational.org

3.2.4.1 316 Austenitic Stainless Steel

The processing industries are experiencing unexpectedly short service life with equipment and piping fabricated from 316L stainless steel. It is speculated that the alloy is being produced with concentrations of chromium, nickel and molybdenum at the low end of the range specified for the 316L stainless steel. Consequently, the present 316L alloy is less resistant to corrosion, particularly to crevice corrosion. The situation raises several questions. How aware is the steel industry of the uncertainty with respect to the 316L alloy? Would simply increasing the concentration of molybdenum in the alloy, to the high end of the specified range, improve the resistance to localized corrosion? Is it possible to produce a 316L stainless steel (a "new" alloy) with the highest specified concentrations of chromium, nickel and molybdenum to obtain performance equivalent to the earlier 316L alloy? Assuming that sanitary tubing and the associated fittings in this "new" alloy became readily available, does it represent a cost effective alternative to the 904L, 2205 and AL6XN alloys? There is a concern in the processing industries, particularly in the food industry, that a significantly shorter service life is presently obtained from the 316L stainless steel equipment and piping. Industries use stainless steels to meet the standards that have been established for sanitary or hygienic processes, e.g., "3-A Accepted Practices for Product and Solution Pipelines." The austenitic stainless steels, 304, 304L, 316 and 316L, have become the workhorses of the food, beverage and dairy industries, representing a highly versatile and cost effective choice for the fabrication of process systems.

All stainless steels contain iron and chromium, with other elements such as nickel, manganese, molybdenum nitrogen and copper, introduced to further modify

the physical properties of the material. Advances in the techniques used in the manufacture of stainless steels have resulted in cleaner, purer products, the compositions of which can be closely controlled. Chromium imparts unique corrosion properties to the stainless steel, properties that are significantly different from those of carbon steels, low alloy steels and cast iron. For example, at concentrations of chromium above 11% by weight, the rate of general corrosion of a stainless steel is practically negligible. This corrosion resistance is attributed to the formation of a thin, passive film, generally considered to be chromium oxide, at the surface of the stainless steel. The addition of nickel stabilizes the austenite crystal structure in the steel, making it more weldable, less brittle and easier to shape and bend than the other crystal structures in which a stainless steel may exist. Manganese also stabilizes the crystal structure of the stainless steel and this metal is frequently used as a partial substitute for nickel. Molybdenum and nitrogen both enhance the resistance to pitting and crevice corrosion and nitrogen also tends to stabilize the austenite crystal structure. The carbon content of 304L, 316L and 317L stainless steels is specified to be 0.03% (maximum), reduced from 0.08% in the 304,316 and 317 steels. This is important since carbon reacts to form chromium carbide during annealing, welding and forming processes and the presence of carbide at grain boundaries leads to the onset of intergranular corrosion when the alloy is in service.

The concentrations of carbon, chromium, nickel and molybdenum in the stainless steels, that are used extensively in the fabrication of process equipment, process piping and process systems, are summarized in Table 3.4.

Table 3.3 The Composition of Stainless Steel

SS	Carbon	Chromium	Nickel	Molybdenum	Manganese	Nitrogen	Copper
304	0.08	18-20	8-15	---	2	---	---
304L	0.03	18-20	8-15	---	2	---	---
316	0.08	16-18	10-14	2-3	2	---	---
316L	0.03	16-18	10-14	2-3	2	---	---
317	0.08	18-20	11-15	3-4	2	---	---
317L	0.03	18-20	11-15	3-4	2	---	---
904L	0.02	19-23	23-28	4-5	---	---	1.5
AL6XN	0.03	20-22	25	6-7	0.4	0.2	0.2
2205	0.03	21-23	4.5-6.5	2.5-3.5	---	0.15	---

The alloys also contain 0.03% sulfur, 1% silicon, 0.045% phosphorus, with the balance being iron.

All the alloys have the austenitic crystal structure, except for 2205, which contains both austenitic and ferritic structures and is referred to as a duplex alloy.

3.3 Martensitic stainless steels

Martensitic stainless steels (MSS) are essentially alloys of chromium (12-16wt %) and carbon (0.06-0.15wt %) that exhibit martensitic structure of body centered tetragonal (BCT) crystal in the hardened condition. They are ferromagnetic, hardenable by heat treatment and they are generally less resistance to corrosion than some other grades of stainless steels. Elements such as niobium, silicon, tungsten, and vanadium can be added for MSS to modify the tempering response after hardening. Small amounts of nickel may also be added to improve the toughness. Sulfur or selenium is added to some grades to improve the machinability. Based on ASTM standards, the grades of martensitic stainless steels are referred as A410, A420, etc. Martensitic stainless steels are specified when the application requires good tensile strength, creep and fatigue strength in combination with moderate corrosion resistance and heat resistance up to approximately 650^{o}C. Martensitic stainless steels are also used in petrochemical equipment, stream turbine, gas turbine, etc., (Davis 1996).

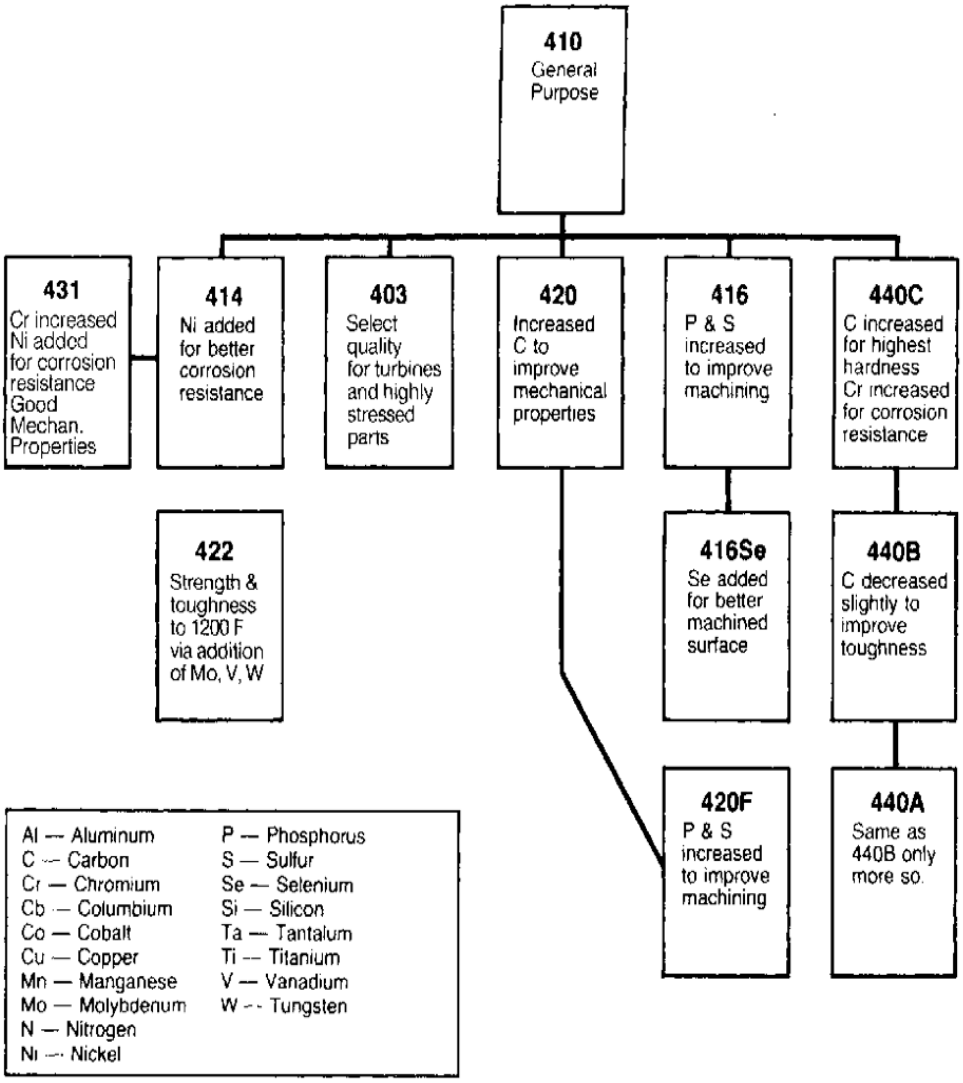

Figure 3.3 Martensitic Stainless Steel Family. (Davis 1996).

3.3.1 440 Martensitic Stainless Steel

Type 440 Stainless Steel, known as "razor blade steel," is a hardenable high-carbon chromium steel. When subjected to heat treatment, it attains the highest hardness levels of any grade of stainless steel. Type 440 Stainless Steel, which comes in four different grades, 440A, 440B, 440C, 440F, offers good corrosion resistance along with abrasion resistance. All grades can be easily machined in their annealed state;

they also offer resistance to mild acids, alkalis, foods, fresh water, and air. Type 440 can be hardened to Rockwell 58 hardness.

Stainless steels are high-alloy steels which have high corrosion resistance compared to other steels due to the presence of large amounts of chromium. Based on their crystalline structure, they are divided into three types such as ferritic, austenitic, and martensitic steels. Another group of stainless steels are precipitation-hardened steels. They are a combination of martensitic and austenitic steels.

Grade 440 stainless steel is a high carbon martensitic stainless steel. It has high strength, moderate corrosion resistance, and good hardness and wear resistance. Grade 440 is capable of attaining, after heat treatment, the highest strength, hardness and wear resistance of all the stainless alloys. Its very high carbon content is responsible for these characteristics, which makes 440 particularly suited to applications such as ball bearings and valve parts [65].

Corrosion resistance implies good resistance to the atmosphere, fresh water, foods, alkalis and mild acids; best resistance in the hardened, tempered and passivated condition. A smooth polished surface also assists in improving corrosion resistance. The corrosion resistance of grade 440C approximates that of grade 304 in many environments.

Heat resistance implies not recommended for use in temperatures above the relevant tempering temperature, because of reduction in mechanical properties by over-tempering.

Thanks to the outstanding properties of each of the grades, all grades of Type 440 Stainless Steel can be found in a number of products including:

- Pivot pins
- Dental and surgical instruments
- High quality knife blades
- Valve seats
- Nozzles
- Oil pumps
- Rolling element bearings

Each grade of Type 440 Stainless Steel is made up of a unique chemical composition. It should be noted that the only major difference between the grades is the level of carbon.

Type 440A

- Cr 16-18%
- Mn 1%
- Si 1%
- Mo 0.75%
- P 0.04%
- S 0.03%
- C 0.6-0.75%

Type 440B

- C 0.75-0.95%

Type 440C and 440F

- C 0.95-1.20%

All of the Type 440 Stainless Steels offered by Continental Steel meets or exceeds some of the toughest standards including ASTM, QQ, and MIL-S.

3.3.2 410 Martensitic Stainless Steel

Type 410 Stainless Steel is a hardenable martensitic stainless steel alloy that is magnetic in both annealed and hardened conditions. It offers users high levels of strength and wear resistance, along with the ability to be heat-treated. It provides good corrosion resistance in most environments including water and some chemicals. Because of Type 410's unique structure and benefits, it can be found in industries that demand high strength parts such as petrochemical, automotive, and power generation. Other uses of Type 410 Stainless Steel include:

- Flat Springs
- Knives
- Kitchen utensils
- Hand Tools

Applications requiring moderate corrosion resistance and high mechanical properties are ideal for Alloy 410. Examples of applications that frequently use Alloy 410 include:

- Cutlery
- Steam and gas turbine blades
- Kitchen utensils
- Bolts, nuts, screws
- Pump and valve parts and shafts
- Mine ladder rugs

- Dental and surgical instruments
- Nozzles

To be sold as Type 410 Stainless Steel, an alloy must have a certain chemical composition, which includes:

- Cr 11.5-13.5%
- Mn 1.5%
- Si 1%
- Ni 0.75%
- C 0.08-0.15%
- P 0.040%
- S 0.030%

Continental Steel offers high-quality Type 410 Stainless Steel in a wide range of sizes and shapes including coils and cut lengths. As with all the stainless steel supplied by Continental Steel, their Type 410 meets all the toughest industry specifications including AMS, and ASTM.

General Properties: Alloy 410 is the basic, general purpose martensitic stainless steel that is used for highly stressed parts and provides good corrosion resistance plus high strength and hardness. Alloy 410 contains a minimum of 11.5% chromium which is just sufficient enough to demonstrate corrosion resistance properties in mild atmospheres, steam, and many mild chemical environments. It is a general purpose grade that is often supplied in the hardened but still machineable condition for applications where high strength and moderate heat and corrosion resistance are

required. Alloy 410 displays maximum corrosion resistance when it has been hardened, tempered, and then polished [65].

Specifications: UNS S41000

Standards

- ASTM/ASME: UNS S41000
- EURONORM: FeMi35Cr20Cu4Mo2
- DIN: 2.4660

Corrosion Resistance

- Good corrosion resistance to atmospheric corrosion, potable water, and to mildly corrosive environments
- Its exposure to everyday activities (sports, food preparation) is generally satisfactory when proper cleaning is performed after exposure during use.

- Good corrosion resistance to low concentrations of mild organic and mineral acids [65].

3.4 Corrosion of Stainless Steel

3.4.1 Introduction

Harry Brearley of the Brown-Firth research laboratory in Sheffield, England is credited as inventing stainless steel in 1913, [27]. Stainless steel alloys are commonly used as construction materials for key rust-resistant components in most of the major industries: chemical, construction, petroleum, power, process, etc.

Stainless steel is a general term for a large group of corrosion resistant alloy steels. These stainless steels are iron-based alloys containing at least 11wt%

chromium [16]. This amount of chromium gives the stainless steel the ability to form a protective or passive film that resists corrosion. This protective film is self-forming and self-healing and this makes stainless steel resistant to corrosion [28]. The stability of the passive film is enhanced by increasing the chromium content [29]. At about 10.5% chromium, a weak film is formed and will provide mild atmospheric protection. By increasing the chromium to 17-20%, which is a typical concentration in type 440 series of martensitic stainless steels, the stability of the passive film is increased and therefore more corrosion resistance is gained. However, stainless steels cannot be considered to be 100% corrosion resistant. The passive state can be broken down under certain conditions and corrosion can result [30].

As stated above, stainless steel has a good corrosion resistance, but is not resistant to corrosion in all environments and might suffer from certain types of corrosion in some media. Corrosion of stainless steels can be categorized as one of: crevice corrosion, general corrosion, inter-granular corrosion, pitting corrosion, stress corrosion cracking and/or galvanic corrosion [48].

General and pitting corrosion are the most likely types of corrosion and most relevant to our present study; so further information about these two types of corrosion will be described in this thesis. The general corrosion is a uniform attack and is the most commonly encountered type of corrosion. It is characterized by a chemical or electrochemical reaction which proceeds uniformly over the entire surface of the exposed material. This general corrosion happens where none of the alloying elements in the material could form a protective layer and normally this is the case during the active and transpassive dissolution of materials [49]. Thus, the metal becomes thinner and eventually fails. The general corrosion of stainless steels normally occurs in acids and hot caustic solutions, and corrosion resistance of the stainless steel usually

increases with increasing levels of chromium, nickel and molybdenum. Moreover, other alloying elements are added to the stainless steel alloys to modify their structure and enhance properties such as formability, strength and cryogenic toughness. Further information about the effects of alloying elements will be covered in the next section.

3.4.2 Effects of Alloying Elements

The properties of metals can be modified by adding alloying elements. In this way, the properties of stainless steel can be adapted so that it can be used in specific environments. In the following section, brief information about the benefits of each ingredient added to stainless steel is presented [31]:

Chromium: is the main element that improves the corrosion resistance of the alloy by forming a passive film on the surface. Chromium provides resistance to oxidizing environments and resistance to pitting and crevice attack. Other elements in the alloy can influence the effectiveness of chromium in forming or maintaining the surface film.

Nickel: is added to stabilize the austenitic structure of the stainless steel and enhance the mechanical properties and fabrication characteristics. Nickel also promotes re-passivation if the film is damaged.

Molybdenum: next to chromium, molybdenum provides the largest increase in corrosion resistance in stainless steel. Molybdenum, in combination with chromium, is very effective in stabilizing the passive film in the presence of chlorides. It is effective in preventing crevice or pitting corrosion.

Manganese: also stabilizes the austenite. In association with nickel, it performs many of the functions attributed to nickel but by substituting manganese for nickel, and then combining it with nitrogen, strength is also increased.

Nitrogen: It is used to stabilize the austenitic structure of stainless steel. It enhances the resistance of stainless steel to pitting and crevice corrosion especially in the presence of molybdenum [32].

Carbon: it increases the strength of steel and is considered as a very strong austenitizer. In low carbon grades stainless steels, carbon is kept in 0.005% to 0.03% level to maintain the desired properties and mechanical characteristics. Carbon can combine with chromium forming chromium carbide precipitation usually at grain boundaries. This may have a negative effect on corrosion resistance by removing some of the chromium from solid solution in the alloy and, as a result, reducing the amount of chromium available to ensure corrosion resistance [31].

Titanium and Niobium: They are used to reduce the sensitization of stainless steel to reduce the possibility of inter-granular corrosion when the stainless steel is welded or heat treated. Titanium and niobium interact with carbon to form carbides, leaving the chromium in solution so that a passive film can form.

Copper and Aluminum: These materials, along with titanium, can be added to stainless steel to precipitate its hardening. These elements form a hard intermetallic microstructure during the soaking process at an elevated temperature.

Silicon: It is added to some alloys for high temperature oxidation resistance. Figure 3-5 summarizes how these elements can influence the corrosion behavior of stainless steel [33].

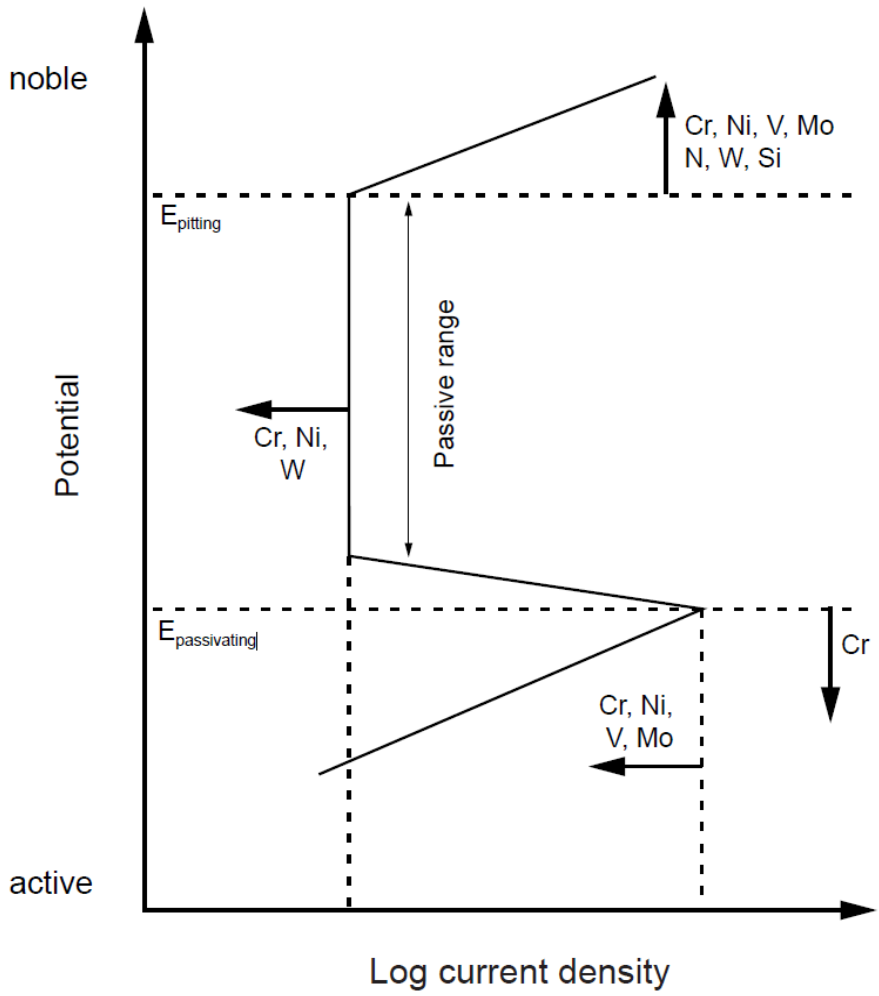

Figure 3.4 Schematic summary of the effects of alloying elements on the anodic polarization curve of stainless steel [33].

3.5 Corrosion by Acetic Acid

3.5.1 Introduction

Acetic acid (CH_3COOH) is one of the most important intermediates and the most frequently used carboxylic acid. When pure, acetic acid is a clear, colorless liquid with the smell of vinegar. At ambient temperature, 25^oC, pure acetic acid boils at 118^oC and its freezing point is only slightly below room temperature at 16.7^oC [99].

Acetic acid is classified as a weak acid, because it does not completely dissociate into its component ions when dissolved in aqueous solution [100]. Acid dissociation constant (Ka) is a quantitative measure of the strength of the acid in solution. It is equal to the concentration of the products divided by the concentration of reactants. For acetic acid, it can be written as:

$$CH_3COOH_{(aq)} \rightarrow CH_3COOH^-_{(aq)} + H^+ (aq) \quad (3.3)$$

$$Ka = [CH_3COO] * [H^+] / [CH_3COOH] \quad (3.4)$$

The acid dissociation constant (Ka) value for acetic acid is 1.8 Å~ 10^{-5} (mol/L) at 25^oC.

3.5.2 Corrosivity

In general terms, carboxylic acid aggressiveness increases with decreasing number of carbon atoms in the alkyl chain [101, 102]:

$$C_4H_9COOH < C_3H_7COOH < C_2H_5COOH < CH_3COOH < HCOOH \quad (3.5)$$

Usually, acetic acid is not considered to be a highly aggressive medium; however, it can severely attack most materials at higher temperatures, near its boiling point, upon aeration and if it contains impurities, for example oxidizing agents, chlorides, formic acid or acetic anhydride [33].

In acetic acid systems, steel is attacked quite rapidly at all concentrations and temperatures and is normally unacceptable for use in acetic acid environment. Also, field experience with the 400 series stainless steel group indicates high rates of corrosion and pitting attack [103].

The 440 stainless steel alloy is most commonly used in equipment for processing acetic acid. However, the behavior of this alloy is greatly affected by impurities in the acid. Contamination with chloride ions can cause pitting, rapid stress corrosion cracking and accelerated corrosion of 440 stainless steel [104]. Similar to chloride, the presence of other halides such as bromide (Br) in the acetic acid environment may lead to corrosion problems for stainless steel alloys [105]. A number of field failure investigations and laboratory studies, carried out on 440 stainless steel type, in acetic acid environments have been reported in the open literature.

Sekine et al. [106, 107] worked extensively on the corrosion behavior of stainless steels in different concentrations of acetic acid. They concluded that the corrosion rate depends markedly on concentration, temperature, solution conductivity, water and oxygen content. It was found that 316 stainless steel had sufficient corrosion resistance at room temperature in each acid concentration. In boiling acetic acid, a maximum corrosion rate of 0.09 mm/year was measured for the 316 stainless

steel and this was in 90 vol. % acid concentrations. Also, they concluded that chromium and molybdenum mainly contribute to corrosion resistance in aqueous solution, while nitrogen contributes only slightly. In the presence of aggressive ions such as chloride and bromide in acetic acid environments, Ashiru et al. reported severe pitting corrosion problems in terephthalic acid production plant [108]. The materials of construction were 316L stainless steel and 2205 duplex stainless steel. It was concluded that pitting corrosion was caused by process upset and the presence of aggressive chloride contaminant in the acetic acid media. Also, Li et al. [109] reported relatively serious intergranular corrosion and pitting in 316L stainless steel packing of a solvent recovery tower in a terephthalic acid plant. Inter-granular corrosion attack was due to the lack (depletion) of chromium in the grain boundaries while the pitting problem was caused by the damage to the local passivation film due to the presence of bromide ions in the acetic acid solution.

CHAPTER 4

CARBON STEEL CORROSION

4.1 Introduction

The high cost of corrosion affects numerous industries, domestic applications and public sectors worldwide and highlights the need for improved corrosion resistance measures. Effective corrosion inhibition has a high economic value as the annual corrosion cost is estimated to reach 3–4% GDP in developed countries.[59] In oil, gas and chemical industries alone, corrosion is one of the most challenging tasks, and it is assumed that it costs 170 billion USD per year.[60,61] It is not only the high cost of corrosion, but also the health and environmental risks associated with potential failure of the oil and gas equipment that drive the developments of corrosion resistant materials and improved corrosion mitigation strategies worldwide. Low-cost carbon steels are used as the preferred construction material across industries and are considered the more economical option than the costly corrosion resistant alloys. Carbon steels typically contain less than 1.5% carbon content along with the minute presence of Mn, Si, P and S. Based on the percentage of carbon, the classification is further divided into three forms, namely low carbon steels (<0.25% C), medium carbon steels (0.25–0.70% C) and high carbon steels (0.70– 1.05% C). Variation in the percentage of carbon content allows to attain different mechanical properties such as strength, ductility, hardness, etc. Based on the steel properties, related to carbon content, plain carbon steels are further divided into certain grades, such as grade 1008 (0.08wt% C), which is good for forming and has good ductility; grade 1018 (0.18wt% C); it is useful for general applications and good for welding; grade 1030 (0.30wt%

C), which has low hardenability; grade 1045 (0.45wt% C), which has applications in power transmission and shafting; and X-65, which is a seamless grade and weldable.

Carbon steels are used in a wide range of applications, such as structural components, industrial pipes, and kitchen appliances. With regard to applications in the oil and gas industry, the two major forms of corrosion are carbon dioxide (CO_2) corrosion, which is also known as sweet corrosion, and hydrogen sulphide (H_2S) corrosion, which is most commonly known as sour corrosion. Among these two, CO_2 corrosion has attracted a lot of attention to researchers since 1949 because oil wells normally contain CO_2.

Carbon steels, in general, are susceptible to corrosion under the conditions at industrial operations and high levels of corrosion inhibition are important for safe and cost-effective operations that extend the limits of use of carbon steels alone. In oil and gas industries, corrosion inhibition can occur naturally through crude oils due to the presence of certain chemical species such as nitrogen, sulphur, aromatic resins, etc. [66,67] The most utilized corrosion inhibition measure is however the use of organic or inorganic inhibitors that protect the steel surface by forming a protective film of a passive nature.[68] Corrosion inhibitors typically contain nitrogen, sulphur and oxygen, and hydrophobic hydrocarbon chains in their structures. Corrosion inhibitors adsorb on the steel surface (either through physical or chemical adsorption) and change the surface and interface free energies. It is postulated from earlier studies that inhibitors alter the wettability of a surface. [69] Physical adsorptions is an electrostatic change whereas chemical adsorption occurs through a bond formation by sharing an electron. As the use of inhibitors for preventing corrosion of carbon is often the most economical option, it is of significant interest to the industry to define the application limits of film forming corrosion inhibitors. Commercial inhibitor

formulations virtually never use a single molecule due to the observed synergistic effects that enhance their performance. However, there is no clear explanation in the open literature as to how chemical components of the corrosion inhibitor formulations self-assemble on metal surfaces to protect synergistically against corrosion. Most importantly, the formation of corrosion-protective films is expected to be strongly affected by the nature of the metallic substrate, i.e. carbon steel. It is clear that a definition of limits and potential extension of the use of carbon steels in different corrosive environments is only achievable with a detailed understanding of the mechanisms of carbon steel corrosion and its inhibition. This review therefore focuses on the importance of texture, surface morphology, surface energy and defects for the corrosion of carbon steels. We discuss in detail the methods of analysis of carbon steel surfaces under corrosive conditions, and in the absence and presence of corrosion inhibitors. In particular, we assess the applicability and limitations of analytical methods that have been utilized on carbon steels; and those that have been applied to other metallic substrates, but could have potential applications for studies on carbon steel substrates.

4.2 Role of Texture in Corrosion of Carbon Steels

Surface texture, also addressed as preferred orientations, is one of the important parameters investigated in relation to corrosion. Surface texture develops in alloys and metals during their mechanical deformation such as rolling, forging, drawing, etc. and the established preferred orientations can introduce significant changes to the material properties, including changes in friction and wear properties. Besides mechanical deformation, texture development can also occur during phase transformation,

recrystallization, grain growth, etc. [70,71] Surface texture can also be associated with special morphology and roughness of the surface, but this review uses the term surface texture with relation to crystallographic orientation. The importance of texture in corrosion investigations lies in its relation to corrosion resistivity of the materials. It is an established fact that the activation energy for dissolution of a densely packed surface is higher than that of a loosely packed surface. The opposite effect is known for surface energy, with a dense plane having a lower surface energy than a loosely packed surface. It is expected that dense planes dissolve at relatively slow rates compared to the low dense (loose) planes. [72] It has been established that crystals that are oriented towards low surface energy (i.e. highly dense planes) can result in increase in corrosion resistance [73].

Texture is also important for welded structures as crystallographic orientation and crystallite interface are strongly correlated with corrosion resistance. The microstructural difference in the weld nugget and the surrounding area, due to precipitation, affects the texture of the steel through microstructural gradient generation. As many failures in the industry are related to the corrosion at welded areas, it is highly desirable to understand and examine the texture at weldments in corrosion investigations. [74,75] Similarly, texture is an important parameter in surface chemical reactions as highly textured crystal faces promote the solid–liquid interfacial reactions. [75,76] The significance of texture in corrosion has been proven by numerous researchers. This thesis focuses on establishing the role of texture in corrosion behavior of carbon steels in corrosive environments.

Bateni et al. [79] investigated the effect of carbon-steel texture on the corrosion process. Under corrosive conditions, the fiber texture and cube texture developed,

which was different from the texture developed in dry wear test, i.e. Goss texture and gamma fiber. In a corrosive environment, NaCl behaves as a lubricant and develops a different orientation distribution function (ODF) by reducing the metallic contact. It is noticed that the same load (9.6 N) applied for dry wear test and the test under corrosive media depicted different ODF. It was stated that shear stress reduction leads to less shear texture formation and resulted in the disappearance of Goss and brass texture in corrosion wear situation. This is due to NaCl acting as a lubricant and reducing frictional force. It was also observed that the weight loss rate under corrosive wear condition was lower than the dry wear condition because of the same lubrication formation by NaCl.

Recently, Baik et al.[80] studied sulphide stress corrosion cracking of carbon steels with the help of strain rate measurement and found strong correlation between sulphide stress corrosion cracking and strain rate test results, which is indirectly related to the surface texture. This is because the movement of dislocations is easier at a certain plane of crystals, known as dense pack plane ((111) (for FCC metals with high atomic density) in BCC iron. This is in agreement with an earlier study showing that pit initiation occurs in sequence of (110) > (100) > (111) whereas pit propagation takes place in the following order (100) > (110) > (111). [24]

Texture generation can be influenced by numerous factors, such as impurities, stacking fault, inherently stored deformation energy, casting and rolling conditions, grain size and shape, grain boundary angle, shear bending, precipitation. Rabbe et al. [84] observed cube type fiber orientation in low carbon steels and showed that active slip system steel which got hot rolled in the austenitic regime shows random austenitic texture and texture gradient across the thickness, and undergoes

recrystallization due to low stacking fault energy. It has been observed that Si and Cr affect the texture in terms of the generation of alpha fiber.

Park et al. [81] investigated corrosion of steels samples, alloyed with Cu and Sb, under aggressive corrosion environment (16.9 vol% H_2SO_4 and 0.35 vol% HCl at 60 °C, pH 0.3). The authors compared corrosion properties of the steels formed by hot rolling and cold rolling. The interesting facts revealed by this study were that the corrosion rate of cold rolled steel was higher than the hot rolled steel. This study again proved the importance of mechanical deformation in corrosion behavior of steels as well as alloys. This was linked closely with the texture of steel as in cold rolled steel, the grain refinement and orientation were the key factors for corrosion. [85] It was observed that a large number of grains were oriented with {001} along with {101} and {111} in cold rolled steel whereas in the case of hot rolled steel {111} crystallographic orientation, it was found dominant along with {101} and {001}. Lower corrosion resistance of cold rolled steel compared to hot rolled steel is related to the high surface energy in {100} direction as low surface energy plane offers slow dissolution rate of atoms due to its closed atomic packing and results in high corrosion resistance.

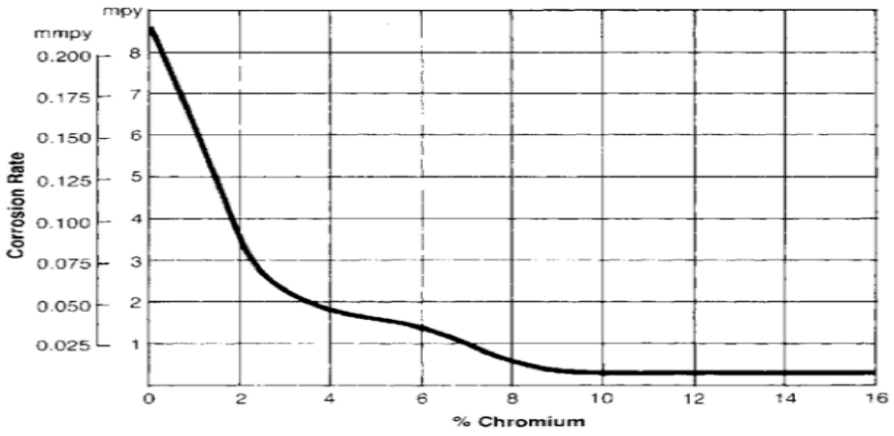

Figure 4.1 Effect of Chromium content on Corrosion Rate.

It has been demonstrated that deformation conditions, such as hot rolling and cold rolling parameters, affect the texture development in steel. Rolling schedule, rolling temperature, reheating time and temperature, etc. are some of the important parameters to consider for texture development. Texture varies over the entire thickness of the specimen

Cold rolled low carbon steel was studied by Xu et al. [82] with four different microstructures, namely ferritic, acicular ferritic, coarse polygonal ferritic and bainitic. All specimens were cold rolled and annealed in the temperature range of 853–953 K. Polygonal ferrite exhibited string texture along {223} <110>, similarly acicular and bainitic showed string texture along {001} <110> and during annealing, all samples exhibited fibrous texture ({111} <uvw>) (with 70–90 reduction). This study elucidated the importance of microstructure and deformation condition with texture.

The deformation procedure affects corrosion such as in cold rolled steel, showing low corrosion resistance due to externally applied tension as well as due to texture. Cold deformation often introduces deformation twinning and dislocation arrays, which are accepted as one-dimensional crystal defects. The defects generated on the surface during cold deformations may be more important than texture for cold rolled steels. Cold worked stainless steel (316 type) exhibits high diffusivity for Cr and easy carbide nucleation by offering low free energy barrier. Earlier explanations in this section have already established the relationship between the deformation process with texture and corrosion resistance. [83]

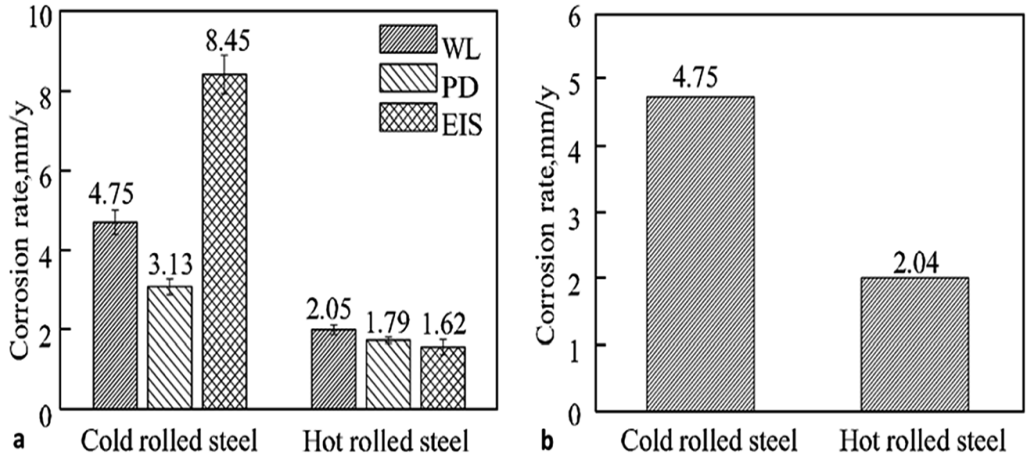

Figure 4.2 (a) Comparison of the corrosion rates of cold and hot rolled steel by weight loss (WL), potentiodynamic polarization (PD) and electrochemical impedance spectroscopy (EIS) measurements; (b) comparison of weight loss measurements for cold and hot rolled steel after 6 h immersion in 16.9vol% H_2SO_4 and 0.35vol% HCl solution at 60 _°C (pH-0.3).

Deformation conditions also affect stacking fault energy. This is responsible for the change in the phase stability and phase transformation. Volume fraction and distribution of phases are other specific parameters that affect the corrosion properties of steels.

The importance of phases in the structure of carbon steels is further highlighted by their effect on the inhibitor applications for enhanced corrosion resistance. Oblonsky et al. [86] explained the importance of phases in the inhibitor molecules' attachment to carbon steel, showing that octadecyldimethyl benzylammonium chloride (ODBAC) attached to ferritic–pearlitic microstructures through physical adsorption, but did not adsorb to the martensitic phase in the carbon steel.

Naderi et al. [87] studied the effect of inhibitors on differently heat treated steels and found slightly lower corrosion in pearlitic steel due to the protective oxide film formation compared to martensitic steel in 1 M HCl solution, whereas in the presence of inhibitors N,N'-ortho-phenylen acetyle acetone imine (S1) and 4-[(3-{[1-(2-hydroxy phenyl)methylidene]amino}propyl)ethanemidol]- 1,3-benzenediol (S2), pearlitic steel exhibited better adsorption of inhibitors than martensitic steel.

The effect of texture on inhibitor adsorption could be very useful to study in the near future as Herrera et al. [88] have shown that heat treatment affects texture evolution. It was observed that cold rolling with large thickness reduction changed the texture of steel (SAE 1050) such as gamma <111>//ND, alpha <110>//RD and gamma prime <223>//ND, whereas after annealing with 50 and 80% reduction, gamma and gamma prime were completely invisible. As explained earlier, heat treatment affects the corrosion resistance and this could be related to texture evolution and the adsorption of inhibitors might be influenced by certain specific textures. This highlights the need for extensive investigations in this area in order to get deep insights into the mechanism of corrosion inhibitor adsorption.

Kandeil et al. [89] investigated the effect of surface texture on corrosion behavior of carbon steel and developed a regression equation for corrosion potential and polarization potential, correlating the corrosion rate, corrosion potential and polarization potential with surface properties.

In the assessment of texture and its role in corrosion, one needs to consider dislocation effects. Dislocations are considered as one dimensional defects in materials and are closely related to the texture development as high dislocation density introduced by tensile deformation causes weakening of the crystallographic

orientation. This phenomenon is closely related to corrosion as high corrosion rates were obtained at sites where dislocations intersect the surface.

4.3 Effects of Surface Energy and Morphology on Corrosion of Carbon Steels

In the previous section, we have described the importance of texture for corrosion of carbon steels and also proposed the ways through which texture could be controlled. There are however other parameters such as microstructure, chemical composition, defects (e.g. stacking fault energy, dislocation, precipitates, point defects) and surface energy of crystal planes, etc. that also affect the corrosion properties of steel. The relationship of texture with microstructure, phase composition and the relation of texture with stacking fault and defects are critical. Passive films contain a number of point defects such as interstitial cations (donors) and oxygen vacancies (donor) and/or cation vacancies (acceptor). Movement of cations through the oxide film contribute to the formation of a passive film and increased oxygen leads to an incompact passive film. An interstitial cation can render a metal more easily dissolvable, resulting in decreasing corrosion resistance. [90,91] Corrosion, texture and surface energy are interrelated as shown in the case of aluminum alloys, where the surface energy of aluminum was at maximum when low corrosion resistance was observed. [92]

Crystallographic planes with high surface energy offer adsorption sites for atoms and thus assist with the development of surface films. Film formation could occur due to the effect of the surface energy or through variations in the surface texture as shown by Perlovich et al. [93] It has been observed that texture-induced stress results in the formation of a film on the steel substrate. A high surface energy (low atomic density) crystallographic plane offers sites for water adsorption or proton adsorption and causes hydrogen evolution (hydrogen reaction process), whereas a low

surface energy plane (high atomic density) presents a site for hydrogen-reduction reaction. [94] Adsorption of hydrogen in a high surface energy plane causes corrosion with dissolution of atoms in that plane. Also, the evolution of hydrogen leads to development of pores on the surface, which is detrimental for corrosion resistance of the steel substrate. Similarly, an increase in the carbon content in grain boundary increases the chances of cleavage fracture by increasing the surface energy. The surface energy of pure austenite was found to be higher than that of pure ferrite, whereas, in the case of a hydrogen-containing system, a decrease in surface energy was observed for both austenite and ferritic phases (Fig. 4a). This study described the role of chemical constituents of steel in contributing to its surface energy as well as the durability of steel in relation to its surface energy as incorporation of carbon in austenitic steel widely affected its surface energy, but had lesser effect on ferritic steel (Fig. 4b).

Surface energy can be altered by alteration of texture, as discussed earlier, which in turn influences the corrosion resistivity of the steel substrate. Another aspect of addressing surface energy is hydrophobicity. A well-established concept of hydrophobicity is very important for corrosion studies of metals or alloys. It is proven that high hydrophobicity prevents liquids from staying on the solid surface for an extended period of time and leads to less exposure of solid surface with liquid by decreasing the contact area between them. Therefore, it is required to understand the surface energy and morphology effects for corrosion studies. Hydrophobicity is related to surface energy as high hydrophobicity requires low surface energy. [95] It is however important to understand that low surface energy alone cannot be considered as the deciding factor for a super-hydrophobic surface. There are other factors that need to be considered, such as surface morphology, including hierarchical

morphology as described earlier in this section, [95–96], surface roughness as increasing surface roughness causes high hydrophobic surface generation [97,98].

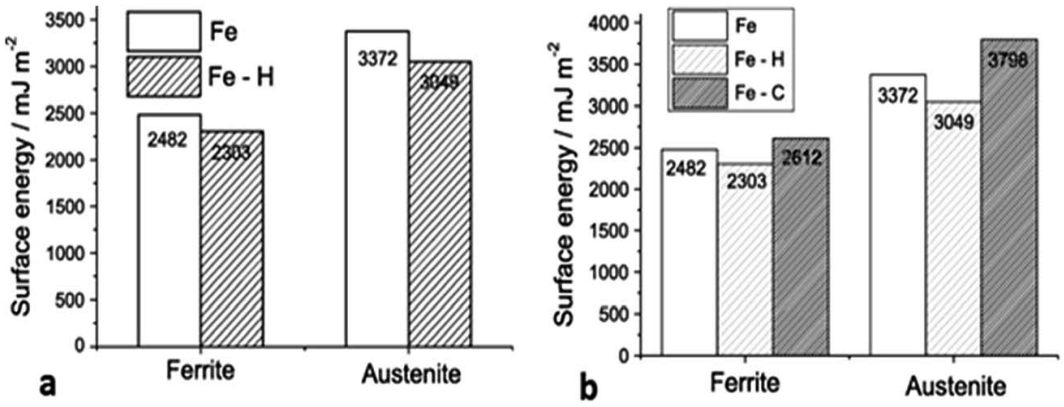

Figure 4.3 (a) Comparison of ferrite and austenite surface energy under hydrogen and hydrogen free condition, exhibiting hydrogen addition caused reduction on surface energy for both ferrite and austenite; (b) computed surface energy of ferrite and austenite [under pure (metallic form) and hydrogen, carbon containing system] exhibited lower surface energy for hydrogen containing system for ferrite and austenite than Fe and Fe–C system. [99]

For corrosion protection, it is necessary that a steel surface has little contact with corrosive media and a surface must have hydrophobic characteristics that can be developed either by increasing the roughness of a surface, which has low surface energy or by low surface energy material coatings on a rough surface. However, a study by Yu et al. [100] showed that super hydrophobic surfaces cannot always prevent corrosion. Certain rolling characteristics should be maintained. Rolling is a mechanical deformation process, which is a well-known process for texture development of materials as discussed in the previous section, but its relation to surface energy in terms of hydrophobicity has not been largely addressed. The development of a hydrophobic surface film using film forming corrosion inhibitors is nowadays rather a conventional way of increasing resistivity of carbon steel surfaces.

An important emerging alternative to the conventional formation of corrosion-protective surface films is morphological modification of the steel and the consequent development of hierarchical morphology generation. Zhang et al. [101] developed a super hydrophobic surface in steel by texturing with the help of a hydrogen fluoride (HF) and a hydrogen peroxide (H_2O_2) solution mixture and the super-hydrophobicity was examined by contact angle measurements (Fig 4.4), which depicts the transformation of hydrophilic bare steel surface to hydrophobic surface. Morphological observation through scanning electron microscopy (Fig 4.5) revealed that the surface contained islands covered with nano-flakes that lead to the hierarchical-surface generation, which is very important for securing hydrophobic nature of the surface. A hierarchical surface is a surface of multiple roughness, which is the origin for the observed hydrophobicity of this surface (Fig 4.6). After 24-hour immersion of textured (modified) steel in 3.5% NaCl solution, the contact angle was not significantly changed which suggested stability of the surface for long duration, while Fig 4.6b shows high corrosion resistance of modified steel surface due to the "cushion" and capillarity effect. Super hydrophobic textured steel does not allow water and Cl_ to reach the bare steel surface.

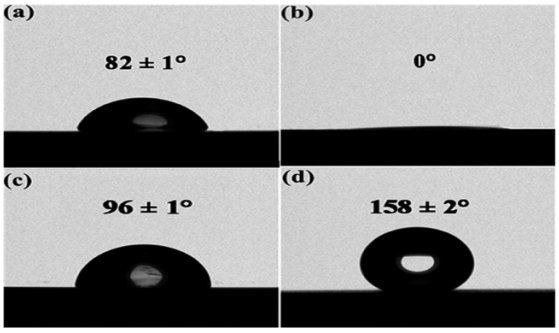

Figure 4.4 Contact angle measurements on (a) the bare steel, (b) the textured steel, (c) the modified bare steel, and (d) the modified textured steel. Modification of textured steel depicted its hydrophobic nature. [101]

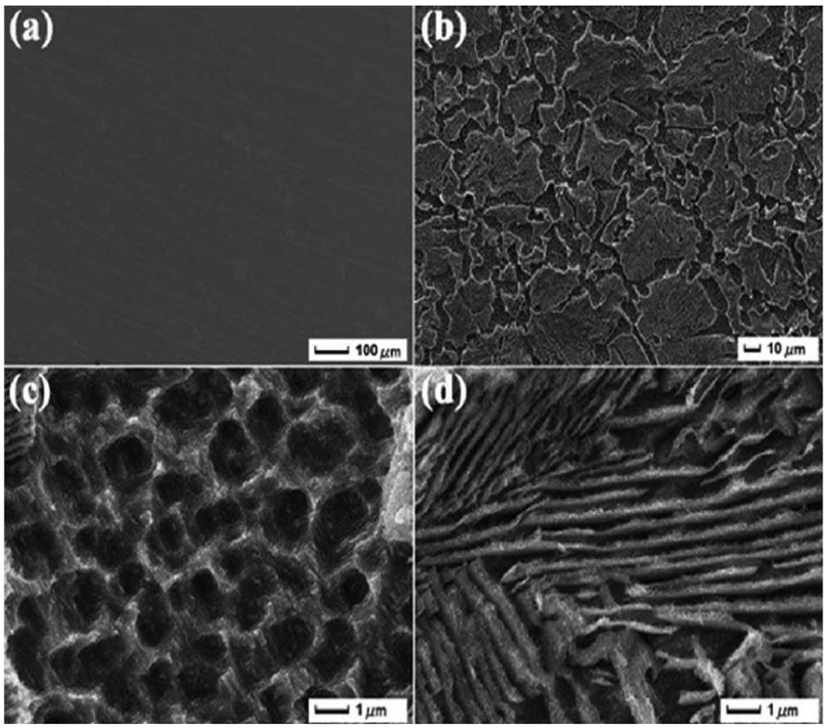

Fig. 4.5 Morphological images recorded via SEM clearly elucidate the differences for (a) the bare steel and (b) the textured steel surface. (c and d) Magnified images of (b). [101]

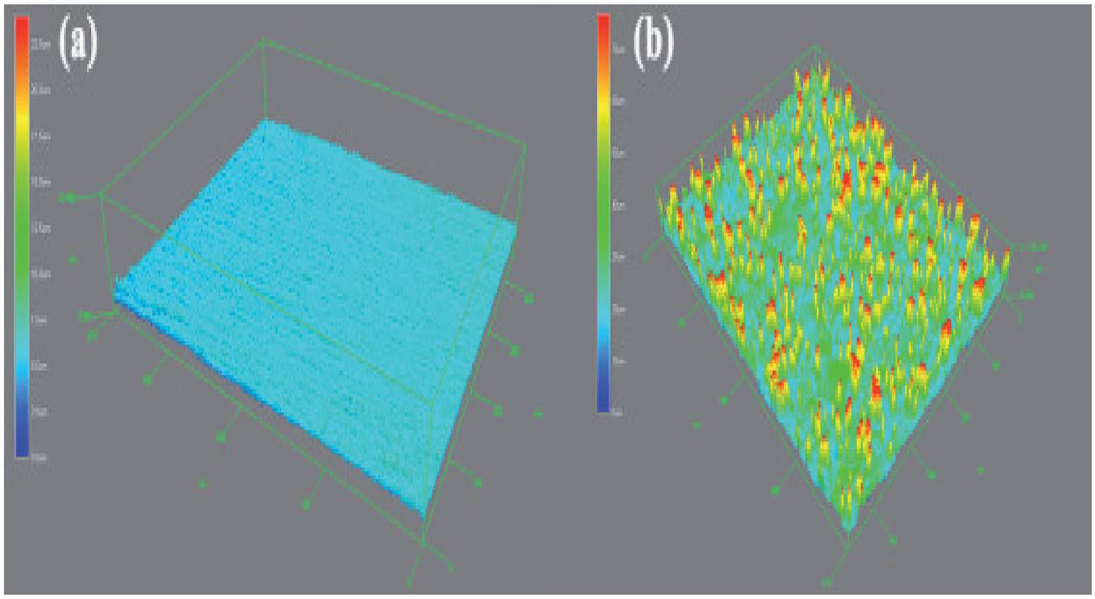

Fig. 4.6 Surface profile variations in (a) the bare steel and (b) the textured steel surface. [101]

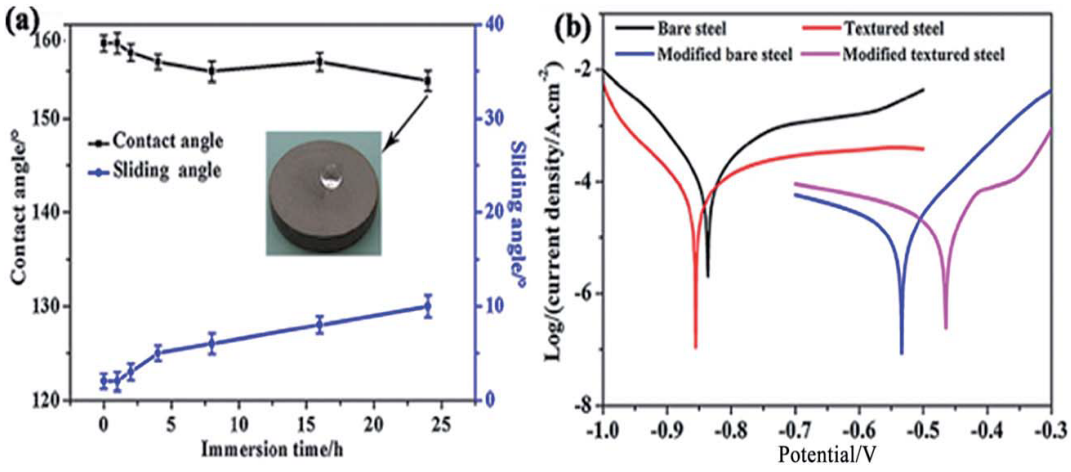

Fig. 4.7 (a) Establishing relationship between the contact angle and sliding angle of the super hydrophobic surface with the immersion time (3.5% NaCl solution); (b) exhibited the effect of surface modification on polarization behavior as polarization curves for the bare steel, the textured steel, the modified bare steel, and the modified textured steel are found different. [101]

A similar approach, involving a template and chemical etching of the substrate was adopted by Yuan et al. [102] This study is beyond the scope of this review as it dealt with iron, but is highly significant as it establishes chemical etching as an important technique for the development of hydrophobic surfaces. It has been observed that the hydrophobic surface has a hierarchical structure. [103] Wu et al.[104] protected mild steel by a one-step electro deposition process of a SiO_2 film, which was hydrophobic in nature. Deposition was done through sol–gel process with tetra-ethoxysilane and dodecyltriethoxysilane precursors. A rough surface with low surface energy was achieved and this study brought attention to the importance of surface roughness in corrosion science. Atomic force microscopy is a technique suitable for identification of the surface roughness, which is discussed in this review. The importance of morphology of the protective surface layer as well as its hydrophobicity have been established. A surface layer with significant roughness and less surface energy, that is

hierarchically structured, can increase the corrosion resistivity of the steel. The adherence of the surface film to the substrate (an alloy or metal) also plays a significant role as low adherence of the surface film to the steel substrate always causes high interface energy and thus provides instability of the interface.

Ramachandran et al. [105] investigated corrosion resistive properties of a super-hydrophobic surface of cast iron and identified the relation between surface energy and electric potential by application of the Lippmann law of electro-wetting and Lechatelier principle. This study described the behavior of a hydrophobic surface in terms of the observed decreasing corrosion potential for hydrophobic surfaces. The methodology could be adopted for plane carbon steels when investigating the behavior of a hydrophobic surface in terms of corrosion potential.

As far as the mechanism of corrosion prevention through hydrophobic surface formation is concerned, it has been documented that a super-hydrophobic surface can trap air in its structure, due to its hierarchical nature. This leads to improved corrosion protection of the underneath surface through restricting the corrosive ions to strike the surface of the steel substrate [106].

It is certainly an emerging field in corrosion science to determine the behavior of carbon steel morphology and texture with respect to both the surface energy and interface energy. Furthermore, we realize that a clear relationship between the hydrophobicity and rolling texture of carbon steels has not been established. We observe from the literature that hierarchical morphology of surface films improves the corrosion resistance due to the multiple-roughness structure. Hierarchical structures can be developed through residue or particle deposition. Another method of generating hierarchical structures is to modify the steel surface, which is typically

achieved through etching. [108] It is also important to note that the mechanical stability and phase stability of the films and structures have not been investigated, but are of significance to the mechanistic studies on corrosion inhibition of carbon steels. Mechanical stability of hierarchical films or morphology could be determined using atomic force microscopy (AFM), where the force required to remove surface film with the AFM tip is measured (scratch test), whereas phase stability could be determined through X-ray diffraction spectroscopy (XRD) or high-temperature XRD.

Another area which is yet to be investigated is the effect of the metallic, non-metallic inclusions and intermetallic phases on the hierarchical structure development. These areas demand extensive investigation as far as carbon steel corrosion is concerned. Furthermore, the mechanistic investigations into the formations of the hierarchical structures on steel surfaces and their corrosion inhibition properties should consider other influencing factors, such as porosity and surface roughness, that are already described for development of surface films (of nonhierarchical structure) on carbon steels. It has been shown, for example, that the formation of iron carbonate layer on carbon steel exposed to carbon dioxide media is affected by the velocity of the carbon dioxide gas. This in effect changes the porosity of the iron carbonate surface film and its protectiveness against corrosion. [109] Future developments of hydrophobic carbon steel surfaces and the mechanistic studies on their formations and modifications will require advanced investigations that consider the properties of carbon steel structures addressed in this review. Such advanced studies, combined with competent theoretical techniques, could reveal the mechanisms involved in the process of corrosion of carbon steels.

4.4 Carbon Martensitic stainless steels

The data presented in Table 4.1 are straight-chromium 400 Series types that are hardenable by heat treatment. They are magnetic. They resist corrosion in mild environments. They have fairly good ductility, and some can be heat treated to tensile strengths exceeding 200,000 psi (1379 MPa). Type 410 is the general-purpose alloy of the martensitic group.

Table 4.1 Chromium 400 Series

Martensitic Stainless Steel			
Type	Equivalent UNS	Type	Equivalent UNS
403	S40300	420F	S42020
410	S41000	422	S42200
414	S41400	431	S43100
416	S41600	440A	S44002
416Se	S41623	440B	S44003
420	S42000	440C	S44004

4.4.1 Mechanical properties

The martensitic grades are so named because when they are heated above their critical temperature (1600ºF or 870ºC) and cooled rapidly, a metallurgical structure known as martensite is obtained. In the hardened condition, the steel has very high strength and hardness, but to obtain optimum corrosion resistance, ductility, and impact strength, the steel is given a stress- relieving or tempering treatment (usually in the temperature range of 300-700ºF (149-371ºC)).

Tables 4.1 and 4.2 give the chemical compositions and mechanical properties of martensitic grades in the annealed and hardened conditions.

The martensitic stainless steels fall into two main groups that are associated with two ranges of mechanical properties: low- carbon compositions with a maximum hardness of about Rockwell C45 and the higher-carbon compositions, which can be hardened up to Rockwell C60. (The maximum hardness of both groups in the annealed condition is about Rockwell C24.) The dividing line between the two groups is a carbon content of approximately 0.15%.

In the low-carbon class are Types 410, 416 (a free-machining grade) and 403 (a "turbine-quality" grade). The properties, performance, heat treatment, and fabrication of these three stainless steels are similar except for the better machinability of Type 416. On the high-carbon side are Types 440A, B, and C. Types 420, 414, and 431, however, do not fit into either category. Type 420 has a minimum carbon content of 0.15% and is usually produced to a carbon specification of 0.3-0.4%. While it will not harden to such high values as the 440 types, it can be tempered without substantial loss in corrosion resistance. Hence, a combination of hardness and adequate ductility (suitable for cutlery or plastic molds) is attained. Types 414 and 431 contain 1.25–2.50% nickel, which is enough to increase hardenability, but not enough to make them austenitic at ambient temperature. The addition of nickel serves two purposes: (1) it improves corrosion resistance because it permits a higher chromium content, and (2) it enhances toughness. Martensitic stainless steels are subject to temper embrittlement and should not be heat treated or used in the range of 800 to 1050ºF (427-566ºC) if toughness is important.

Impact tests on martensitic grades show that toughness tends to decrease with increasing hardness. High-strength (high- carbon) Type 440A exhibits lower toughness than Type 410. Nickel increases toughness, and Type 414 has a higher level of toughness than Type 410 at the same strength level.

Martensitic grades exhibit a ductile-brittle transition temperature at which notch ductility drops very suddenly. The transition temperature is near room temperature, and at low temperature of about -300ºF (-184ºC), they become very brittle. This effect depends on composition, heat treatment, and other variables.

Clearly, if notch ductility is critical at room temperature or below, and the steel is to be used in the hardened condition, careful evaluation is required. If the material is to be used much below room temperature, the chances are that quenched-and-tempered Type 410 will not be satisfactory. While its notch ductility is better in the annealed condition down to -100ºF (-73ºC), another type of stainless steel is probably more appropriate.

The fatigue properties of the martensitic stainless steels depend on heat treatment and design. A notch in a structure or the effect of a corrosive environment can do more to reduce fatigue limit than alloy content or heat treatment. Another important property is abrasion or wear resistance. Generally, the harder the material, the more resistance to abrasion it exhibits. In applications where corrosion occurs, however, such as in coal handling operations, this general rule may not hold, because the oxide film is continuously removed, resulting in a high apparent abrasion/corrosion rate. Other mechanical properties of martensitic stainless steels, such as compressive yield and shear strength, are generally similar to those of carbon and alloy steels at the same strength level. The property of most interest is

modulus of elasticity. The moduli of the martensitic stainless steels (29 x 10^6 psi) (200 GPa) are slightly less than the modulus of carbon steel (30 x 10^6 psi) (207 GPa) but are markedly higher than the moduli of other engineering materials, such as aluminum (10 x 10^6 psi) (67 GPa). The densities of the martensitic stainless steels (about 0.28 lb. per cu. in.) (7780 Kg/m^3) are slightly lower than those of the carbon and alloy steels. As a result, they have excellent vibration damping capacity.

The martensitic stainless steels are generally selected for moderate resistance to corrosion, relatively high strength, and good fatigue properties after suitable heat treatment. Type 410 is used for fasteners, machinery parts and press plates. If greater hardenability or higher toughness is required, Type 414 may be used, and for better machinability, Types 416 or 416 Se are used. Springs, flatware, knife blades, and hand tools are often made from Type 420, while Type 431 is frequently used for aircraft parts requiring high yield strength and resistance to shock. Cutlery consumes most of Types 440A and B, whereas Type 440C is frequently used for valve parts requiring good wear resistance.

High-carbon martensitic stainless steels are generally not recommended for welded applications, although Type 410 can be welded with relative ease. Hardening heat treatments should follow forming operations because of the poor forming qualities of the hardened steels.

Table 4.2 Chemical Analysis of Martensitic Steels

Martensitic Stainless Steels **Chemical Analysis %**									
Type	C	Mn	P	S	Si	Cr	Ni	Mo	other
410	0.15	1.00	0.040	0.030	1.00	11.50/13.50			
440A	0.60/0.75	1.00	0.040	0.030	1.00	16.00/18.00		0.75	
440B	0.75/0.95	1.00	0.040	0.030	1.00	16.00/18.00		0.75	
440C	0.95/1.20	1.00	0.040	0.030	1.00	16.00/18.00		0.75	

4.5 Corrosion characteristics – High Temperature

Corrosion Resistance

When stainless steels are exposed at elevated temperatures, changes can occur in the nature of the surface film. For example, at mildly elevated temperatures in an oxidizing gas, a protective oxide film is formed.

In more aggressive environments, with temperatures above 1600ºF (871ºC), the surface film may break down with sudden increase in scaling. Depending on alloy content and environment, the film may be self-healing for a period of time followed by another breakdown.

Under extreme conditions of high temperature and corrosion, the surface film may not be protective at all. For these reasons, the following data should serve only as a starting point for material selection, not as a substitute for service tests. Stainless steel has been widely used for elevated-temperature service; therefore, fundamental and practical data concerning their resistance to corrosion are available.

4.5.1 Oxidation

In non-fluctuating-temperature conditions, the oxidation resistance (or scaling resistance) of stainless steels depends on chromium content. Steels with less than 18% chromium (ferritic grades primarily) are limited to temperatures below 1500ºF (816ºC). Those containing 18-20% chromium are useful to temperatures of 1800ºF (982ºC), while adequate resistance to scaling at temperatures up to 2000ºF (1093ºC) requires a chromium content of at least 22%, such as Types 309, 310 or 446. The maximum service temperature based on a rate of oxidation of 10 mg. per sq. cm. in 1000 hours is given for several stainless steels in Table III for non- fluctuating temperature. The corrosion resistance of several stainless steels in steam and oxidizing flue gases are compared with their corrosion resistance in air. In many processes, isothermal (constant temperature) conditions are not maintained and process temperatures vary. Expansion and contraction differences between the base metal and the protective film (or scale) during heating and cooling cause cracking and Spalling of the protective scale. This allows the oxidizing media to attack the exposed metal surface. The Spalling resistance of the Martensitic stainless steels is greatly improved at higher nickel levels. Nickel reduces the thermal expansion differential between the alloy and the oxide film and thereby reduces stresses at the alloy-oxide interface during cooling. Also, Type 446 and the proprietary ferritic chromium-molybdenum stainless steels have a fairly low coefficient of thermal expansion, which tends to enhance Spalling resistance.

A number of proprietary austenitic stainless steels that rely on silicon, aluminum, or cerium additions for improved oxidation resistance are listed in ASTM A240 and other product specifications.

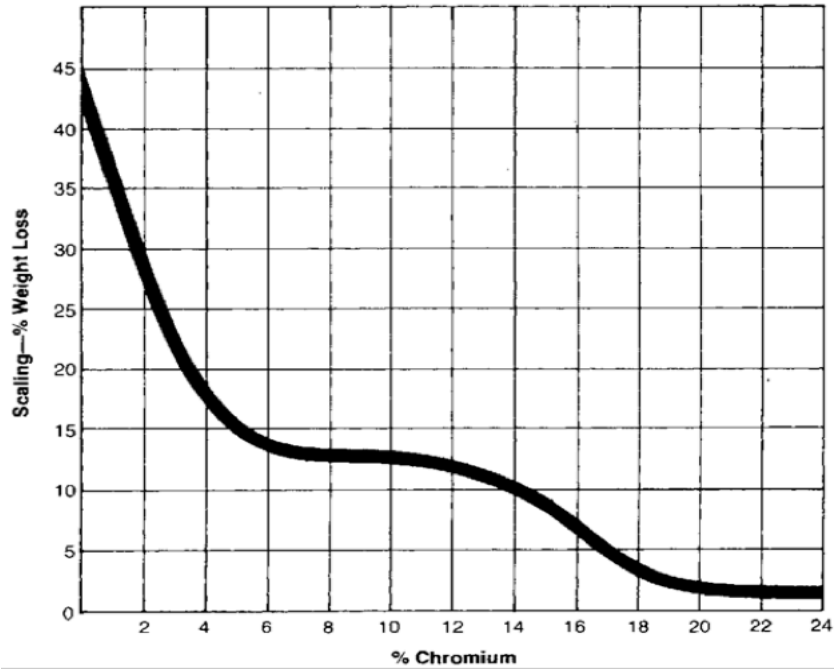

Figure 4.8 Effect of Chromium Content on Scaling resistance.

4.5.2 Effect of Atmosphere

Much attention has been given to the compatibility of stainless steels with air or oxygen. However, trends in the design of steam and other forms of power generation have resulted in a growing interest in oxidation in such environments as carbon monoxide, carbon dioxide, and water vapor. Exposure to mild conditions in these environments leads to the formation of the protective oxide film described earlier, but when conditions become too severe, film breakdown can occur. The onset of this transition is unpredictable and is sensitive to alloy composition. Although the reaction mechanisms are probably similar in air, oxygen, water vapor, and carbon dioxide, reaction rates may vary considerably. For example, similar scaling behavior has been observed in air and oxygen except that the scale break-down occurs more rapidly in oxygen. For this reason, results obtained in air should be applied with care when considering service in pure

oxygen. An increase in corrosion rates can be expected in the presence of water vapor. Type 302 undergoes rapid corrosion in wet air at 2000ºF (1093ºC), whereas a protective film is formed in dry air. The higher nickel Type 330 is less sensitive to the effects of moisture; so it is assumed that increased chromium and nickel permits higher operating temperatures in moist air. Types 309 and 310 are superior at temperatures greater than 1800ºF (982ºC), and Type 446 is usable at temperatures approaching 2000ºF (1093ºC).

It is difficult to indicate maximum service temperatures in steam, one reason being the sensitivity of corrosion rate to surface condition. (Cold worked surfaces tend to exhibit reduced corrosion effects in steam service.) Most austenitic stainless steels can be used at temperatures up to 1600ºF (871ºC), and Types 309, 310, and 446 at higher temperatures. Types 304, 321, and 347 are being used in low- pressure steam systems at temperatures approaching 1400ºF (760ºC). Scale on Types 304, 347, and 316 tends to exfoliate at higher temperatures The oxidation of stainless steels in carbon dioxide and carbon dioxide- carbon monoxide atmospheres at temperatures in the range of 1100- 1800ºF (593-982ºC) is of interest because of their use in gas-cooled nuclear reactors. Type 304 is serviceable in this environment, although some proprietary stainless steels offer better resistance.

A note of caution about stainless steels at high temperatures in *stagnant* oxidizing environments: The protective film breaks down in the presence of certain metal oxides, causing accelerated attack. For instance, austenitic types are susceptible to attack in the presence of lead oxide at temperatures as low as 1300ºF (704ºC). Vanadium oxide, found in fuel ash, may cause failure of Types 309 and 310 at 1900ºF (1038ºC) when water vapor is present. Molybdenum oxide behaves in a similar manner.

Table 4.3 Suggested Maximum Temperature

Suggested Maximum Service Temperatures in Air				
AISI Type	**Intermittent Service**		**Continuous Serivce**	
	°C	**F**	**°C**	**F**
410	815	1500	705	1300
416	760	1400	675	1250
420	735	1350	620	1150
440	815	1500	705	1300
442	1035	1900	980	1800

4.5.3 Flue Gases

The corrosivity of flue gas containing sulfur dioxide or hydrogen sulfide is similar to that of most sulfur-bearing gases. Accordingly, the corrosion resistance of stainless steels in flue gas environments is improved by increased chromium content.

CHAPTER 5

Razor Blade Steel and Material

5.1 Introduction

Cr-Mo stainless steel is used for making razor blades and exhibits a high resistance to corrosion, and also to a process for manufacturing razor blades. High carbon steel containing 1.2% by weight of carbon and 0.4% by weight of chromium are usually used for making razor blades. This material shows a high degree of hardness when heat treated and could make a blade having a high level of cutting quality, but has the drawback of being poorly resistant to corrosion and of rusting easily.

Every razor is normally used in a more or less humid environment. When it is used, it is brought into contact with corrosive substances, such as the constituents of sweat, soap, and shaving foam. Moreover, the nature of water which is used for shaving, and the temperature of the place where the razor is used, are likely to promote the rusting of its blade. The high carbon steel razor blade was primarily intended for providing a high level of cutting quality, and did not usually withstand any repeated use under the conditions as herein stated. Therefore, 13 Cr martensitic stainless steel has come to be used widely as a rust-resisting material for making a razor blade having a high level of cutting quality. Martensitic stainless steel containing 0.6 to 0.7% of carbon and 12 to 13% of chromium, both by weight, is used more often for making razor blades than any other stainless steel. This material has a hardness of HV 620 to 650 when heat treated, and is superior to high carbon steel in rusting and corrosion resistance owing to the 13% Cr it contains.

This material is, however, not completely free from the problem of rusting,

either; when it is used for making razor blades, it is usual a practice to form a coating of e.g. platinum, chromium or chromium nitride (CrN) on the surface of the material by sputtering to improve its corrosion resistance. Although the coating does certainly improve the corrosion resistance of the material, a razor blade made of this material still has an undesirably short life due to the corrosion which occurs at the grain boundary, and the rust which forms between the coating and the substrate. Moreover, the formation of the coating requires additional equipment and incurs an additional cost.

The razor blade is preferably coated with a layer of polytetrafluoroethylene (PTFE) or silicone which reduces friction and renders the blade smoother to the skin.

5.2 Elements of Razor Blade Material

A description of the component elements of the razor blade material and the contents of alloying elements are described here.

(a) C: not less than 0.5%

Carbon is an element necessary for improving the strength of the material. An appropriate carbon content lowers the melting point of the material and improves its productivity. Thus, the carbon content is set to be not less than 0.5%. Preferably, the carbon content is not more than 5.0% in order to inhibit crystallization of graphite. Carbon is an element which is important for the hardness of steel as heat treated, but lowers its corrosion resistance as its proportion increases. We have looked into the optimum proportion of carbon that ensures that the steel has a Vickers hardness of at least 620 when hardened and tempered, as measured under a load of 0.5 kg, while also takes the proportions of the other elements (mainly chromium) into consideration. As a result, the presence of more than 0.45% of carbon has been found to be essential

from the standpoint of hardness as set forth above. The presence of 0.55% or more of carbon has, however, been found to lower the corrosion resistance of steel and necessitate surface treatment for making up its lower corrosion resistance as has been given to the presently available steel containing 0.65% of carbon and 13% of chromium. Therefore, the steel of this type contains more than 0.45%, but less than 0.55%, of carbon. According to a salient feature of the steel of this invention, it has an improved corrosion resistance due to its carbon content which is lower than that of the presently available stainless steel, and nevertheless, a satisfactorily high level of hardness as heat treated owing to its specific carbide density, as will be described.

(b) Cr: 9.0 to 14.0%

Cr is a basic element necessary for providing the material with corrosion resistance, and is required to be not less than 9.0% Cr in order to ensure substantially the same level of corrosion resistance as that of stainless steel. However, Cr content exceeding 14.0% makes the material not only expensive but also susceptible to crystallize coarse network carbides resulting in deteriorated hot-workability and low productivity. In order to prevent the crystallization of carbides, quick quenching is necessary for the material. Therefore, the Cr content is set to be 9.0 to 14.0%. Chromium is one of the most important elements for the rusting and corrosion resistance of steel. At least 12% of chromium is necessary to form a sufficiently passive film to render the steel of this invention resistant to corrosion. The use of too much chromium must, however, be avoided, since its formation of carbide at the temperature employed for austenitizing steel brings about a reduction in the carbon content of the steel and thereby in its hardness as heat treated. The hardness, which the steel of this invention is required to exhibit when heat treated, can be attained only when it contains not more than 14% of chromium.

(c) Mo: not more than 8.0%

Mo improves corrosion resistance. Mo is effective for not only preventing coarsening of Cr-containing carbides but also preventing precipitation of other carbides, since it occupies precipitation sites of Cr-containing carbides that are susceptible to be coarse and is effective for lowering a diffusion activity of carbon because of a high affinity for carbon. However, when the Mo content is significant, a brittle phase precipitates to deteriorate the material's corrosion resistance and toughness, the brittle phase comprising Mo-containing carbides (including Mo2C) and composite borides (including $Mo_2(Fe, Cr)B_2$, $Fe_{13}Mo_2B_5$, Mo_3B and Mo_2B). Thus, an upper limit value is set to be 8.0%. Preferably, the Mo content is not less than 0.5% in order to obtain the above effects. While the invented material is directed to an Fe-based alloy containing the above components with specific contents, respectively, it is effective for the material to contain B (boron) and Si in order to further improve characteristics of the material.

(d) B+Si: not more than 8.0%

Both the elements B and Si promote a transformation of the alloy structure of the material into amorphous phase. However, a significant amount of the elements prevents such a structural transformation and causes brittle phase to precipitate resulting in deteriorated toughness, the brittle phase comprising composite borides (including $Mo_2(Fe, Cr)\ B_2$,

$Fe_{13}Mo_2B_5$, Mo_3B and Mo_2B), Fe_3Si. Thus, an upper limit of a total content of one or both of the elements is set to be 8.0%. Preferably, the content is not less than 0.5% in order to obtain the above effects.

It should also be noted that other elements promoting the structural

transformation into amorphous phase can be added into the material as long as basic actions by the above chemical composition and a microstructure described below are not deteriorated. Such elements may be P, Nb, Zr, Ta, Al, Ga, Ni, Co and Cu.

(e) Coating With polytetrafluoroethylene (PTFE)

The razor blade material is characterized by that it may be used with a coating of polytetrafluoroethylene (PTFE). Thereby, a shaving feel, which is one of important properties of the razor blade, can be remarkably improved.

As mentioned above, it is effective to use the quenching solidification method in order to obtain the invention razor blade material. In this case, When the solidification rate is a level of critical cooling rate of 5><104 K/second, the invention razor blade material may be as solidified by quenching, and it is possible to attain the blade material having a thickness of not less than 30 pm. However, it should be noted that an excess thickness is inappropriate in order to attain the amorphous structure, and that the upper limit of thickness of the material as solidified by quenching, which is attainable at the cooling rate mentioned above, is an order of 100 pm. Therefore, the thickness of the invention material is set to be a range of 30 to 100 pm.

A razor blade is usually coated with a resin, such as polytetrafluoroethylene (PTFE) or silicon, after a cutting edge has been formed on it, so that it may be smooth to the skin, and on that occasion, it is heated at a temperature of 350° C. to 400° C. Silicon is the most, effective element for restraining any reduction that occurs to the hardness of steel when it is heated when a resin coating is formed. In this connection, the presence of at least 0.4% of silicon is essential to ensure that the steel maintain a Vickers hardness of at least 620.

(f) Silicon and Manganese

Silicon, however, forms a solid solution in steel, and thereby embrittles it and lowers its cold workability. It also forms hard non-metallic inclusions, such as Si02. The addition of too much silicon is, therefore, likely to make the formation of a proper cutting edge difficult, or result in an edge which is easily broken. Under these circumstances, the addition of more than 1.0% of silicon has been found undesirable. Therefore, the steel of this invention contains 0.4 to 1.0% of silicon.

Manganese is also used as a deoxidizing agent. It exists in the form of a solid solution in steel, and also forms manganese sulfide and manganese silicate as non metallic inclusions. The hard inclusions formed by silicon must be removed from the steel, as they remain unchanged even by a strong force applied for cold working the steel, and eventually disable the formation of a proper cutting edge on a razor blade and also have an adverse effect on its properties. On the other hand, manganese sulfide and manganese silicate hardly present any problem in the formation of a razor blade or from the standpoint of its properties, since they are sufficiently soft to be deformable into a very small thickness by cold working. It, therefore, follows that any and all unavoidable non-metallic inclusions need be fixed in the form of soft ones, such as those formed by manganese. At least 0.5% of manganese is necessary to form manganese sulfide. At least 0.5% of manganese is necessary to form manganese silicate when the proportion of silicon as herein above defined is taken into consideration. The addition of too much manganese must, however, be avoided, as it lowers the hot workability of steel. Therefore, the steel of this invention contains 0.5 to 1.0% of manganese.

5.3 TECHNOLOGY

The technology for the manufacture of safety razor blades is a closely held trade secret with a few manufacturers in the world.

Manufacture of safety razor blades is a technology by itself and utilizes state-of the-art equipment and machinery. Brief outline of the process of manufacture includes the following:

1. Drawing of the blade strips from the spools;
2. High Speed Punching of the blade blanks in high speed punch presses (950- 1000 SPM (Splits Per Minute);
3. Bliss Press operations;
4. Heat Treatment - (automatic electric hardening systems);
5. Cutting operations;
6. Grinding;
7. Stropping (lapping with leather belts);
8. Coating;
9. Printing (rotogravure printing of brand name, etc.);
10. Quality Check;
11. Packing and Dispatch (automated).

From a historic perspective, the Indian male had to put up with the so-called "safety" razor blades, which gave more cuts on the face than the number of good shaves each morning. A mandate that safety razor blades, manufactured in the country, should be covered by the certification implementing a scheme of the Indian Standards Institution (now Bureau of Indian Standards) and carries the ISI mark.

Tests conducted by the institution revealed that all major brands of safety razor blades failed to come up to the relevant Indian standards. This failure of the

manufacturers was despite the imported raw material, imported machinery (even the dies were imported) and, as some claimed, imported know-how.

Notwithstanding the "imported technology", while one blade would just give a single, satisfactory shave, the best performance seldom exceeded five shaves. The price differential between the lowest and the highest brand was in the ratio of 1:6. The reason was that the defective pieces and rejects, segregated during the online quality checks, were earmarked and graded for the lower priced brands.

One particular brand X of carbon steel blade did not even give one nick free shave. The manufacturer, when confronted, cleverly retorted that what was labeled was meant to be a "blade", not a "shaving blade". On further questioning regarding its use, the manufacturer recommended it "for pencil sharpening".

The Bureau of Indian Standards (BIS) certification scheme was introduced in 1956 and later various items of mass consumption, which had health and safety implications, were brought under compulsory ISI marking through different enactments.

The blades are produced in accordance with the following specifications:

- Stainless Steel Safety Razor Blades (Second Revision Amendments 3) - Reaffirmed – 1996 **IS 7371 – 1982**
- Safety Razors Amendments 3 - Reaffirmed –1991 **IS 7370 1974**
- Twin Blade Razor Handles Hermal - Reaffirmed-1998 **IS 13777 – 1993**
- Twin Blade Cartridges Shaving Systems Amendments 2 - Reaffirmed 1996 -**IS 13031-1990**

Since there are only two major multinational companies manufacturing the above item under foreign collaboration and having monopoly in the market, the detailed technological aspects of manufacture is almost a trade secret. Safety razor blades

currently are produced in large scale sector only. There are many types of blades in the market, for e.g., single edge, double edge, sandwiched and bonded. Safety razor blades are items of consumption. Being a commodity of mass and daily consumption, the industry provides good scope for investment.

The manufacture of razor blades involves a variety of operations such as punching and hardening. List of plant and machineries required are as follows:

1. Punch machine
2. Fully automatic press
3. Automatic electric hardening machine
4. Automatic etching machine
5. Varnishing machine
6. Cutting machine
7. Grinding and polishing machine
8. Tool grinder and miscellaneous tools and accessories.

The razor blades are mostly being manufactured by the foreign firms in India, although Indian firms are also in the field but their product is not up to the mark. Therefore, high quality razor blades have ample scope in Indian as well as foreign market.

5.4 Raw Materials

BLADE MATERIAL PROPERTIES

The material properties that are generally of most interest when choosing the optimum material for a particular cutting application include the following:

- Wear Resistance
- Toughness or Shock Resistance
- Corrosion Resistance
- Influence on Edge Characteristics
- Shape Control during Heat Treat
- Cost
- Availability

Materials most commonly used in blade applications include the following:

- 1095 Carbon Steel
- Heat-Treated Stainless Steels
- 301 Stainless, 17-4 & 17-7 PH Stainless
- High Speed Steels
- Tool Steels
- Extreme-Wear Tool Steels
- Tungsten Carbide
- High-Performance Zirconia Ceramic
- Coatings
- Martensitic Stainless Steels.

1095 Carbon Steel

Available in either Rc 50 spring temper or custom hardened and tempered up to Rc 62, AISI 1095 is an economical material choice where corrosion is not expected to be a problem. While most blade manufacturers use AISI 1095, normally 1.25 Carbon Steel is used. 1095 steel has 0.95% carbon while 1.25 steel has 1.25% carbon.

This increased carbon content allows the blades to be heat treated to a higher hardness and offers better wear resistance. This steel is a good, economical choice when fair wear resistance is required and corrosion is not a problem.

Heat-Treated Stainless Steels

Suitable for industrial and medical applications, these 400 series martensitic steels are much more corrosion-resistant than carbon steels and can be sharpened to equally-keen edge sharpness. Razor Blade Stainless steel in thicknesses from 0.010”-0.062” thick can also be used.

High-Speed Steels

High-speed steels also have excellent temper resistance, holding their hardness even when exposed to temperatures up to 1,000 ° F, which can also be considered.

Coatings

With many materials, desirable qualities can be enhanced by applying wear resistant TiN, TiC, TiCN, ceramic (aka boron carbide), or Armoloy® coatings or dry film lubricant coatings such as Teflon. However, the following coatings are used extensively for safety razor blade manufacturing.

TITANIUM NITRIDE (TIN) - This familiar gold-like coating is economical as it adds some lubrication and wear-resistance.

SOLID TUNGSTEN CARBIDE - Unique grades, ultra-fine and sub-micron grain tungsten carbide, offer the best blend of wear resistance and toughness. Polishing all edges and surfaces to a 2 RMS finish is possible. Each cutting edge is microscopically inspected at 50X, to assure customers a perfect blade. Carbide blades can last hundreds of times longer; so they can be an excellent choice in high production applications or where a superior cut is needed. These blades can be re-sharpened, further increasing their cost effectiveness.

SAPPHIRE - Sapphire has superior sharpness and durability characteristics than that of even carbide or ceramic. Sapphire's true benefit is that is can withstand much higher heat applications than solid carbide or ceramic materials. This translates into even faster production speeds for increased productivity, decreased down time, decreased scrap, and higher profits. Classified grades of this precious stone for razor blade applications have been developed recently.

The raw materials that are used for the manufacture of safety razor blades are the following:

- Carbon Steel for safety razor blade - Amendments-2 Reaffirmed 1994 **IS 10198 – 1982**.
- Cold Rolled Steel Strips for Carbon Steel Razor Blades - Reaffirmed 1992 **IS 9476 – 1980.**
- Cold Rolled Stainless Steel Strips for razor blades - Amendments 2 – Reaffirmed 1990 **IS 9294 – 1971**

Raw material required for razor blade is steel strip which is imported from other countries. The commonly used dimensions of steel strip are as follows:

- 0.881 x 0.0024" thick
- 0.881 x 0.004" thick
- 0.881 x 0.0032" thick
- 0.881 x 0.005" thick

There is no single thin blade material that is appropriate for all cutting applications. There are a wide range of hardened stainless steels, flat ground tool steels, and many other wear resistant materials from which to choose from various manufacturers across the globe. "Optimize, not Compromise" when selecting a blade material to ensure the right mix of properties for each individual application should be the watchword in selecting materials for manufacture.

The ideal blade material would be highly wear and shock resistant, economical, available in a wide range of thickness and finish, readily sharpened to a fine quality edge, possess outstanding corrosion resistance, and have no distortion after heat- treatment.

5.5 MACHINERY AND EQUIPMENT

The selection of machinery and equipment generally depends on the product/products to be manufactured and their processes of manufacture. Since the product is being manufactured under monopolistic lines, with state-of-the-art machinery and equipment, it is suggested that new units which intend to be manufactured can be designed and developed using the state-of-the-art machinery and equipment..

The following process operations have to be taken into consideration during selection and installation of the machinery & equipment for manufacturing:

- Drawing of the blade strips from the spools
- Bliss Press operations
- Heat Treatment - (automatic electric hardening systems)
- Cutting operations
- Grinding
- Stropping (lapping with leather belts)
- Coating
- Printing (rotogravure printing of brand name, etc.)
- Quality Check
- Packing and Dispatch (automated)
- High Speed Punching of the blade blanks in high speed punch presses (950-1000 SPM (Splits Per Minute).

CHAPTER 6

EXPERIMENTAL TECHNIQUES AND INSTRUMENTATION

6.1 Introduction

The primary motivation of the experimental work was to draw comparisons and characterize the corrosion behavior of martensitic stainless steel blades, when immersed in concentrations of 3.5% NaCl and 3.5% of acetic acid in room temperature. The experimentation and instrumentation that were employed in this research can be grouped as follows:

1) Weight loss measurements,

2) Scanning electron microscopy (SEM) and energy-dispersive X-ray (EDX spectroscopy).

6.2 Weight Loss Tests

Weight loss tests are a very widely used corrosion measurement and monitoring technique. They are simple to understand and provide a direct measure of the corrosion rate, allow a direct comparison of the relative resistance to corrosion of one sample with another under comparable or standard conditions, and provide a sound basis for estimating the likely active life of process equipment. There are numerous standard techniques for weight loss testing [4, 23].

The samples of razor blades may have one of a given number of geometries (usually a small flat rectangular sheet or cylinder). The samples are surface finished, and the surface area is determined. Care should be taken to avoid cross-

contamination, for example, new polishing paper should be used to avoid contamination of the metal surface. The blade is degreased (washed in a suitable solvent) after which it should not be touched directly; it is then dried and accurately weighed. The blade should then be exposed to the corrosive environment of interest. If the sample is to be stored, it should be kept in a desiccator.

Given that surface preparation can be achieved by any one of a number of methods, it is very important that comparisons be made only between coupons that were prepared in a similar manner. Various methods can be used to support the samples when they are in a corrosive medium. These include plastic wire, glass holders and test racks. Once a blade is immersed into a corrosive environment, a notable consideration is the length of time of exposure to the environment. Misleading results may be obtained if an incorrect choice is made, due in part to the fact that the initial rate of attack is often greater than the average over a longer period [5]. There are standard procedures that can be used to plan exposure test time, such as ASTM and NACE Standards [4, 23].

Following its immersion in the test solution, the sample should be closely inspected for, e.g. visual signs of localized attacks such as pitting or deposits which can help identify the causes of corrosion. Next, any corrosion products adhering to the sample should be removed from the surface to allow accurate determination of corrosion weight loss. Cleaning methods are either mechanical (scraping or brushing) or chemical (using solvents). Chemical cleaning is generally preferable, but the solution used will be specific to the metal being cleaned. Normally, the sample undergoes a number of equivalent cleaning cycles with the sample being weighed after each one [4]. Mass loss is plotted against the number of cleaning cycles, see Figure 6.1. Two lines are obtained; AB and BC. The former corresponds to removal

of corrosion products, the latter to removal of base metal. The required corrosion mass loss (W) occurs at point B, the intercept of the two lines [4]. More accurate results will be obtained by testing more than one blade and averaging the mass lost.

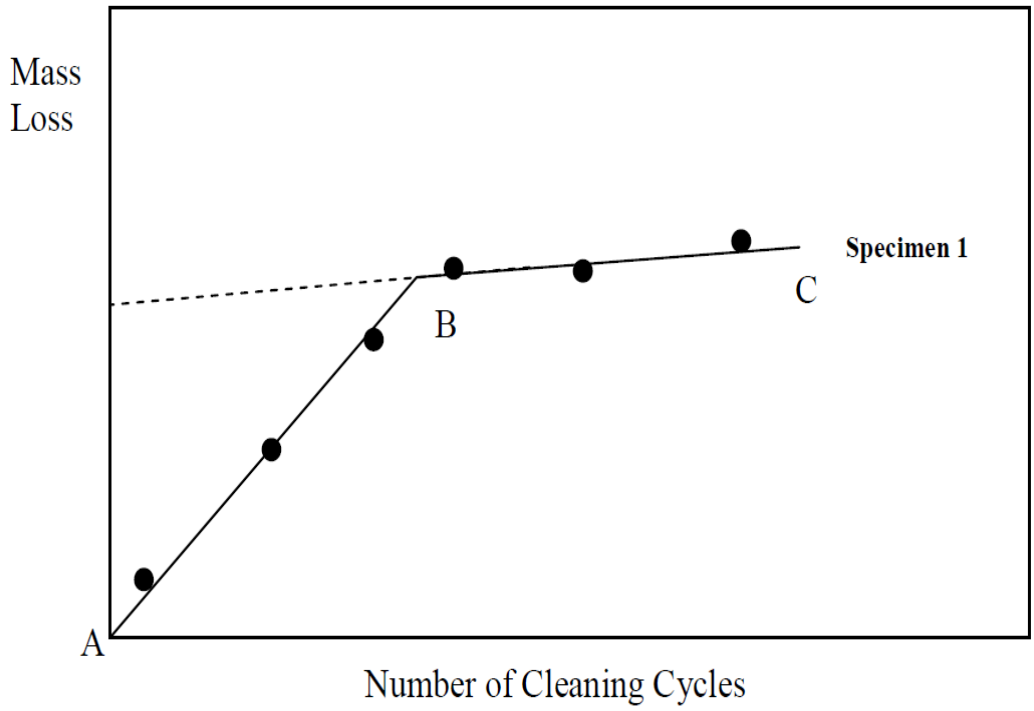

Figure 6.1 Theoretical mass loss of a corroded sample resulting from repeated cleaning cycles.

Corrosion rate can be calculated from the measured weight loss as [4, 24]:

Corrosion Rate (g/cm2.d) = **(K x W)/ (A x T x D).**

K is a constant [4], W is the mass lost from sample in g, T is the exposure time in days, A is the sample exposure area in cm^2, and D is the sample density in g/cm^3.

Corrosion rate can be expressed in millimeters per year (mm/y), mils per year (mpy) or milligrams per square centimeter per day (mg/cm^2d). Conversion between these units can be seen in Table 6.1 [25].

Table 6.1 Conversion factors between some of the units commonly used for corrosion rates.

Unit	Mdd	$g/m^2/d$	um/yr	Mm/yr	Mils/yr	In./yr
Milligrams per square decimeter per day (mdd)	1	0.2	36.5/d	0.365/d	1.144/d	0.00144/d
Grams per square meter per day ($g/m^2/d$)	10	1	365/d	0.365/d	14.4/d	0.0144/d
Micrometers per year (μm/yr)	0.0274d	0.00274d	1	0.001	0.0394	0.0000394
Millimeters per yr (mm/yr)	27.4d	2.74d	1000	1	39.4	0.0394
Mils per year (mils/yr)	0.696d	0.0696d	0.0696d	0.0254	1	0.001
Inches per year (in/yr)	696d	69.6d	25400	25.4	1000	1
Note: d is metal density in grams per cubic centimeter (g/cm^3).						

6.3 Scanning electron microscopy (SEM) and energy-dispersive X-ray (EDX spectroscopy).

Figure 6.2 shows a schematic diagram of the major components of the SEM. Generally, a beam of electrons are generated by the electron gun (located at the top of the column of the SEM instrument). This electron beam travels through a series of electromagnetic fields and lenses, which focus the electron beam onto the surface of the sample. For stable operation, a high vacuum is normally essential for the operation of the SEM. If the SEM contained a gas, the electron beam could react with it, ionizing the gas with the possibility that it could react with both the electron beam source causing burn out and contaminate the sample.

The interaction between the beam and the sample surface will result in emission of electrons and photons. The emitted electrons include back scattered electrons (BSE) and secondary electrons (SE), while the emitted photons include X-rays that can be used for elemental analysis (details given below). Various detectors are employed to record these emissions and the output of these is processed to produce relevant images/data [26, 27]. The backscattered electrons are most valuable for showing variation in surface composition of the analyzed sample [27, 28]. The secondary electron is an electron which has escaped from the sample with energy of less than 50 eV. These electrons provide information about the morphology and topography of the sample surface. If the specimen experiences a net loss or gain of electrons, it will gain a positive or negative charge causing image distortion and loss of resolution. Such effects can be overcome simply by earthing the specimen and using an electrically conducting sample or coating the specimen with a gold or carbon

film [29]. In our work, the detection was performed by using a SEM interfaced with EDX machine to observe the sample surfaces before and after corrosion.

Energy Dispersive X-ray Spectroscopy (EDS)

The surface analysis performed on backscatter electrons (BES) displays compositional contrast that results from different atomic number elements and their distribution. Energy Dispersive Spectroscopy (EDS) allows one to identify what those particular elements are and obtain compositional information of various elements (Atomic % for example).

Energy-dispersive X-ray spectroscopy (EDS, EDX, or XEDS), sometimes called as energy dispersive X-ray analysis or energy dispersive X-ray microanalysis (EDXMA), is a surface analytical technique used for the elemental analysis or chemical characterization of a sample. EDS analysis often relies on the fact that each element has a unique atomic structure allowing unique set of peaks on its X-ray emission spectrum. The excitation caused by the incident beam leads to the ejection of an electron from an inner shell, while creating an electron hole pair. An electron from an outer, higher-energy shell then fills the hole. The difference in energy between the higher-energy shell and the lower energy shell may be released in the form of an X-ray. As the energies of the X-rays are characteristic of the difference in energy between the two shells and of the atomic structure of the emitting element, EDS allows the elemental composition of the specimen to be measured.

Bombardment of a specimen with high energy electrons produces X-rays; the wavelength of these X-rays depends on the elements that are present in the sample. An electron in the primary beam with sufficient energy can excite an electron in an inner shell of one of the atoms of the sample causing it to leave the atom entirely or

move to a higher unoccupied energy level. The hole, as a result of this process, can be filled by an outer (higher energy) electron, an X-ray photon is emitted of energy equal to the energy difference between the two atomic shells and thus is characteristic of the atom from which the photon was emitted. This is the basis of Energy Dispersive X-Ray Spectroscopy (EDX), which is often used together with SEM [27]. EDX is a useful technique for elemental analysis or chemical characterization of the sample. EDX can be used for spot analysis in which the electron beam is positioned carefully onto a point of interest on the sample surface. Also, it may be employed for analysis of selected area as well as for line scans. In our work, the detection was performed by using SEM interfaced with EDX to observe the sample surfaces before and after corrosion.

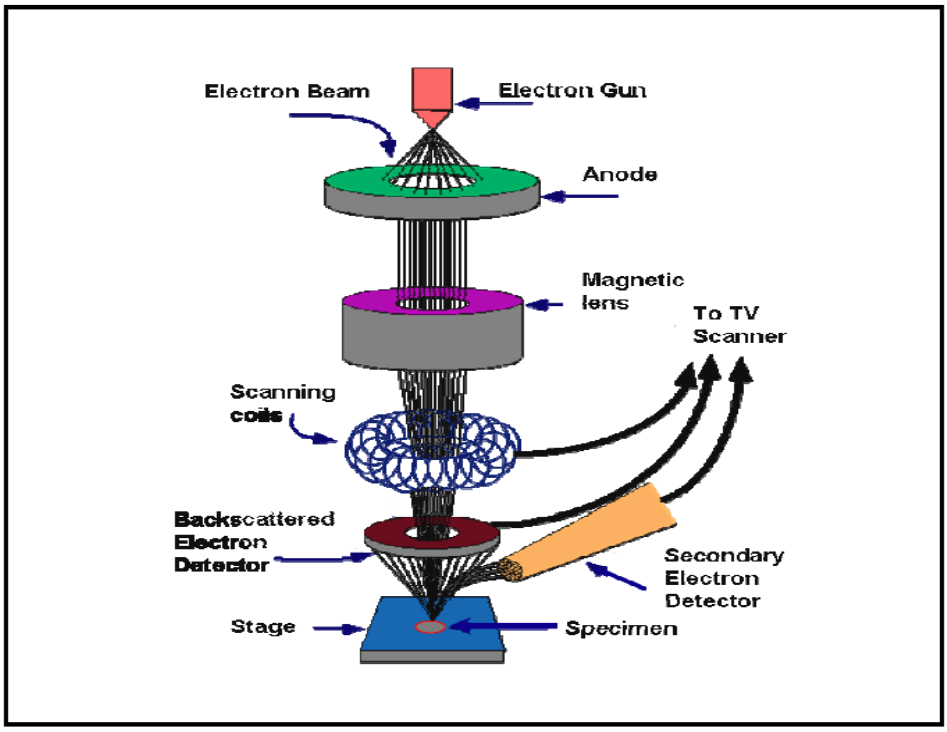

Figure 6.2 Schematic diagram of major components of SEM. [3]

CHAPTER 7

RESULTS AND DISCUSSION

7.1 NaCl and Acetic Acid

Upon retrieval of the blades after a period of 6 days, the blades were cleaned and analyzed to determine the metal loss and surface morphology. The results showed that generally, weight loss in both the blades is equal but creates a huge impact on surface morphology of both the blades.

First approach

This approach is a modified version of ASTM G48 test. Specimen's resistance to pitting corrosion were tested in sodium chloride solution and acetic acid to examine their weight loss.

Table 7.1 First set up for NaCl

Duration of Exposure	144 hrs
Temperature	Room Temperature

Table 7.2 First set up for Acetic Acid

Duration of Exposure	144 hrs
Temperature	Room Temperature

Second approach

This approach follows exact guidelines of the ASTM G 48 test. Examination on weight loss of specimen in NaCl and Acetic Acid is carried out.

Table 7.3 Weight Loss of Blade

	Duration of Exposure 144hrs		
Blade in Solution	Initial weight (gm)	Final weight (gm)	Weight loss in (gm)
NaCl	0.2288	0.2255	0.0033
Acetic Acid	0.2288	0.2254	0.0034

In Figures 7.1 and 7.2, the change in color of the solution due to the corrosion of the blade in NaCl, for 144 hrs, are shown. Change in color of the solution shows that the blade is corroded.

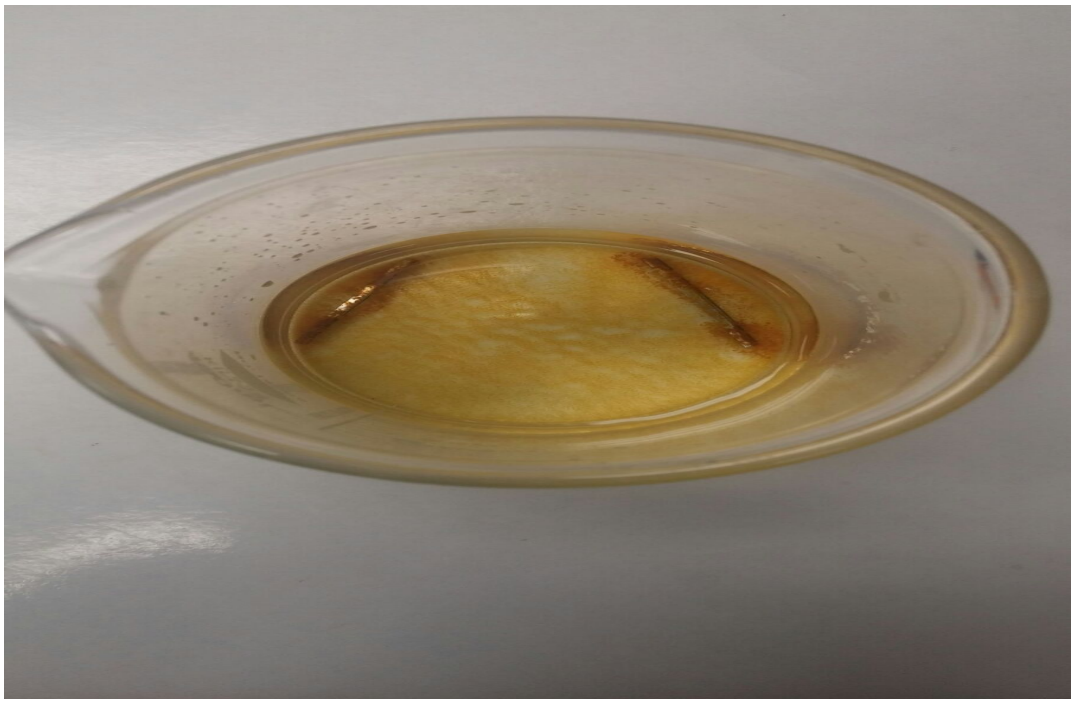

Figure 7.1 Color Change in solution when Blade is dissolved in NaCl solution for 144hrs.

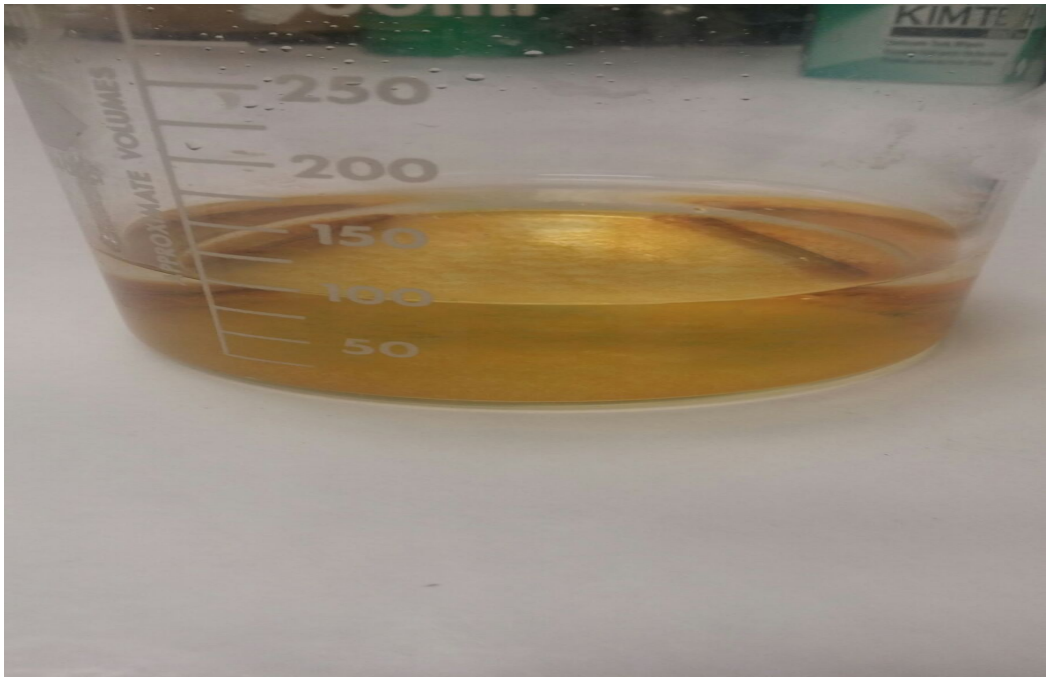

Figure 7.2 Blade dissolved in 100ml of NaCl in glass beaker.

After treating the blade in the solution for 144 hours, it was taken out. Mass loss of blade were measured on weighing scale, as shown in Figures 7.3 -7.5, to get the idea of corrosion and surface deterioration.

Figure 7.3 Weight of blade before exposure to acid.

Figure 7.4 Weight of blade after exposure to acetic acid.

Figure 7.5 Weight of blade after exposure to NaCl.

Figure 7.3 shows the weight of a new untreated blade. Figure 7.4 shows the weight loss of blade when it is exposed to acid for several hours. The corrosion rate and weight loss in blade increases with increase in time of exposure to acid.

7.2 Microstructural Analysis of Blades By SEM

7.2.1 Surface Analysis of Blades in NaCl

Figures 7.6-7.10 show the SEM micrographs of the blade after 144hrs of exposure. The morphology of the upper oxide layer in the micrograph is seen in the surface-view images. After 144h, the oxide layer was mostly flat, while increased oxide porosity was observed only in the thicker regions. The oxide layer was rougher and there were more porous regions. Fig 7.8 shows images of the bulk. Segregated particles were found in the bulk or at the grain boundaries.

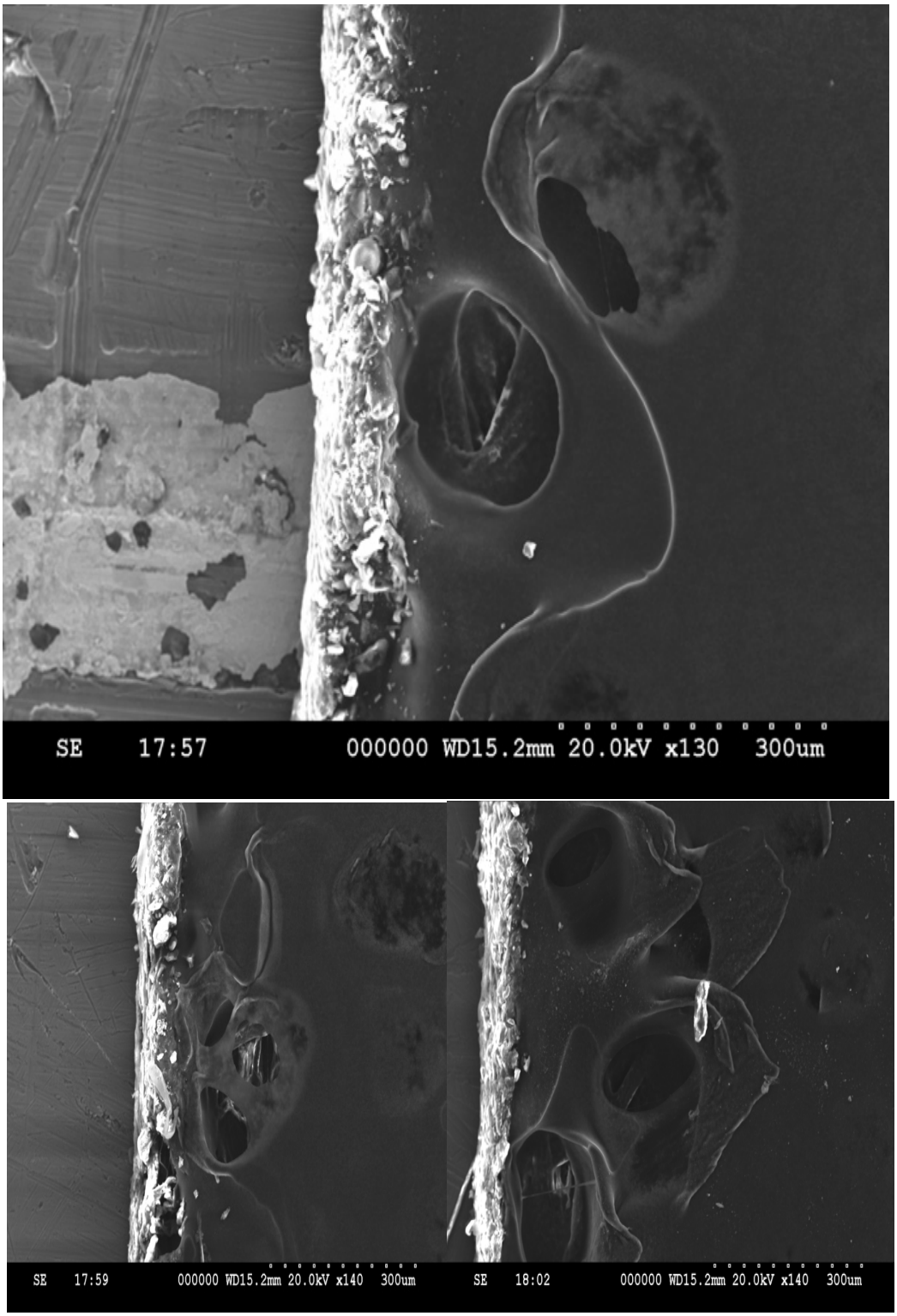

Figure 7.6 Represents increased oxide porosity near the boundaries of blade.

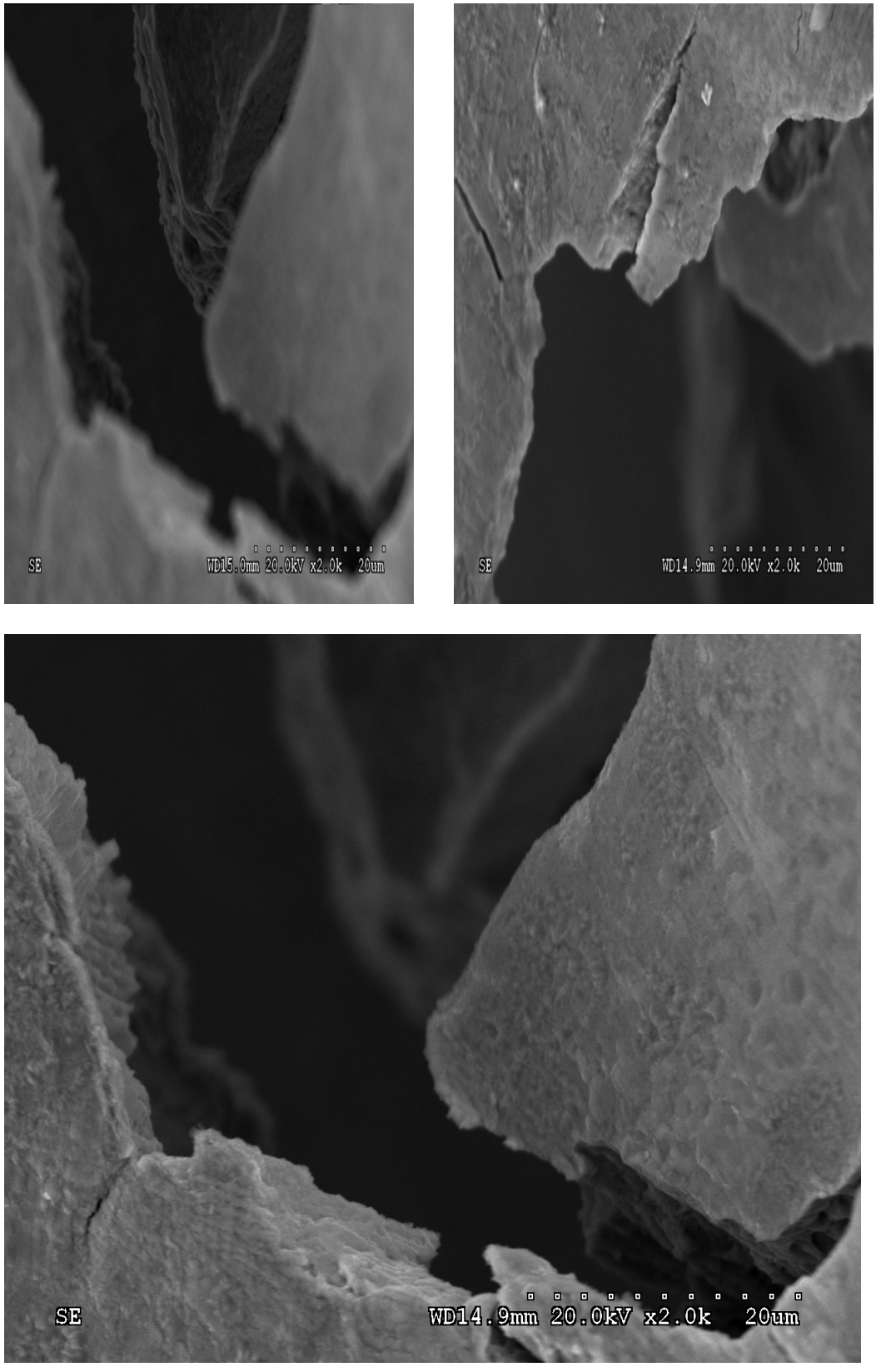

Figure 7.7 Represents surface crack.

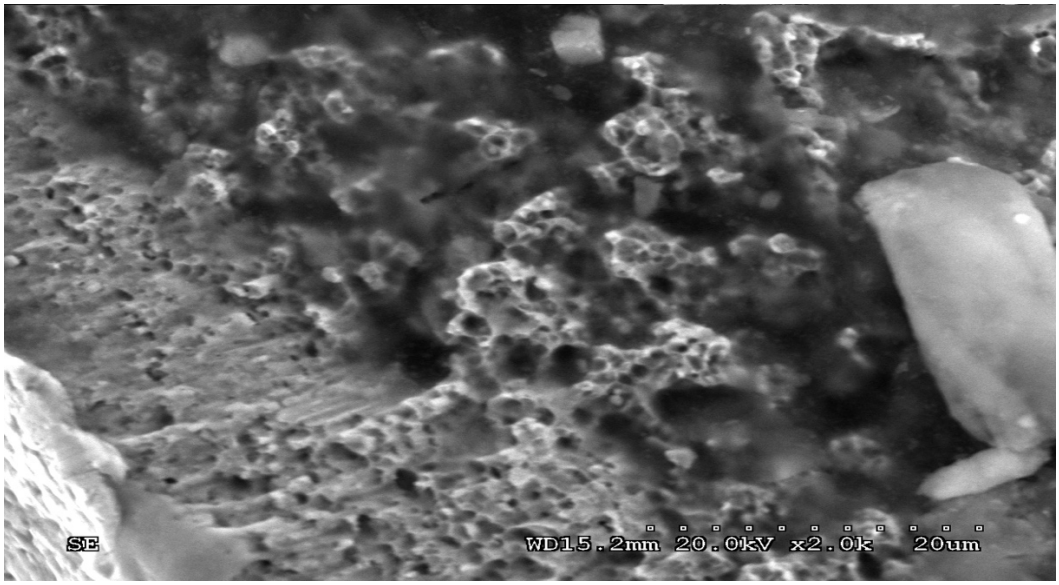

Figure 7.8 Segregated particles in the bulk.

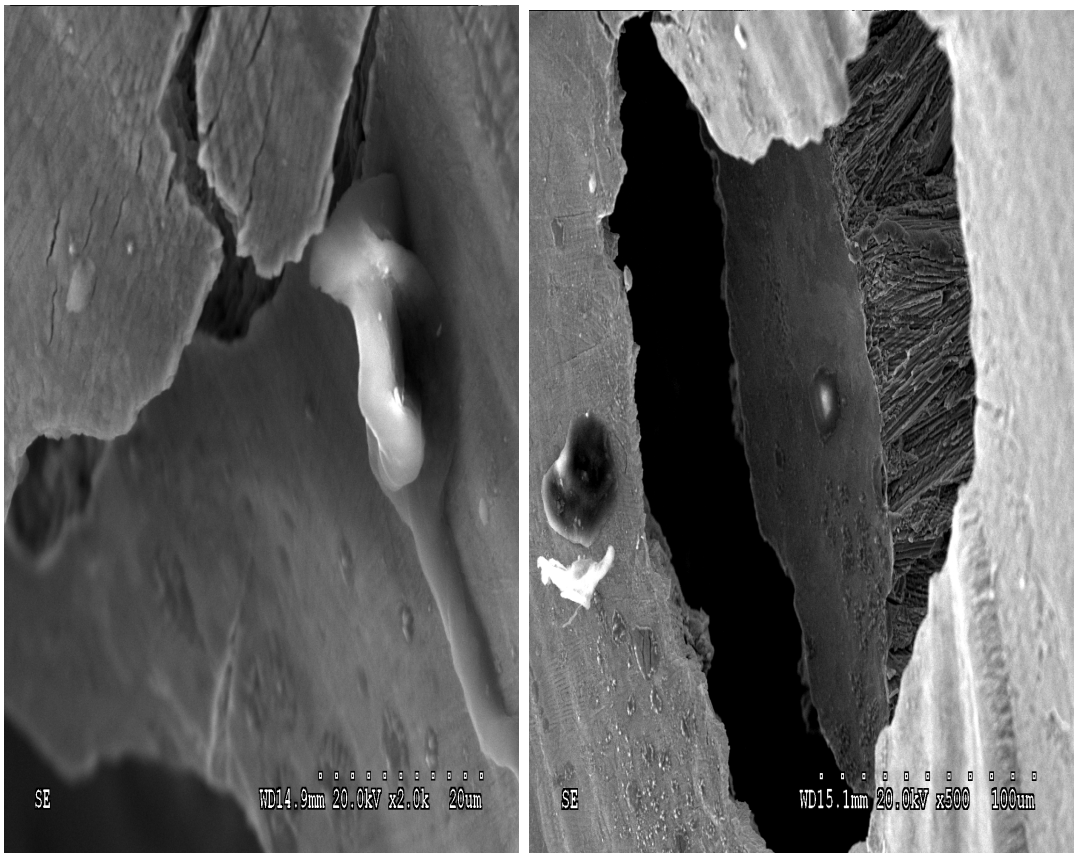

Figure 7.9 shows the depth of pit hole on the surface.

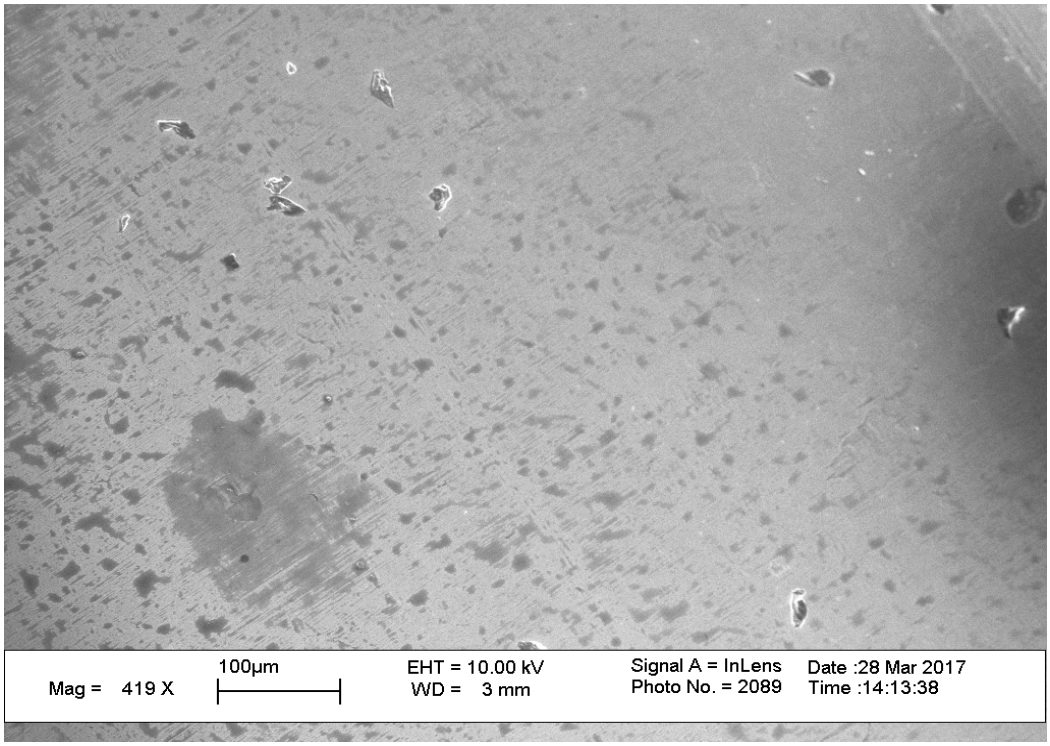

Figure 7.10 Pit holes over the surface of blade.

7.2.2 Surface analysis of Blades in Acetic Acid

In this experiment, blades have been exposed in 3.5% acetic acid for 144 hours. After cleaning the blades, they were observed under SEM as shown in Figure 7.11 and 7.12.

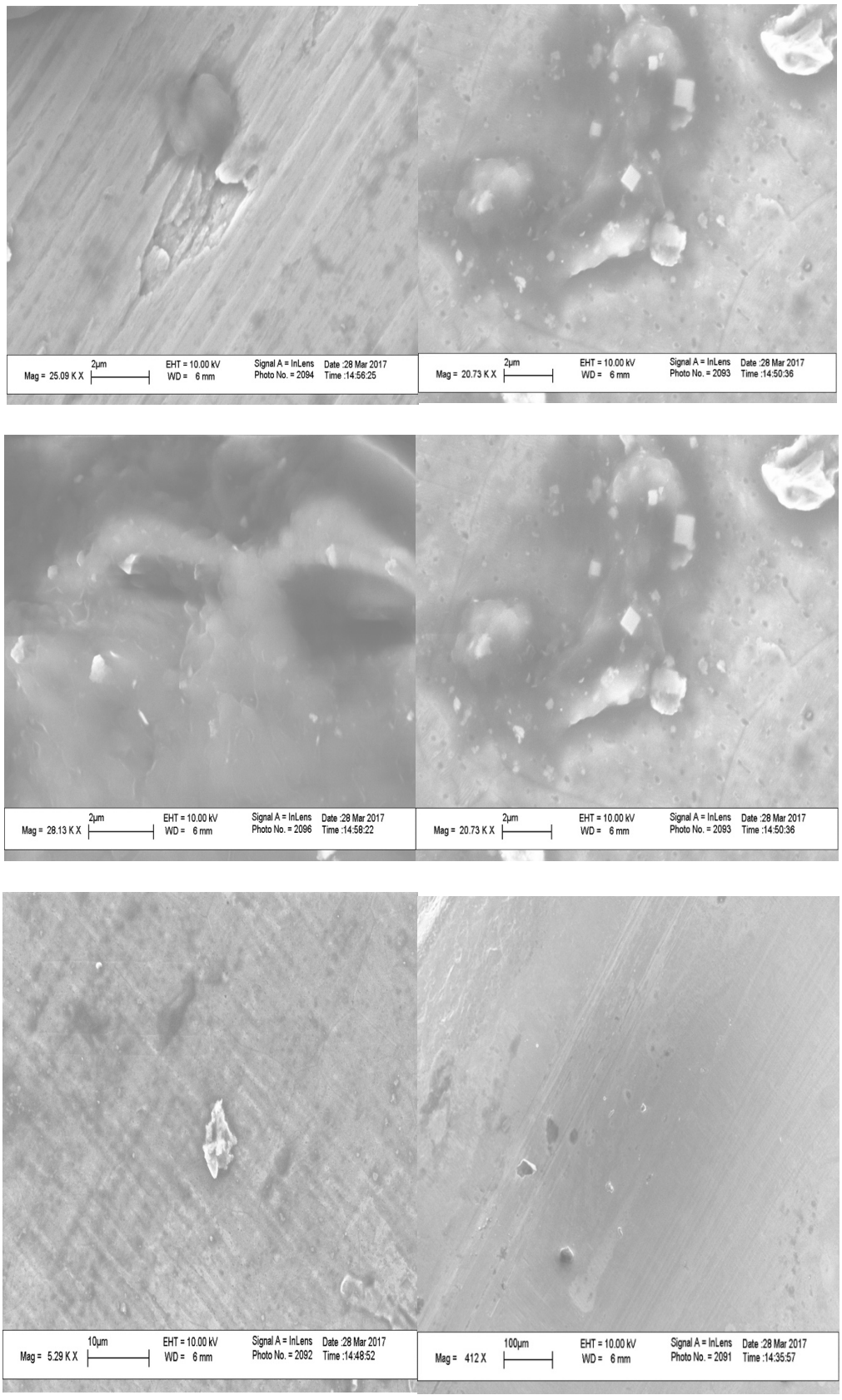

Figure 7.11 Represents the surface deterioration as well as pit and crevice corrosion.

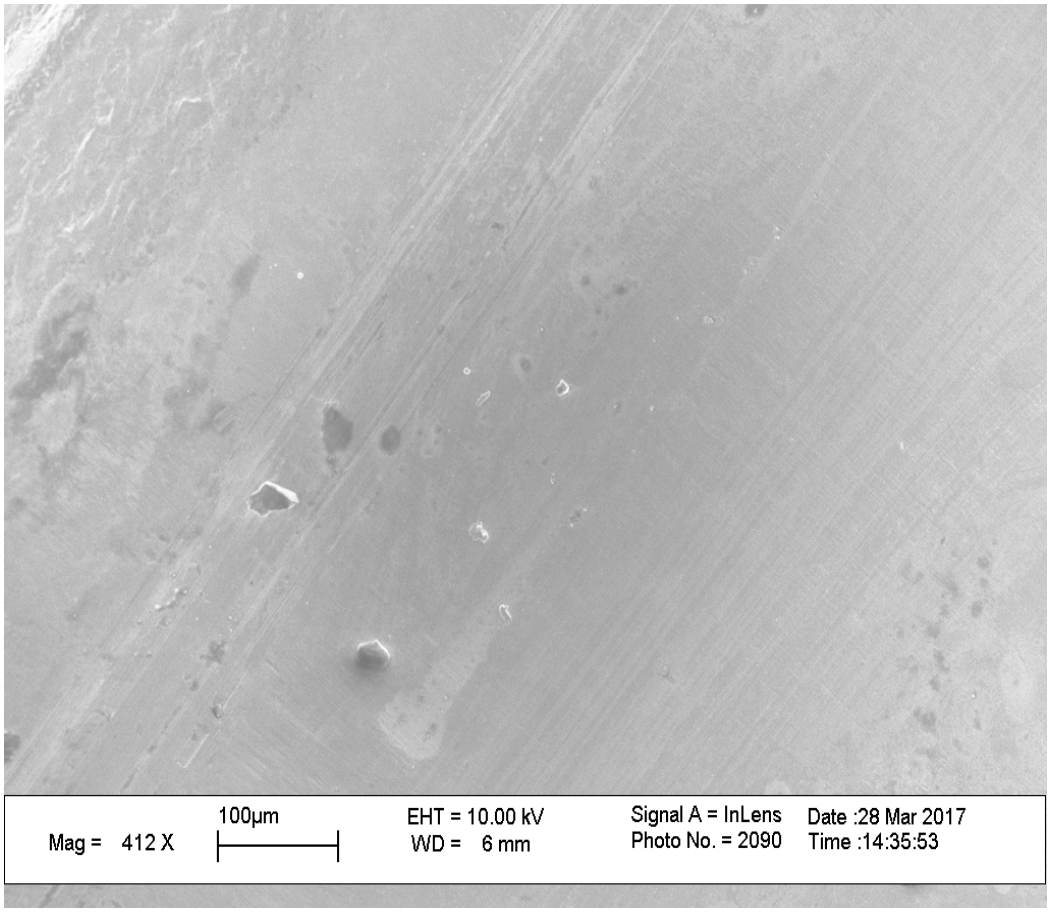

Figure 7.12 Pit holes on surface of blade.

7.3 EDX Analysis of Blades

7.3.1 Martensitic 440 razor blade

EDX spectra were acquired on the surface of the blade.

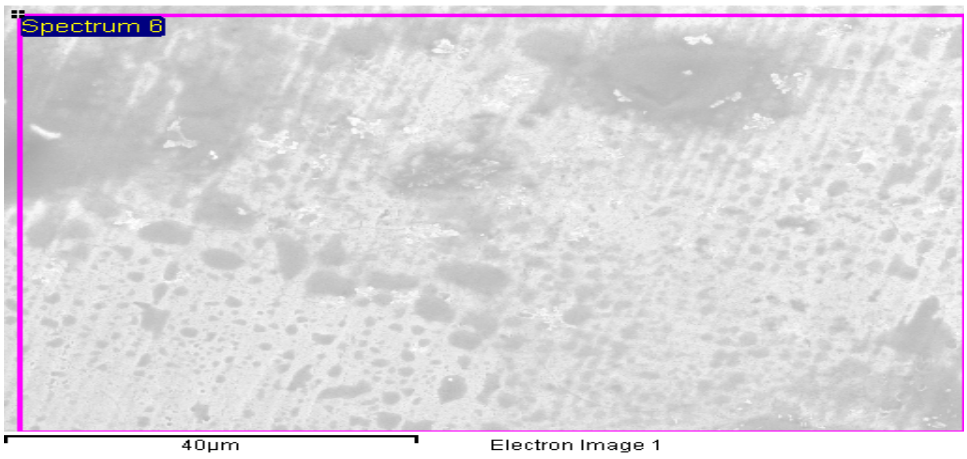

Figure 7.13 EDX analysis of the surface of the blade.

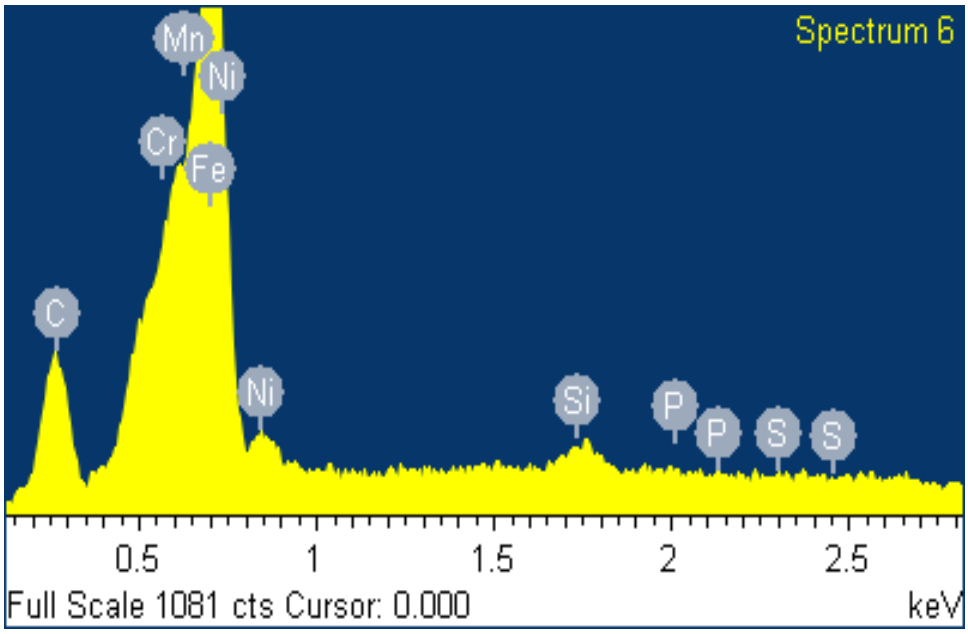

Figure 7.14 EDX analysis showing the chemical analysis of blade.

DATA FROM EDX:

Spectrum processing: No peaks omitted

Processing option: All elements analyzed (Normalized)

Number of iterations = 2

Table 7.4 Standard Elements in Blade:

C	$CaCO_3$	1-Jun-1999 12:00 AM
Si	SiO_2	1-Jun-1999 12:00 AM
P	GaP	1-Jun-1999 12:00 AM
S	FeS_2	1-Jun-1999 12:00 AM
Cr	Cr	1-Jun-1999 12:00 AM
Mn	Mn	1-Jun-1999 12:00 AM
Fe	Fe	1-Jun-1999 12:00 AM
Ni	Ni	1-Jun-1999 12:00 AM

Table 7.5 Composition of Elements in Blade

Elements	C K	Si K	P K	S K	Cr L	Mn L	Fe L	Ni L	Totals
Weight%	6.02	0.51	0.02	0.00	21.61	1.60	66.65	3.59	100.00
Atomic%	22.59	0.82	0.03	0.00	18.72	1.31	53.77	2.76	

7.3.2 Analysis of blade after exposure to NaCl

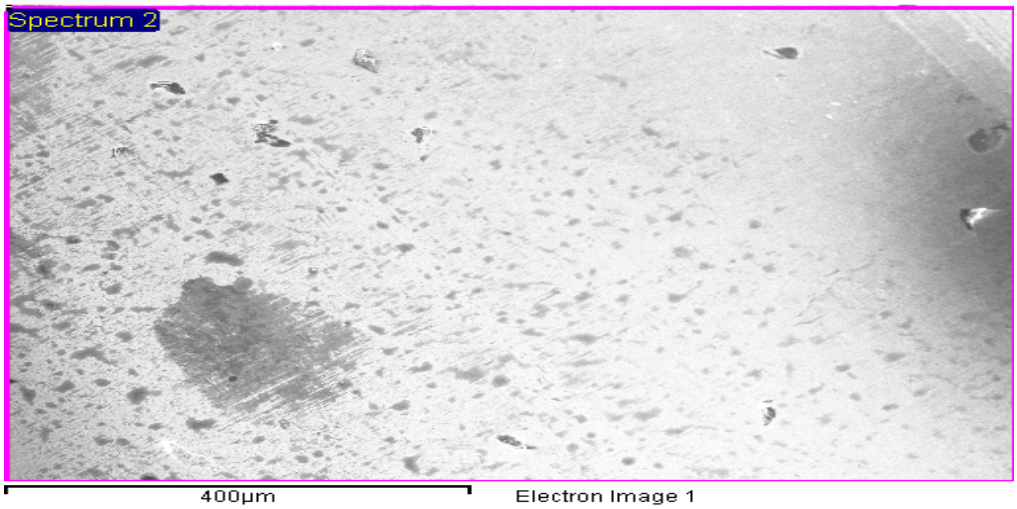

Figure 7.15 EDX analysis of surface of blade.

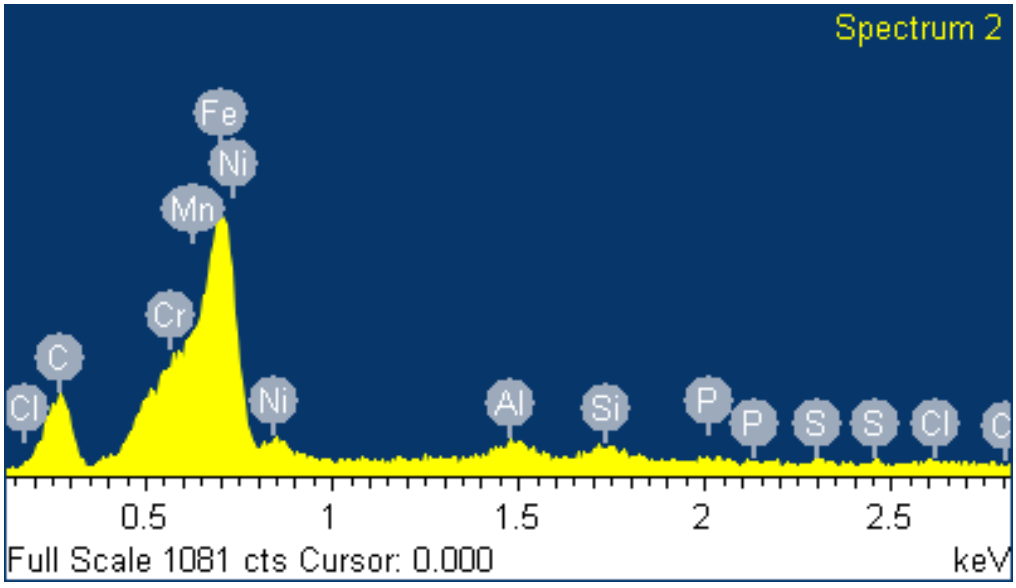

Figure 7.16 EDX analysis showing the chemical analysis of blade.

Data from EDX

Spectrum processing: No peaks omitted

Processing option : All elements analyzed (Normalized)

Number of iterations = 1

Table 7.6 Standard Elements in Blade treated in NaCl

Standard
C $CaCO_3$ 1-Jun-1999 12:00 AM
Al $Al2O_3$ 1-Jun-1999 12:00 AM
Si SiO_2 1-Jun-1999 12:00 AM
P GaP 1-Jun-1999 12:00 AM
S FeS_2 1-Jun-1999 12:00 AM
Cl KCl 1-Jun-1999 12:00 AM
Cr Cr 1-Jun-1999 12:00 AM
Mn Mn 1-Jun-1999 12:00 AM
Fe Fe 1-Jun-1999 12:00 AM
Ni Ni 1-Jun-1999 12:00 AM

Table 7.7 Composition of Elements in Blade treated in NaCl

Elements	C K	Al K	Si K	P K	S K	Cl K	Cr L	Mn L	Fe L	Ni L	Totals
Weights%	7.81	0.61	0.53	0.18	0.18	0.18	19.55	2.08	65.16	3.71	100
Atomic%	27.63	0.97	0.80	0.25	0.24	0.2	15.99	1.61	49.60	2.68	

7.3.3 Analysis of blades after exposure to Acetic Acid

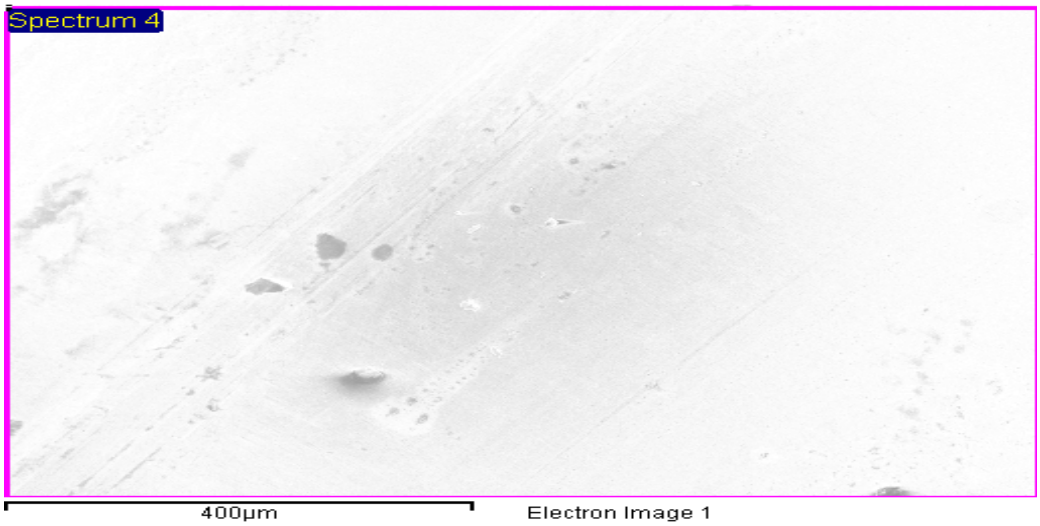

Figure 7.17 EDX analysis of surface of blade.

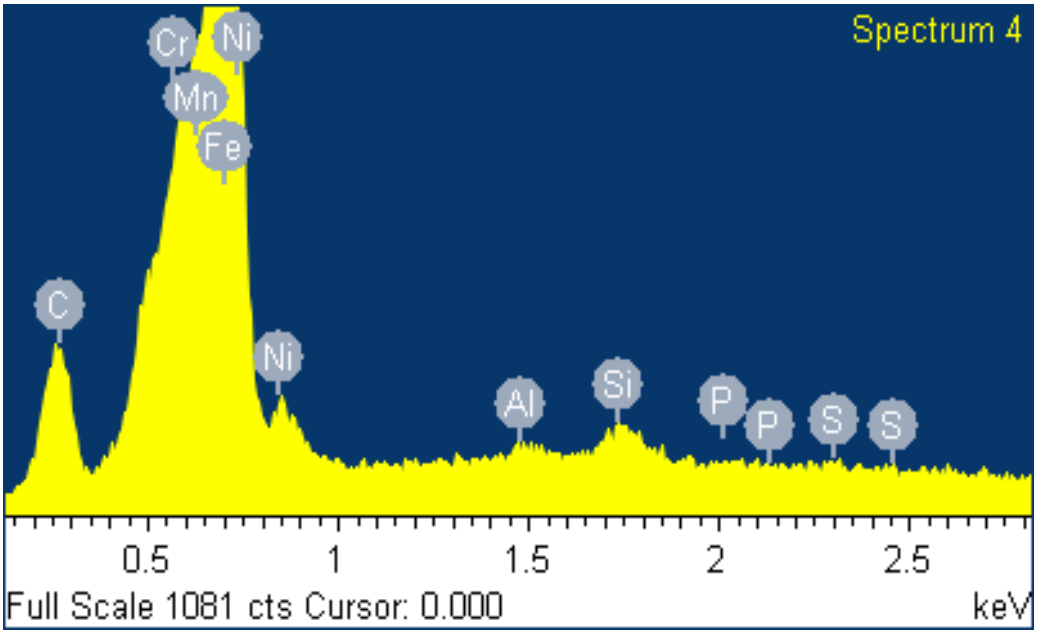

Figure 7.18 EDX analysis showing the chemical analysis of blade.

DATA FROM EDX:

Spectrum processing: No peaks omitted

Processing option: All elements analyzed (Normalised)

Number of iterations = 2

Table 7.8 Standard Elements in Blade treated in Acetic Acid

Standard
C CaCO3 1-Jun-1999 12:00 AM
Al Al2O3 1-Jun-1999 12:00 AM
Si SiO2 1-Jun-1999 12:00 AM
P GaP 1-Jun-1999 12:00 AM
S FeS2 1-Jun-1999 12:00 AM
Cr Cr 1-Jun-1999 12:00 AM
Mn Mn 1-Jun-1999 12:00 AM
Fe Fe 1-Jun-1999 12:00 AM
Ni Ni 1-Jun-1999 12:00 AM

Table 7.9 Elements Composition in Blade treated in Acetic Acid

Elements	C K	Al K	Si K	P K	S K	Cr L	Mn L	Fe L	Ni L	Total
Weight%	4.99	0.19	0.45	0.04	0.08	21.02	1.20	68.57	3.45	100.00
Atomic%	19.29	0.33	0.75	0.06	0.11	18.76	1.01	56.96	2.73	

CHAPTER 8

CONCLUSION AND RECOMMENDATION

8.1 General Conclusions

In this research, corrosion performance of Martensitic stainless steels, 440 Razor blade, after immersion in 3.5% of Acetic acid and 3.5% of NaCl, is presented. The major conclusions are as follows:

1. Corrosion behavior of Martensitic 440 razor blade stainless steels at room temperature changes significantly with increase in acetic acid concentration and NaCl acid.

2. In NaCl and acetic acid, steels exhibit a much greater corrosion rate.

3. Blade experiences uniform and pitting corrosion in acid and no passive surface film is formed. The EDX results indicate a continual oxidation of C, Fe, Cr, Mo and Ni on the surface of the 440 stainless steel blade subsequent to emersion in acids. Also, the contribution of the pits to the total weight loss was at least 60 % after 6 days of immersion.

4. As steel undergoes corrosion in acids, there tends to be an inverse relationship in the weight loss and corrosion rate. While weight loss tends to increase over time, the highest being at the time that the corrosion process is initiated, corrosion rate tends to decrease simultaneously.

After 6 days of exposure to corrosive environments, synthetic seawater gives pitting and crevice corrosion results on stainless steels that are comparable to one month of exposure in natural seawater. Mechanism of pitting corrosion of stainless steel blade in sodium chloride solution involves the formation of an intermediate complex of chloride ion with the passive metal followed by successive dissolution.

The susceptibility of pitting corrosion of Martensitic stainless steel increases with the increase in chloride ion concentration in acidic chloride media. The pitting potential (Epit) decreases with increase in chloride ion concentration. The pit formed under droplets of chloride solutions was a shallow type, which indicates that the pit propagates preferentially to horizontal direction. The pitting corrosion mechanism of Type 440 steel, under thin droplet layers containing chloride ions, has been proposed on the basis of these experimental results.

The results obtained in the present work revealed that the passive film formed on the surface of the AISI 440 blade in the chloride solutions and acetic acid contains oxides of the two main elements, i.e., Cr and Fe as Cr-oxides and Fe-oxides. A slight decrease in the chromium oxide content, close to the oxide/solution interface, after 144 h exposure in NaCl and acetic acid was observed.

This thesis presents corrosion data and microstructural analysis data of martensitic stainless steel blade exposed to NaCl and acetic acid. The corrosion tests lasted for 144h.The microstructural data have been collected through SEM analysis in the grain interior and at grain boundaries of the bulk of the materials and at the superficial oxide layer developed during the corrosion exposure. The microstructural characterization of the materials, subjected to corrosion tests, provides insight into the corrosion behavior of such materials where the surface deterioration of blade, crack and pit holes on surfaces can be observed. These are of interest to industries and research laboratories that are focused on developing better performing materials to be used in harsh environments.

8.2 RECOMMENDATION

1. Further experiments can be carried out to provide better understanding of the corrosion performance of the two stainless steels 316 and 440 in acetic acid environments in the presence of Br ions. Below are some of the proposed future works:

- Follow the polarization technique to measure the corrosion rate and analyze the sample with SEM prior to passivation; this may give more insight into surface processes at this stage. Studying any possible effect(s) of flow rate on the corrosion behavior of these alloys would be interesting.

- In order to evaluate the extent of metallic dissolution from the surface of steels, the content of dissolved elements, Fe, Cr, Mo or Ni, in the test solution could be evaluated by using Atomic Absorption Spectrometer (AAS).

- Study the behavior of the constituent elements: iron, chromium, nickel and molybdenum in their pure state and compare with typical alloys with the aim of knowing which element(s) may possibly facilitate the passivity to corrosion in test solutions.

- Study the depth of pit holes by using depth profilometery.

2. Apply Nano-titanium and diamond like carbon thin film coating on blades to reduce the corrosivity and protect it from pitting corrosion. Measure the coated blades and compare with the results of uncoated blades.

3. Perform corrosion studies on blades from various manufacturers and compare corrosion rates of blades in NaCl and acetic acid with bromide ions.

REFERENCES

1. Fotana N.D., M.G. and Green, "Corrosion Engineering", 3rd, McGraw-Hill, Singapore.

2. Uhlig, H.H. and Revie, R.W., "Corrosion and Corrosion control", 3 ed., McGraw-Hill, New York (1987).

3. Shreir, L.L., Jarman, R.A. & Burstein, G.T., "Corrosion" Vol.1, Metal/ Environment Reactions, 3 ed. John Wiley, New York, (1984). 3rd edition 1994

4. West, J.M., "Basic Corrosion and Oxidation", Ellis Horwood Ltd., West Sussex (1980).

5. Roberge, P.R., "Handbook of Corrosion Engineering" McGraw- Hill, U.S.A., (2000).

6. Stansbury, E.E. and Buchanan, R.A., "Fundamentals of Electrochemical Corrosion", ASM International, (2000).

7. Tretheway, K. R. and Chamberlain," J. Corrosion Science and Engineering", 2nd

8. Shreir,L.L.,"Corrosion", Metal/Environment Reactions, Newnes Butten worths, 2 Edition. , Longman, London, (1996).

9. West, J. M., "Electrode position and Corrosion Processes", Van Nostrand Reinhold Company, 2 ed., vol.1, (1976).

10. Steigerwald, R. F.," Corrosion", No.24,p. 1, (1968). ed.,(1971).

11. From internet on, Technical Hand book of Stainless, Atlas steels, Corrosion resistance at the http://www.corrosion.ksc.nasa.gov, (2001).

12. Hoar T.P.," Corrosion Science" ,7 , 341 , (1967)

13. Uhlig H.H,"History of passivity, Experiments and Theories" , Passivity of the 4th Sysmposium on Passivity , edited by Frankenthal and J. Kruger, Electrochemical. Soc. Princton, N.J (1978).

14. Wagner C.," Corrosion Science" ,(1965)

15. Kabanove B., Burstein R., and Frumkin A., "Discussions Faraday Society, 1, 259,(1947)(as quoted in 2).

16. Frankenthal,R., "Journal of the Electrochemical Society",114,542, (1967)

17. Mc Adam, D. J. and Gell, G.W., "Pitting and its Effect on the Fatigue Limit of Steels Corroded Under Various Conditions" Journal of the Proceedings of the American

Society for Testing Materials, Vol.41,(1928).

18. Nguyen, T.H. and Foley, R.T." On the Mechanism of Pitting of Aluminum," Journal of the Electrochemical Society, Vol.126, No.11,1979.

19. Frankel G.S., "Pitting Corrosion of Metal"; A Review of the Critical Factors, J. Electrochemical Society, Vol. 145, 1998.

20. From internet on "Pitting Corrosion" ch.9, KAIST, at http://corrosion.kaist.ac.kr.

21. Baroux B., Further Insights on the Pitting Corrosion of Stainless Steels, "Corrosion Mechanisms in Theory and Practice", 2nd Edition

22. Smialowska- Szklarska Z., "Pitting Corrosion of Metals", NACE,(1986). ed. ,P. Marcus, Ed,.

23. George E. Dieter, Mechanical Metallurgy, McGraw-Hill Book Company, 1988.

24. G.S. Frankel, Pitting Corrosion Metals Handbook, Ohio State University 1994

25. Japanese Standards Association, JIS Handbook, Ferrous Materials and Metallurgy I,

2002.

26 Fong-Yuan Ma (2012). Corrosive Effects of Chlorides on Metals, Pitting Corrosion, Prof. Nasr Bensalah (Ed.), ISBN: 978-953-51-0275-5, InTech, Available from: http://www.intechopen.com/books/pittingcorrosion/ corrosive-effects-of-chlorides-on-metals

27. Frankel G.S., Stockert L., Hunkeler F., and Boehmi H., " Corrosion", Vol.43, (1987) (cited in 19).

28. Pessall N.and Liu C.," Electrochemical Acta", Vol.16,(1971)(cited in 19).

29.Hisamatsu Y. Yoshii T., and Matsumura Y.," Electrochemical and Microscopical Study of Pitting Corrosion of Austenitic Stainless Steel", Localized Corrosion, Vol.NACE-3,R.W. Staeble ,B,F. Brown, J. Kruger and A. Agrawal, Ed.,NACE,(1974)(cited in 19).

30.Williams D.E., Stewar J., and Balkwill P.H., Corrosion Science, Vol.36,(1994) (cited in 19).

31. Ezuber H. and Newman R.C., Growth-Rate Distribution of Metastable Pits. Critical Factors in Localized Corrosion, Vol. PV 92-9,(1992) (cited in 19).

32. Pistorius P.C. and Burstein G.T.," Corrosion Science", Vol. 33 (1992) (cited in 19

33. Pistorius P.C. and Burstein G.T.," Corrosion Science", Vol. 36 (1994) (cited in 19).

34.Wood G.C., Sutton W.H., Richardson J.A, Riley T.N.K., and Malherb A.G.," The Mechanism of Pitting of Aluminum and Its Alloys", Localized 130 Corrosion, R.W. Staehle, B.F. Brown, J. Kruger, and A.Agrawal, Ed.,NACE,(1974) (cited in 19).

35. Pride S.T., Scully J.R, and Hudson J.L.," J. Electrochemical society" Vol.141,(1994) (cited in 19).

36 57.Arnvig P.E. and Biogard A.D., Paper 437," Corrosion 96", NACE,(1996) (cited in 19).

37. Arnvig P.E. and Davision R.M., Paper 209," Process 12th

38. Brigham R.J. and Tozer E.W.," Corrosion", Vol.29,(1973) (cited in 19). International Corrosion Congress",(Houston, TX),(1993) (cited in 19).

39. Brigham R.J. and Tozer E.W., Corrosion, Vol.30,(1974) (cited in 19).

40.Qvarfort R.," Corrosion Science", Vol.28,(1988) (cited in 19).

41.Qvarfort R.," Corrosion Science", Vol.29,(1989) (cited in 19).

42. Laycock N.J., Moayed M.H., and Newman R.C.," Prediction of Pitting Potentials and Critical Pitting Temperatures", Critical Factors in Localized Corrosion II,Vol.PV95-15(1995) (cited in 19).

43. Pourbaix M., et al.," Corrosion science",Vol.3,(1963).

44. Leckie H.P. and Uhlig H.H.,"J. Electrochemical Society", Vol.113,(1966) (cited in 19).

45.Kolotyrkin J.M., Golovina G.V., and Florianovich G.M., SSSR D.A.N., Vol.148,(1963).

46. Fokin M.N., Kurtepov M.M., and Bachkareva V.J., Sbornik Pokorrozji, Moskov(1965).

47. Pourbaix, M.," Corrosion Science". 30,963, (1990).

48. Sandwith Colin and Randy K. Kent, University of Washington, MDE Engineers, Inc."Corrosion – Related Failures".

49. Tuthill A.H. and Schillmoler C.M.," Guidelines for Selection of Marine Materials", Ocean Science and Engineering Conference, Marine Technology Society, Washington, (1965)(cited in 71).

50. Stein A.A., MIC in the Power Industry," Microbiologically Influenced Corrosion", Korbin G., Ed., NACE International, (1993)(cited in 6).

51. Little B., Wagner P., and Mansfeld F.," Microbiological influenced Corrosion of Metals and Alloys", Int. Mater. Rev., Vol.36,(1991)(cited in 6).

52. Laycock N. J. and Newman R.C.,"Corrosion Science",Vol. 39,(1997) (cited in 19).

56. Shibata T.and Takeyama T.," Corrosion" , Vol.33,(1977) (cited in 19).

57. Sedriks A. J.," Corrosion of Stainless Steels", Wiley-Inter science , (1996) (cited in 19).

58 http://www.arcelormittal.com/stainlesseurope

59 F. U. Renner, A. Stierle, H. Dosch, D. M. Kolb, T. L. Lee and J. Zegenhagen, Nature, 2006, 707–710.

60 S. D. Cramer and B. S. Covino, Corrosion: fundamentals, testing and protection, ASM International Handbook, 2003, vol. 13A.

61 F. M. Song, D. W. Kirk, J. W. Graydon and D. E. Cormack, Corrosion, 2004, 60, 736–748.

62 W. Villamizar, M. Casales, J. G. Gonzalez-Rodriguez and L. Martinez, J. Solid State Electrochem., 2006, 11, 619–629.

63 J. L. Crolet, Predicting CO2 corrosion in oil and gas industry, European Federation of Corrosion Publications, Work. Party Report, Inst. Mater, London, 1994, SSN 1354–5116, No. 13.

64 A. Ikeda, M. Ueda and S. Mukai, Corrosion, 1983, 83.

65 L. A. I. Kestens and R. Petrov, Ceram. Trans., 2009, 200, 207– 216.

66 S. Nesic, Corros. Sci., 2007, 49, 4308–4338.

67 H. S. Hernandez, F. L. Linares, J. Bruzual and J. G. Luzon, NACE International, 2003, 1, 03330.

68 M. A. Migahed, Prog. Org. Coat., 2005, 54, 91–98.

69 S. Papavinasam, A. Doiron, T. Panneerselvam and R. W. Revie, Corrosion, 2007, 63, 704–712.

70 M. Godec and M. Jenko, Mater. Tehnol., 2000, 34, 359–364.

71 Z. N. Farhat, Wear, 2001, 250–251, 401–408.

72 M. Liu, D. Qiu, M.-C. Zhao, G. Song and A. Atrens, Scr. Mater., 2007, 58, 421–424.

73 R. Xin, Y. Luo, A. Zuo, J. Gao and Q. Liu, Mater. Lett., 2012, 72, 1–4

74 Y. S. Sato, H. Kokawa, K. Ikeda, M. Enomoto, S. Jogan and T. Hashimoto, Metall. Mater. Trans. A, 2001, 32, 941–948.

75 D. P. Field, T. W. Nelson, Y. Hovanski and K. V. Jata, Metall. Mater. Trans. A, 2001, 32, 2869–2877.

76 M. F. Suarez and R. G. Compton, J. Phys. Chem. B, 1998, 102, 7156–7162.

77 E. Hill, R. R. Lloyd-Williams, R. G. Compton and J. H. Atherton, J. Solid State Electrochem., 1999, 3, 327–330.

78 K. Y. Tam, R. G. Compton, J. H. Atherton, C. M. Brennan and R. Docherty, J. Am. Chem. Soc., 1996, 118, 4419–4426.

79 M. R. Bateni, J. A. Szpunar, X. Wang and D. Y. Li, Wear, 2005, 259, 400–404.

80 Y. Baik and Y. Choi, Phys. Met. Metallogr., 2014, 115, 1318– 1325.

81 S. A. Park, J. G. Kim, Y. S. He, K. S. Shin and J. B. Yoon, Phys. Met. Metallogr., 2014, 115, 1285–1294.

82 W. Xu andM. Ferry,Mater. Sci. Technol., 2010, 26, 1159–1172.

83 W. Ozgowicz, A. Grajcar and A. Kurc-Lisiecka, in Corrosion Behaviour of Cold-Deformed Austenitic Alloys, INTECH Open Access Publisher, 2012.

84 D. Raabe, Crystallographic textures of hot rolled steels, 2003,http://pubman.mpdl.mpg.de/pubman/item/escidoc:2018381/ component/escidoc:2018380/Raabe%20textures%20of% 20hot%20rolled%20steels.pdf.

85 J. M. Hallen, V. Venegas and F. Caleyo, International Conference on Fracture, Beijin, China, 16–21 June 2013

86 L. J. Oblonsky, G. R. Chesnut and T. M. Devine, Corrosion, 1995, 51, 891–900.

87 E. Naderi, A. H. Jafari, M. Ehteshamzadeh and M. G. Hosseini, Mater. Chem. Phys., 2009, 115(2–3), 852–858.

88 C. Herrera, N. B. Lima, A. Ferreira Filho, R. L. Plaut and A. F. Padilha, J. Mater. Process. Technol., 2009, 209(7), 3518–3524.

89 A. Y. Kandeil and M. Y. Mourad, Surf. Coat. Technol., 1989, 37(2), 237–250.

90 C. Y. Chao, L. F. Lin and D. D. Macdonald, J. Electrochem. Soc., 1981, 128, 1187–1194.

91 S. M. Moon and S. I. Pyun, Electrochim. Acta, 1998, 43, 3117– 3126.

92 L. Jinlong and L. Hongyun, Surf. Coat. Technol., 2013, 235, 513–520.

93 Y. A. Perlovich, M. G. Isaenkova, P. N. Medvedev, V. A. Fesenko and S. San Thu, Inorganic Materials: Applied Research, 2015, 6, 259–266.

94 G. L. Song, R. Mishra and Z. Xu, Electrochem. Commun., 2010, 12, 1009–1012.

95 J. T. Woodward, H. Gwin and D. K. Schwartz, Langmuir, 2000, 16, 2957–2961.

96 P. Roach, N. J. Shirtcliffe and M. I. Newton, So Matter, 2008, 4, 224–240.

97 W. Xu, T. Ning, X. Yang and S. Lu, Appl. Surf. Sci., 2011, 257, 4801–4806.

98 R. N. Wenzel, Ind. Eng. Chem., 1936, 28, 988–994.

99 E. J. Song, H. Bhadeshia and D. W. Suh, Corros. Sci., 2013, 77, 379–384.

100 D. Yu and J. Tian, Colloids Surf., A, 2014, 445, 75–78.

101 H. Zhang, J. Yang, B. Chen, C. Liu, M. Zhang and C. Li, Appl. Surf. Sci., 2015, 359, 905–910.

102 Z. Yuan, J. Bin, X. Wang, M. Wang, C. Peng, S. Xing, J. Xiao, J. Zeng, X. Xiao and X. Fu, Surf. Topogr.: Metrol.Prop., 2014, 2, 25003.

103 L. K. Wu, X. F. Zhang and J. M. Hu, Corros. Sci., 2014, 85, 482–487.

104 R. Ramachandran and M. Nosonovsky, Phys. Chem. Chem. Phys., 2015, 17, 24988–24997.

105 W. Xu, J. Song, J. Sun, Y. Lu and Z. Yu, ACS Appl. Mater. Interfaces, 2011, 3, 4404–4414.

106 T. Liu, S. Chen, S. Cheng, J. Tian, X. Chang and Y. Yin, Electrochim. Acta, 2007, 52, 8003–8007

107 J. Y. Lee, J. Han, J. Lee, J. S. Yeo, J. Y. Lee and J. Han, Nanoscale Res. Lett., 2015, 10(1), 505.

108 L. Li, V. Breedveld and D. W. Hess, ACS Appl. Mater. Interfaces, 2012, 4, 4549–4556.

109 S. Seal, K. Sapre, A. Kale, V. Desai, M. Gopal and P. Jepson, Corros. Sci., 2000, 42(9), 1623–1634.